

4-28-1995

Improved Finite Analytic Methods for Solving Advection-dominated Transport Equation in Highly Variable Velocity Field

Wei Cuifeng
Portland State University

Follow this and additional works at: https://pdxscholar.library.pdx.edu/open_access_etds



Part of the [Civil Engineering Commons](#)

Let us know how access to this document benefits you.

Recommended Citation

Cuifeng, Wei, "Improved Finite Analytic Methods for Solving Advection-dominated Transport Equation in Highly Variable Velocity Field" (1995). *Dissertations and Theses*. Paper 4922.
<https://doi.org/10.15760/etd.6798>

This Thesis is brought to you for free and open access. It has been accepted for inclusion in Dissertations and Theses by an authorized administrator of PDXScholar. Please contact us if we can make this document more accessible: pdxscholar@pdx.edu.

THESIS APPROVAL

The abstract and the thesis of Cuifeng Wei for the Master of Science in Civil Engineering presented April 28, 1995, and accepted by the thesis committee and the department.

COMMITTEE APPROVALS: 

Dr. Shuguang Li, Chair



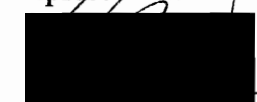
Dr. Scott Wells



Dr. Gerry Recktenwald



Dr. Charles Balogh
Representative of the Office of Graduate Studies



DEPARTMENT APPROVAL :

Dr. Franz Rad, Chair
Department of Civil Engineering

ACCEPTED FOR PORTLAND STATE UNIVERSITY BY THE LIBRARY

by  on 7 July 1995

ABSTRACT

An abstract of the thesis of Cuifeng Wei for the Master of Science in Civil Engineering presented on April 28, 1995.

Title: Improved Finite Analytic Methods for Solving Advection-Dominated Transport Equation in Highly Variable Velocity Field.

Solute transport studies frequently rely on numerical solutions of the classical advection-diffusion equation. Unfortunately, solutions obtained with traditional finite difference and finite element techniques typically exhibit excessive numerical diffusion or spurious oscillation when advection dominates, especially when velocity field is highly variable.

One recently developed technique, the finite analytic method, offers an attractive alternative. Finite analytic methods utilize local analytic solutions in discrete elements to obtain the algebraic representations of the governing partial differential equations, thus eliminating the truncation error in the finite difference and the use of approximating functions in the finite element method. The finite analytic solutions have been shown to be stable and numerically robust for advection-dominated transport in heterogeneous velocity fields.

However, the existing finite analytic methods for solute transport in multiple dimensions have the following disadvantages. First, the method is computationally inefficient when applied to heterogeneous media due to the complexity of the formulation. Second, the evaluation of finite analytic coefficients is when the Peclet number is large. Third, the method introduces significant numerical diffusion due to inadequate temporal approximation when applied to transient problems.

This thesis develops improved finite analytic methods for two-dimensional steady as well as unsteady solute transports in steady velocity fields. For steady transport, the new method exploits the advantages of the existing finite analytic and finite difference methods. The analytically difficult diffusion terms are approximated by finite difference

and numerically difficult advection and reaction terms are treated analytically in a local element in deriving the numerical schemes.

The new finite analytic method is extended to unsteady transport through application of Laplace transformation. Laplace transformation converts the transient equation to a steady-state expression that can be solved with the steady version of the improved finite analytic method. Numerical inversion of the transformed variables is used to recover solute concentration in the physical space-time domain.

The effectiveness and accuracy of the new finite analytic method is demonstrated through stringent test examples of two dimensional steady-state transport in highly variable velocity fields. The results clearly demonstrated that the improved finite analytic methods are efficient, robust and accurate.

**IMPROVED FINITE ANALYTIC METHODS FOR SOLVING
ADVECTION-DOMINATED TRANSPORT EQUATION
IN HIGHLY VARIABLE VELOCITY FIELD**

by
CUIFENG WEI

**A thesis submitted in partial fulfillment of the
requirements for the degree of**

**MASTER OF SCIENCE
in
CIVIL ENGINEERING**

**Portland State University
1995**

ACKNOWLEDGMENTS

I would like to thank my committee, Drs. Shuguang Li (Chair), Scott Wells, Gerry Recktenwald, and Charles Balogh, for their time in reading and giving comments on this work, and also for their encouragement. Especially, I want to thank Dr. Shuguang Li, my advisor, who has spent much time in discussing and solving problems with me, and thoroughly reviewed the thesis. I am also grateful to Charles Balogh, who spent hours explaining and discussing his comments and suggestions in person.

I would like to acknowledge Department of Civil Engineering at Portland State University for financial support of this research.

I would also like to thank CH2M HILL for support and understanding, while I put this work into final form. Particularly I want to thank Mr. Dale Richwine, who has been fully supportive and encouraged me in both academic and professional work during last two years. I would also like to thank Dawn Sanders, who gave me great encouragement.

I would like to thank all the people at Chinese Free Methodist Church for their encouragement, concern, prayers and love. Especially, I want to thank Rev. Joseph Yeung and his wife for their love and support.

I would also like to thank Feng Ruan, whose Random Field Generator provided me a good way to test the improved methods. I want to thank Dr. Vern Bissell, who has spent much time correcting my written English and has provided counsel, encouragement and prayers when I encountered difficulties in my research and writing.

My heartfelt thanks go to my family. Their continual concern, support, encouragement, patience, and love constantly refreshed me when I felt emotionally drained. I have learned much about their true love for me.

Above all, I give thanks to God, and acknowledge Him as the giver of all talents, abilities, and opportunities which have made this possible for me.

Table of Contents

Section	Page
List of Symbols	vi
List of Figures	viii
List of Tables	xi
Chapter	
1. Introduction	1
1.1. Motivation.....	1
1.2. Literature Review	5
1.3. Objective and Scope of Work.....	11
2. Critical Review of Existing Finite Analytic Methods	12
2.1. Basic Idea of Finite Analytic Methods.....	12
2.2. Illustrative Example: One-Dimensional Steady Problem	12
2.2.1. Conventional Finite Difference Approximations	14
2.2.2. Finite Analytic Approximation	15
2.2.3. Discussion and Comparison	17
2.3. Basic Formulation of Finite Analytic Method for Multi-Dimensional Transport	20
2.4. Problems and Limitations of Existing Finite Analytic Methos	24
2.4.1. Computational Efficiency	24
2.4.2. Difficulties in Evaluating Finite Analytic Coefficients	24
2.4.3. Boundary Approximations	26
2.4.4. Transient Extensions.....	27

Table of Contents

(continued)

Chapter	Page
3. Improved Finite Analytic Methods for Steady Transport.....	28
3.1. Governing Equation	28
3.2. Approximation of Local Analytic Solution.....	28
3.2.1. Approximation of Diffusion Terms.....	28
3.2.2. Linear Interpolation Boundary Approximation	34
3.2.3. Improved Linear Interpolation Boundary Approximation	39
3.3. Properties of Improved Finite Analytic Methods	46
4. Improved Finite Analytic Methods for Unsteady Transport.....	61
4.1. Basic Idea.....	61
4.2. Formulation.....	62
4.2.1. Governing Equation.....	62
4.2.2. Laplace Transformation	63
4.2.3. Finite Analytic Approximation in the Laplace Domain	63
4.2.4. Numerical Laplace Inversion	68
4.3. Discussion	69
5. Examples, Results and Discussion.....	71
5.1. Problem Definition.....	71
5.2. Numerical Results	73

Table of Contents

(continued)

Chapter	Page
6. Conclusion and Recommendation	95
6.1. Summary of Original Contributions	95
6.2. Recommendations for Future Work.....	97
Appendix The Improved Finite Analytic Method with Linear Interpolation for Steady Transport	98
References	111

List of Symbols

Alphabetical Symbols

a	Coefficient in numerical solution
C	Solute concentration
\tilde{C}	Laplace transformed solute concentration
D	Dispersion coefficient
g	Initial condition
L	Laplace transformation
N_p	Number of terms truncated from infinite series
p	Laplace transform parameter
P	Interior node in a local element
P', P''	Non-nodal points in a local element
S	Source/sink term in the solute transport equation
\tilde{S}	Transformed source/sink
t	Time
T	Maximum simulation time
U	Combined velocity over each element
u, v	Flow velocities in x and y directions; if with subscripts, velocities at nodes
u_0, v_0	Mean flow velocities in x and y directions
x, y	Spatial Cartesian coordinates
Pe	Peclet number
r, r'	Flow direction in the local element in finite analytic formulation
R	Numerical coefficient in the finite analytic steady-state formulation
R'	Numerical coefficient in finite analytic unsteady-state formulation

Greek Symbols

α, β	Numerical coefficients for one-dimensional advection transport problems
π	Pi = 3.141592654
λ	Decay rate

List of Symbols

(continue)

Greek Symbols

λ_x, λ_y	Correlation scales in x and y directions
σ_{LnK}^2	Variance
$\Delta\eta$	Distance from non-nodal point P' to interior node P
Δ	Difference

Subscripts

E, W, N, S	East, West, North, South, boundaries
EC	East Central (Similarly for WC, SE, NE, etc.)
i, j	Nodal coordinate in the x, y directions
l, m	Nodal coordinate other than i and j
P	Interior point for local element
P'	Non-nodal point on the boundary in local element
P''	Non-nodal point on the boundary in the local element (used in improved linear interpolation scheme)
x, y	Variables in x and y directions

List of Figures

Figures	Page
1-1	Schematic representation of leachate plume from a leaking landfill 1
1-2	Permeability and porosity of cores collected at 1-ft intervals from borehole (IL056) in the Mt. Simon Aquifer in Illinois (data from Bakr, 1976) 3
1-3	Simulation of groundwater flow and solute transport through a synthetically generated random hydraulic conductivity field (domain dimensions in m). (a) Log10 hydraulic conductivity contours; (b) Corresponding hydraulic head contours (high head at left side); and (c) Corresponding solute concentration contours emanating from a continuous sources, plotted at 100 days after the start of injection. (Source: McLaughlin et al., 1993)..... 4
1-4	Concentration profiles for one-dimensional transport of a pulse source obtained with typical finite difference methods (Source Leendertse, 1970)..... 7
2-1	Local element for one-dimensional problem 13
2-2	Numerical coefficients as functions of pecelet numbers..... 18
2-3	A discretized domain and local element of the finite analytic method 20
2-4	Inaccuracy of finite analytic coefficients in cross-hatched region..... 25
3-1	A computational element for finite analytic method with linear interpolation..... 29
3-2	Schematic of comparison of numerical dispersion as function of r_{ij} 38
3-3	Local flowline and P' for $r' = \frac{1}{2}$ 39
3-4	A computational local element for finite analytic method with improved linear interpolation approximation 40
3-5	A local domain for finite analytic method with improved linear interpolation..... 43
3-6	Coefficients for pure diffusion problem ($Pe_x=Pe_y=0$) 48
3-7	Coefficients for transport in horizontal flow ($Pe_x=1, Pe_y=0$)..... 49
3-8	Coefficients for transport in horizontal flow ($Pe_x=20, Pe_y=0$)..... 50

List of Figures

(continued)

Figures	Page
3-9	Coefficients for 2-D transport ($Pe_x=20, Pe_y=6$) 51
3-10	Coefficients for 2-D transport ($Pe_x=20, Pe_y=20$)..... 52
3-11	Coefficients for pure advection problem ($v/u=0$)..... 53
3-12	Coefficients for pure advection problem ($v/u=0.25$)..... 54
3-13	Coefficients for pure advection problem ($v/u=0.5$)..... 55
3-14	Coefficients for pure advection problem ($v/u=0.75$)..... 56
3-15	Coefficients for pure advection problem ($v/u=1.0$)..... 57
5-1	Domain of interest and boundary conditions 71
5-2	Solute transport in homogeneous porous media for $r = 0$ (Peclet number: $Pe_x = 20$) 75
5-3	Solute transport in heterogeneous porous media for $r = 0$ ($\sigma^2_{LnK} = 1.0$; mean Peclet numbers: $Pe_x = 16.7, Pe_y = 0.0$) 76
5-4	Highly variable velocity flow field realization ($\lambda_x = \lambda_y = 8.0$ m; $\sigma^2_{LnK} = 1.5$; mean flow velocity: $u_0 = 0.0417$ m/day) 77
5-5	Solute transport in homogeneous porous media for $r = 0.5$ (Peclet numbrs: $Pe_x = 20; Pe_y = 10$) 78
5-6	Solute transport in heterogeneous porous media for $r = 0.5$ ($\sigma^2_{LnK} = 1.5$; mean Peclet numbers: $Pe_x = 16.7; Pe_y = 8.7$) 79
5-7	Solute transport in heterogeneous porous media for $r = 0.5$ ($\sigma^2_{LnK} = 1.5$; mean Peclet numbers: $Pe_x = 83.4; Pe_y = 41.7$) 80

List of Figures

(continued)

Figures	Page
5-8 Highly variable velocity flow field realization ($\lambda_x = \lambda_y = 8.0$ m; $\sigma^2_{LnK} = 1.5$; mean flow velocities: $u_0 = 0.0417$ m/day, $v_0 = 0.0208$ m/day)	81
5-9 Solute transport in homogeneous porous media for $r = 1.0$ (Peclet numbers: $Pe_x = 20$; $Pe_y = 20$)	82
5-10 Solute transport in heterogeneous porous media for $r = 1.0$ ($\sigma^2_{LnK} = 1.5$; mean Peclet numbers: $Pe_x = 16.7$; $Pe_y = 16.7$)	83
5-11 Highly variable velocity flow field realization ($\lambda_x = \lambda_y = 8.0$ m; $\sigma^2_{LnK} = 1.5$; mean flow velocities: $u_0 = 0.0417$ m/day, $v_0 = 0.0417$ m/day)	84
5-12 Solute transport in homogeneous porous media for $r = 0$ and $Pe \rightarrow \infty$	86
5-13 Solute transport in homogeneous porous media for $r = 0.25$ and $Pe \rightarrow \infty$	87
5-14 Solute transport in homogeneous porous media for $r = 0.5$ and $Pe \rightarrow \infty$	88
5-15 Solute transport in homogeneous porous media for $r = 1.0$ and $Pe \rightarrow \infty$	89
5-16 Solute transport in heterogeneous porous media for $r = 0$ ($\sigma^2_{LnK} = 1.5$; mean flow velocity: $u_0 = 0.0417$ m/day)	90
5-17 Solute transport in heterogeneous porous media for $r = 0.5$ ($\sigma^2_{LnK} = 1.5$; mean flow velocities: $u_0 = 0.0417$ m/day, $v_0 = 0.0208$ m/day).....	91
5-18 Solute transport in heterogeneous porous media for $r = 1.0$ ($\sigma^2_{LnK} = 1.5$; mean flow velocities: $u_0 = 0.0417$ m/day, $v_0 = 0.0417$ m/day).....	92

List of Tables

Tables	Page
5-1 Total Grid Points and Site Parameters for Nonuniform Fields.....	73

Chapter 1

Introduction

1.1. Motivation

Groundwater contamination, particularly from hazardous wastes, has been recognized in recent years as a widespread problem that poses a serious threat to groundwater resources. Problems of groundwater pollution frequently lead to the contamination of wells or surface water bodies interacting with the associated aquifer. Figure 1-1 presents a typical scenario of groundwater contamination due to subsurface waste disposal and possible pathway for human exposure to contamination.

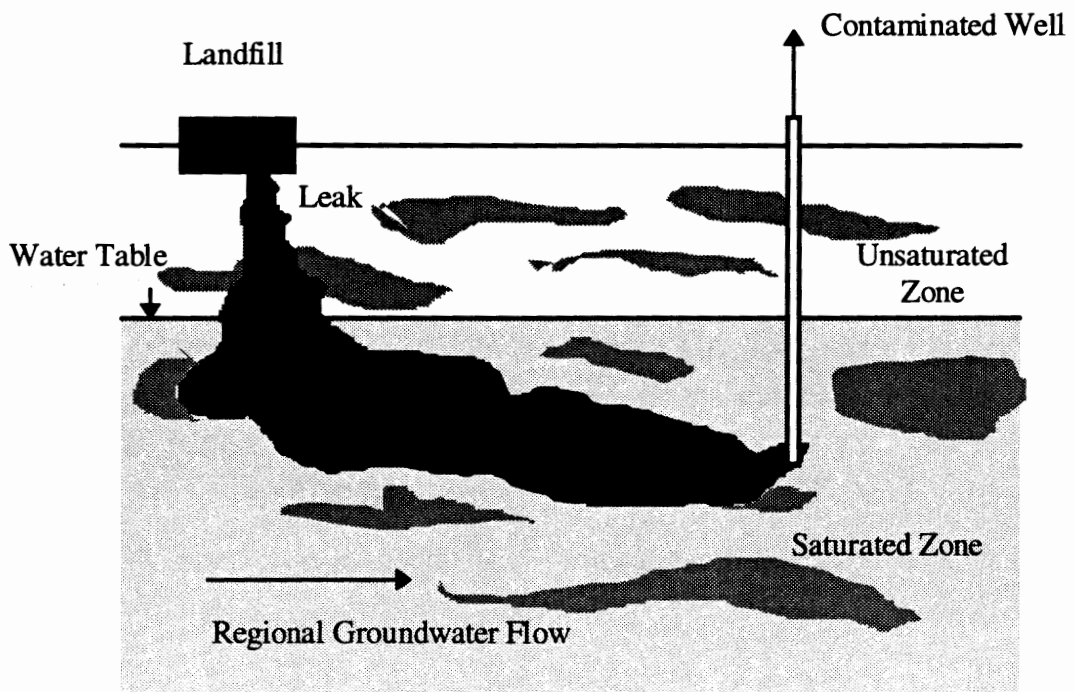


Figure 1-1: Schematic representation of leachate plume from a leaking landfill

One of the factors of groundwater contamination that makes it so serious lies in its long term nature and the fact that it is very difficult to detect and monitor. Wastes buried long ago may cause groundwater contamination that takes decades to be discovered. Although many groundwater contamination sites are small, some of the long term sites are fairly extensive due to the long time period over which contamination has been migrating away from the source. Once a site is found polluted it is often a daunting task to clean up.

The success of groundwater remediation strongly depends on how well one can characterize the groundwater site. Characterization of subsurface contamination, however, can be extremely difficult. Several factors make it difficult to characterize the field-scale transport of soluble contaminants. First, the location and composition of the source of contamination is frequently difficult to determine [Mclaughlin et al., 1993]. Second, site characterization is complicated by the fact that hydrogeological and geochemical properties vary dramatically in space, and possibly over time. Figure 1-2 shows data of permeability collected from a real field site, the Mt. Simmon aquifer, in Illinois [Bakr, 1976]. This is a relatively homogeneous aquifer and the data were collected in the same geologic sandstone unit. The permeability of this material, however, varies over four orders of magnitude. This kind of geological variability is not an exception, but ubiquitous at all field sites [Gelhar, 1993].

Recent theoretical and field investigations have demonstrated that subsurface heterogeneity has a dramatic impact on fate and transport of subsurface contaminants. Variability in hydraulic conductivity, for example, translates into nonuniformity in hydraulic head distribution, which in turn causes irregularities and spatial variability in contaminant plume distribution (see Figure 1-3). All of these problems are familiar to the site managers and planners responsible for site assessments and cleanup programs. If we do not detect contamination because our sampling network is poorly designed, we may greatly underestimate the risk to human health. If we are unable to locate a heterogeneous subsurface contaminant plume accurately, cleanup efforts will be less likely successful.

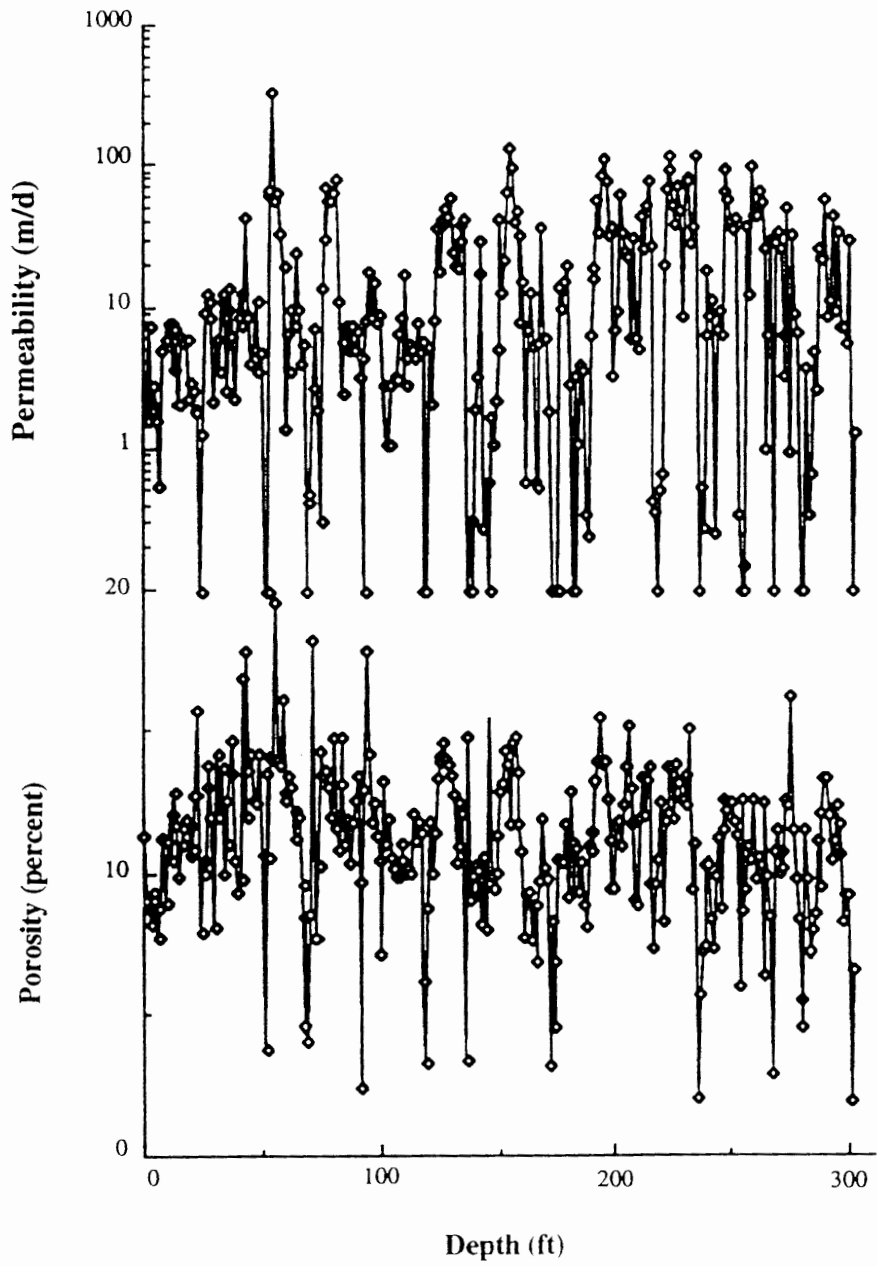
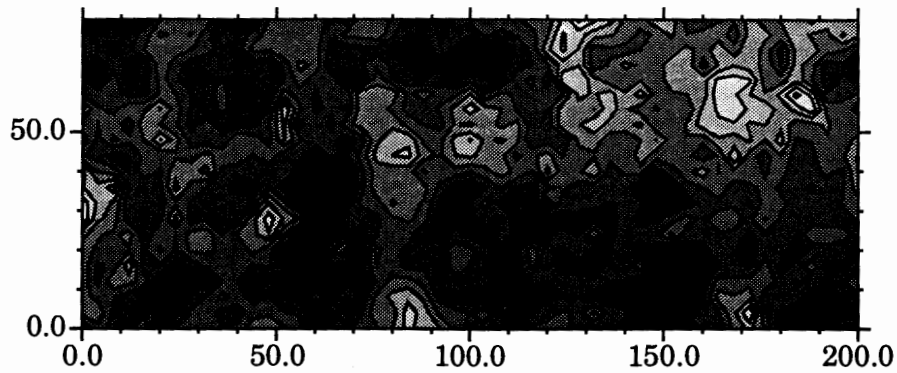
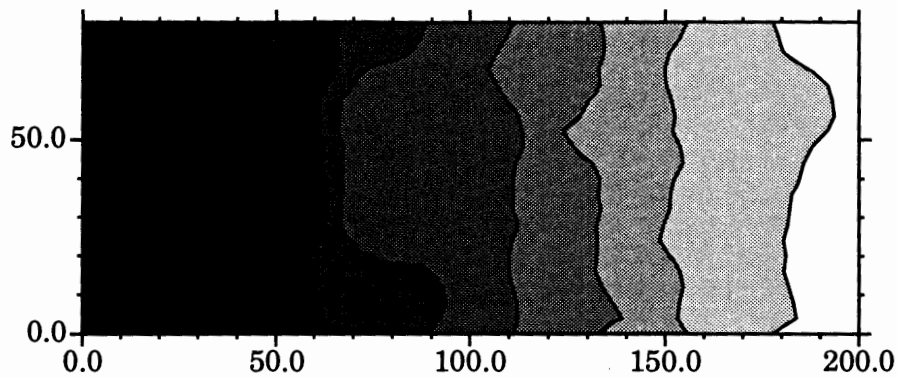


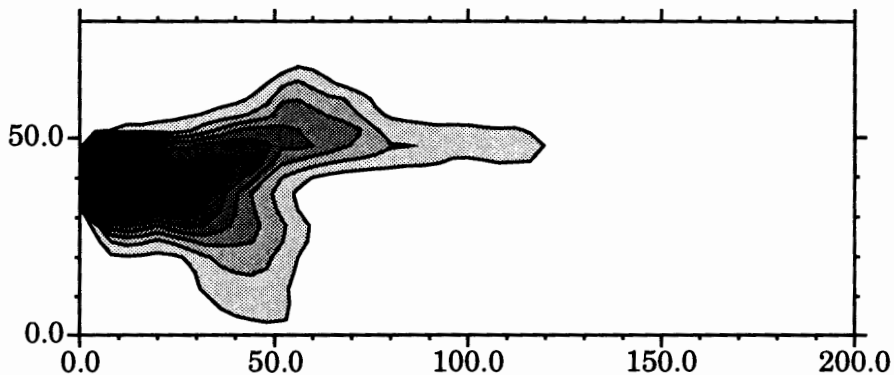
Figure 1-2: Permeability and porosity of cores collected at 1-ft intervals from borehole (IL056) in the Mt. Simon Aquifer in Illinois (data from Bakr, 1976)



(a)



(b)



(c)

Figure 1-3: Simulation of groundwater flow and solute transport through a synthetically generated random hydraulic conductivity field (domain dimensions in m) . (a) Log_{10} hydraulic conductivity contours; (b) Corresponding hydraulic head contours (high head at left side); and (c) Corresponding solute concentration contours emanating from a continuous sources, plotted at 100 days after the start of injection. (Source: McLaughlin et al., 1993)

There are many ways to characterize a contaminated groundwater site. One direct way is to directly measure hydrogeological properties and contaminant concentrations. Field data collected this way are site specific and reflect actual field conditions. However, the amount of data that can be obtained are often limited because of the high cost in sampling. The limited field information, though very valuable, is seldom adequate to provide a complete synoptic picture of what is actually happening on the contaminated site.

An alternative way to characterize groundwater contamination is to utilize a mathematical model. Mathematical models are physically-based and reflect the underlying scientific principles that dictate space and time distribution of contaminant distribution in porous media. When a mathematical model is combined with field data, the model provides a systematic site characterization procedure that is site specific and scientifically defensible. Mathematical models have been increasingly applied for site characterization because of their generality and predictive capabilities. A mathematical model becomes particularly attractive for site managers and planners to evaluate and experiment with various proposed or hypothetical management options under realistic complex field conditions.

This thesis focuses on model based approaches for characterizing groundwater contamination. In particular, the thesis addresses the computational aspect of modeling solute transport and proposes new methods for predicting solute transport in strongly heterogeneous porous media.

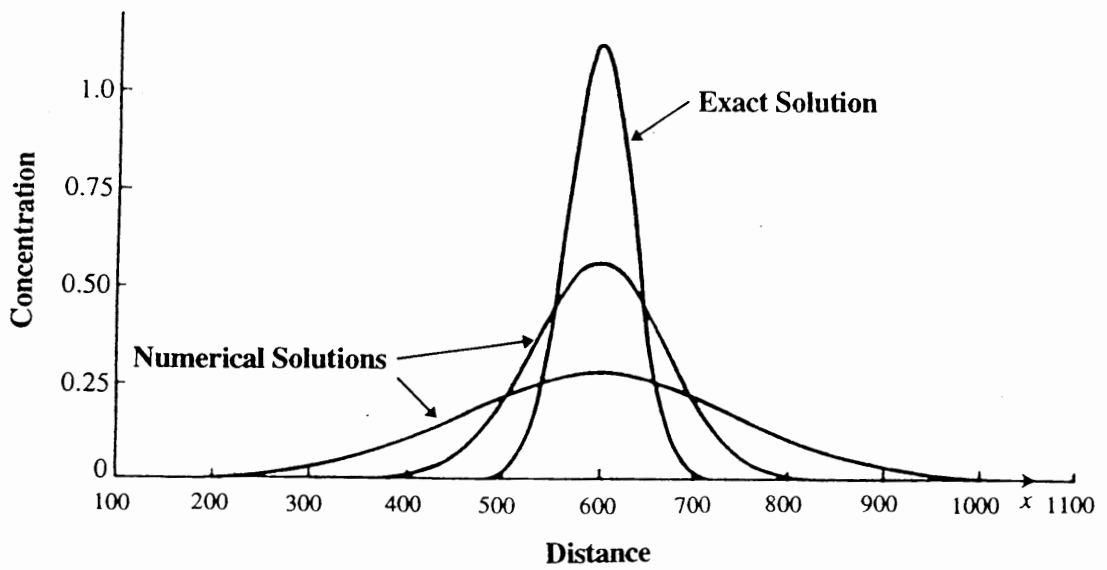
1.2. Literature Review

Because of the practical importance of contaminant transport problems and the well-known theoretical and computational difficulties associated with their solutions, an intense research effort has been devoted to this topic. Considerable attention may likely continue to be focused on this area in the immediate future.

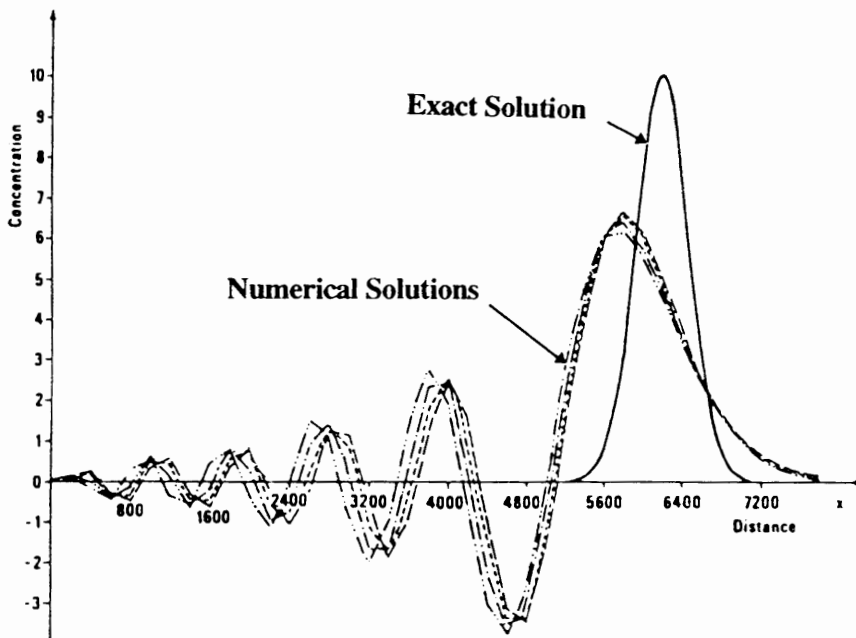
Numerical solution of the solute transport problem has been approached using various methods. These mainly include finite-difference methods, finite element methods, method of characteristics and random walk techniques. These methods are distinguished from one another depending on how the corresponding algebraic representation of the solute transport equation is derived.

The finite difference method was first applied to problems of groundwater flow and solute transport in the mid-1960s [Stone and Brain, 1963; Freeze and Witherspoon, 1966]. The classical finite difference method is probably the oldest and conceptually simplest of the numerical procedures. The finite difference method consists of discretizing the problem area into rectangular cells which are identified with discrete points or nodes. In general, the method contains an approximation of partial derivatives by algebraic expressions involving the values of the dependent variable at limited number of selected points [Bear and Verruijt, 1987]. Development of the approximations is generally done using Taylor series expansion about each point. A set of approximating algebraic equations thereby replaces the original continuous solute transport equation. However, since the Taylor-series formulation based on term-by-term difference approximation largely ignores the character of the solute transport equation, an accurate term-by-term finite difference analog for a partial differential equation does not necessarily lead to higher accuracy for the differential equation [Roache, 1972].

Early finite difference models of the solute transport equation often relied on conventional second-order finite difference approximation. The truncation error in using a second-order finite difference approximation for the advection term, or the first order spatial derivative, introduces spurious oscillations in the numerical solution of the solute transport model. The oscillations can be controlled if upwind (backward) difference is introduced, however, at the expense of numerical diffusion. This phenomenon refers to artificial diffusion which involves errors of the order of magnitude of the second order derivative. The numerical diffusion can be sometimes much larger than the actual physical diffusion, leading to erroneous solution. These numerical problems become especially bad



(a). Numerical Diffusion



(b). Numerical Oscillation

Figure 1-4: Concentration profiles for one-dimensional transport of a pulse source obtained with typical finite-difference methods (Source: Leendertse, 1970)

when the velocity field is heterogeneous [Dagan, 1990] and in those regions with sharp concentration gradients where advection dominates [Price, et al, 1968]. Figure 1-4 presents a graphical illustration of these notorious numerical problems associated with the traditional finite difference method. Some higher order finite difference methods such as the upwind type finite difference methods used QUICK (Quadratic Upstream Interpolation for Convective Kinematics) and QUICKEST [Leonard and Noye, 1990; Chen and Falconer, 1992] were developed to reduce the numerical errors. However, these methods are still often plagued by numerical diffusion or oscillation.

Traditional finite element methods, though much more flexible in handling complex geometries and boundary conditions, are very similar to finite difference methods and share similar numerical characteristics. All the numerical problems encountered in the finite difference solutions often also show in finite element method solutions. In fact, in the case of one dimensional problems, it can be shown that finite element and finite difference method in many situations are identical [Leon and Pinder, 1982].

There are several ways to avoid, or at least to reduce, numerical dispersion in conventional finite difference or finite element method solutions. Mathematically, the obvious solution is to use spatial steps and time steps that are sufficiently small, so that the numerical dispersion is small compared to the physical one. This may not be always feasible from a practical point of view. Note that physical dispersion in porous media can be written, at least as first approximation, as the product of a characteristic dispersivity and a characteristic mean velocity. In a typical porous medium, say a sandy aquifer, the dispersivity for pore scale solute transport is of the order of mean particle size. Obviously it is not realistic, from an engineering point of view, to use a mesh size which is small compared to the sizes of particles. Recent investigations show that physical dispersion tends to increase with the overall problem scale, possibly because of large-scale inhomogeneities in the soil (see Gelhar 1993 for a review on the effect heterogeneity on solute dispersion), these numerical limitations may still remain since grid spacing (and thus grid Peclet number) generally increases with the overall problem scale.

Suggested by the special structure of the advection-dominated transport equation, the modified method of characteristics (MMOC) becomes a choice of many of the more recent solute transport models [e.g., MT3D developed by Zheng 1991 and MOC developed for US Geological Survey]. The MMOC method overcomes some of the difficulties, which conventional finite difference and finite element methods encounter, by decoupling the advective part and the dispersive part in the transport equation and solving them successively. The MMOC approximates the advective component of the transport using backward particle tracking, while treating the dispersion and other terms with a standard finite-difference or finite-element method. The accuracy and efficiency of the MMOC approach is, however, strongly influenced by the particle tracking scheme used. When Courant numbers are large and flow field is strongly nonuniform, particle tracking can become increasingly inaccurate and problematic and often leads to considerable mass balance error [Li and Venkataraman, 1992]. The accuracy of MMOC also strongly depends on backward concentration interpolation, especially when the number of time steps is large as in a longer term simulation. This is because concentration interpolation is necessary at every successive time step and the interpolation error introduced is accumulative over time. The commonly used linear interpolation [Li et al., 1992; Neuman, 1981; Neuman and Sorek, 1982; Douglas and Tussell, 1982; Wheeler and Dawson, 1988; Chiang, et al., 1989] can still lead to significant numerical diffusion [Roache, 1972; Huffenus and Khaletzky, 1981]. Quadratic interpolation [Douglas and Russell, 1982; Baptisa et al., 1984; Roache, 1972; Huffenus and Khaletzky, 1981] reduces numerical damping somewhat but can introduce spurious oscillations [Roache, 1972; Huffenus and Khaletzky, 1981]. High-order interpolation techniques based on more interpolating nodes [Martin, 1975] can reduce numerical diffusion further but may introduce even more severe oscillations [Holly and Preissmann, 1977]. Hermit interpolation technique [Holly and Preissman, 1977; Fischer, 1977] achieves good accuracy at the expense of increased computational effort [Huffenus and Khaletzky, 1981].

The random walk methods have recently become one of the most popular methods for solving solute transport problems [Prickett et al., 1981; Kinzelbach, 1988; Uffink,

1988]. This method is conceptually simple and differs from the previous methods in that it is not a direct numerical solution of the differential equation. In random walk method, the solute source is represented as a collection of particles. These particles are assumed to transport with the groundwater flow. To represent the convective dispersive transport, one keeps track of the coordinates of each particle based on the given mean velocity field modified by adding a random velocity component whose statistics are related to physical dispersion coefficient [Bear and Verruift, 1987]. To determine the concentration in a mesh, one divides the sum of the mass of the particles by the volume of water in the mesh. For this reason, the random walk method does not suffer from numerical diffusion [Bear and Verruift, 1987]. Nevertheless, the price paid for the suppression of numerical dispersion is the random fluctuation of computed concentrations, especially when they are low. Fluctuations can be diminished by increasing the number of particles used. Therefore the random walk method remains, at reasonable computational effort, a relatively crude method as far as the estimation of local concentrations is concerned. Besides, the random walk method can not be applied to the simulation of non-conservative chemical plumes [Tompson and Gelhar, 1990; Uffink, 1985].

To remedy these difficulties, recently, Chen and his co-workers developed an analytically-based numerical approach, or the so called finite-analytic method for solving transport problems [Chen and Li, 1979; Chen and Chen, 1982; Choi and Chen, 1985; Wung and Chen, 1989; Li et al. 1992; and Hwang et al., 1985]. The basic idea of the finite analytic method is to utilize a local analytic solution in a discretized computational element to obtain the algebraic representation of the governing partial differential equation. The approach is novel and it explicitly and systematically takes into account the character of the differential equation in developing the numerical representation. The finite analytic method has been applied to solve a range of fluid flow and heat transfer problems [Chen and Li, 1979; Chen et al., 1981; Wung and Chen, 1989; and Tsai et al., 1993] and very recently, to solute transport problems [Li et al., 1992; and Hwang and Chen, 1985]. However, as will be discussed and demonstrated in this thesis, the existing versions of the finite analytic method, though conceptually attractive, still suffer from the following major

problems and limitations when applied to multi-dimensional problems: (1) the existing finite analytic formulation is complex and inefficient because of the way the local approximate analytical solution is derived; (2) the existing finite analytic solution still suffers, though to a less degree, from numerical diffusion because of the approximate boundary value approximation used in the local analytical solution; (3) one will have difficulties in evaluating the analytic coefficients when Peclet number is greater than 120 because of the limitation of current computers; (4) the existing finite analytic solution for transient transport suffers from severe numerical dispersion because of the inadequate hybrid finite difference approximation for the temporal derivative.

1.3. Objective and Scope of Work

This thesis focuses on finite analytic methods for solving solute transport problems. In particular, the thesis addresses the issues and limitations above, extends and refines finite analytic methods for predicting steady and unsteady solute transports in multiple dimensions in strongly heterogeneous velocity fields.

After the introduction, the thesis is organized in six chapters as follows. In Chapter 2, the principle of the finite analytic method is introduced and illustrated with an one-dimensional steady transport example. Potential problems and difficulties with the existing finite analytic methods are described and discussed. Chapter 3 presents improved finite analytic methods for steady transport problems. Chapter 4 presents improved finite analytic methods for solving unsteady solute transport problems. Chapter 5 demonstrates, with examples and applications, the performance of the improved finite analytic methods. Finally, Chapter 6 concludes the thesis by summarizing the original contribution of this research, and limitations and assumptions which suggest direction for future work.

Chapter 2

Critical Review of Existing Finite Analytic Methods

This chapter presents and critically reviews the existing finite analytic methods for solving solute transport problems.

2.1. Basic Idea of Finite Analytic Methods

The finite analytic method differs from conventional numerical methods in that it does not tamper with the differentials or the derivatives of the governing equation, nor does the analytic method need the shape function which is made to satisfy the integral form of the governing equation. The finite analytic method incorporates the local analytical solution in the numerical solution of linear or linearized partial differential equations. In the finite analytic method, the solution domain is first discretized and the governing equation approximated as a differential equation with constant coefficients in a local computational element. The local differential equation is then solved analytically. The resulting analytical solution is then expressed in an algebraic form and overlapped to cover the entire region of the problem. The assembly of these local analytic solutions results in a system of linear algebraic equations. The system of algebraic equations is then solved to provide the numerical solution of the total problem.

2.2. Illustrative Example: One-Dimensional Steady Transport

In this section, a simple one-dimensional example is used to illustrate the fundamental concept behind the finite analytic method and its relationship with the conventional finite difference methods.

Consider steady solute transport in a uniform velocity field. The governing equation is:

$$u(x) \frac{\partial C}{\partial x} = \frac{\partial}{\partial x} \left[D(x) \frac{\partial C}{\partial x} \right] \quad (2.1)$$

where x is the spatial Cartesian coordinate, $u(x)$ is the advective velocity, $D(x)$ is the diffusion coefficient, and C is the solute concentration.

Equation (2.1) must be solved numerically since velocity and dispersion coefficient are spatially variable. Discretizing the solution domain as shown in Figure 2-1, and

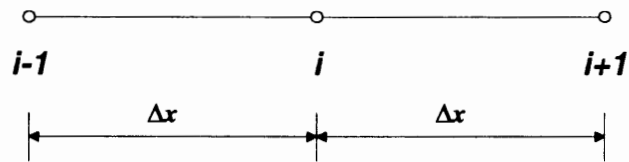


Figure 2-1: Local element for one-dimensional problem

assuming, as in all standard numerical procedures, that velocity and dispersion coefficients can be approximated as locally constant,

$$u(x) = u(x_i) = u_i, \quad x_{i-1} < x < x_{i+1} \quad (2.2)$$

$$D(x) = D(x_i) = D_i, \quad x_{i-1} < x < x_{i+1} \quad (2.3)$$

The governing equation can then be approximated locally as

$$u_i \frac{\partial C}{\partial x} = D_i \frac{\partial^2 C}{\partial x^2} \quad (2.4)$$

2.2.1. Conventional Finite Difference Approximations

In a traditional explicit finite difference method (2.4) is “solved” approximately using Taylor series expansions and leads to a local algebraic representation of the following general form:

$$C_i = \alpha_i C_{i-1} + \beta_i C_{i+1} \quad (2.5)$$

where the coefficients α_i and β_i are

$$\alpha_i = \frac{Pe_i + 2}{4}$$

$$\beta_i = \frac{2 - Pe_i}{4} \quad (2.6)$$

if a central difference scheme is used to approximate the advection portion of (2.4); and

$$\alpha_i = \frac{Pe_i + 1}{Pe_i + 2}$$

$$\beta_i = \frac{1}{Pe_i + 2} \quad (2.7)$$

if an upwind (or backward) difference scheme is used to approximate the advection term.

The symbol Pe_i , referred to as grid Peclet number, is defined as

$$Pe_i = \frac{u_i \Delta x}{D_i} \quad (2.8)$$

The grid Peclet number is dimensionless and represents the relative magnitude of advection versus dispersion.

These finite difference schemes are known to be problematic and can lead to either spurious oscillations or artificial diffusion when advection dominates or when grid Peclet number is large. This is because the truncation error involved in these schemes increases as the grid Peclet number increases. Using Taylor series expansion approach, the central difference equation (2.6) can be derived to an equation with a differential form.

$$D_i \frac{\partial^2 C}{\partial x^2} = u_i \frac{\partial C}{\partial x} + \frac{u_i \Delta x^2}{6} \frac{\partial^3 C}{\partial x^3} + O(\Delta x^3) \quad (2.9)$$

where $O(\cdot)$ reads as “of the order of”.

Thus solving equation (2.6) is in fact equivalent to solving the following modified differential equation. The exact solution of (2.9) is known to be oscillatory when the third order derivative term is significant. Similarly, a modified differential equation for upwind difference equation (2.7) can be obtained

$$u_i \frac{\partial C}{\partial x} = \left(D_i + \frac{u_i \Delta x}{2} \right) \frac{\partial^2 C}{\partial x^2} + O(\Delta x^3) \quad (2.10)$$

Equation (2.10) is of the same form as the original advection dispersion equation but with an additional "numerical" diffusion coefficient term that increases with grid size and magnitude of advective velocity.

2.2.2 Finite Analytic Approximation

The numerical problems illustrated above are caused by error introduced by the truncated Taylor series expansion. These problems can be avoided if (2.4) is solved analytically. Analytical solution is possible because what is sought here is a local representation of the original differential equation. In a local element the governing

equation has been approximated as a differential equation with constant coefficients. So solving (2.4) analytically, yields

$$C(x) = a + b e^{\frac{u_i}{D_i}(x-x_i)} \quad (2.11)$$

where a and b are integration constants, and can be determined by imposing the following local boundary conditions

$$C(x_{i+1}) = C_{i+1} \quad (2.12)$$

$$C(x_{i-1}) = C_{i-1} \quad (2.13)$$

Using (2.12) in (2.13) and solving for the coefficients a and b , in terms of the nodal concentrations, gives

$$a = \frac{C_{i-1} e^{Pe_i} - C_{i+1} e^{-Pe_i}}{e^{Pe_i} - e^{-Pe_i}} \quad (2.14)$$

$$b = \frac{C_{i-1} - C_{i+1}}{e^{Pe} - e^{-Pe}} \quad (2.15)$$

Substituting (2.14) and (2.15) into (2.11) and evaluating the concentration at the mid nodal point, $x = x_i$, (2.11) reduces to an identical finite difference equation as given in (2.5), but with the following modified coefficients

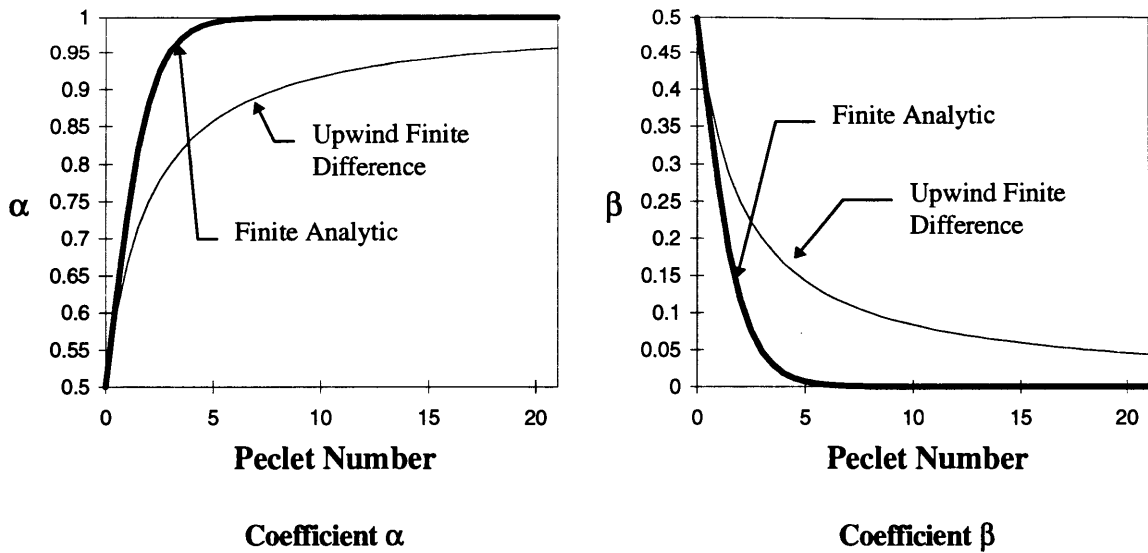
$$\alpha_i = \frac{e^{Pe_i}}{e^{Pe_i} + 1}$$

$$\beta_i = \frac{1}{e^{Pe_i} + 1} \quad (2.16)$$

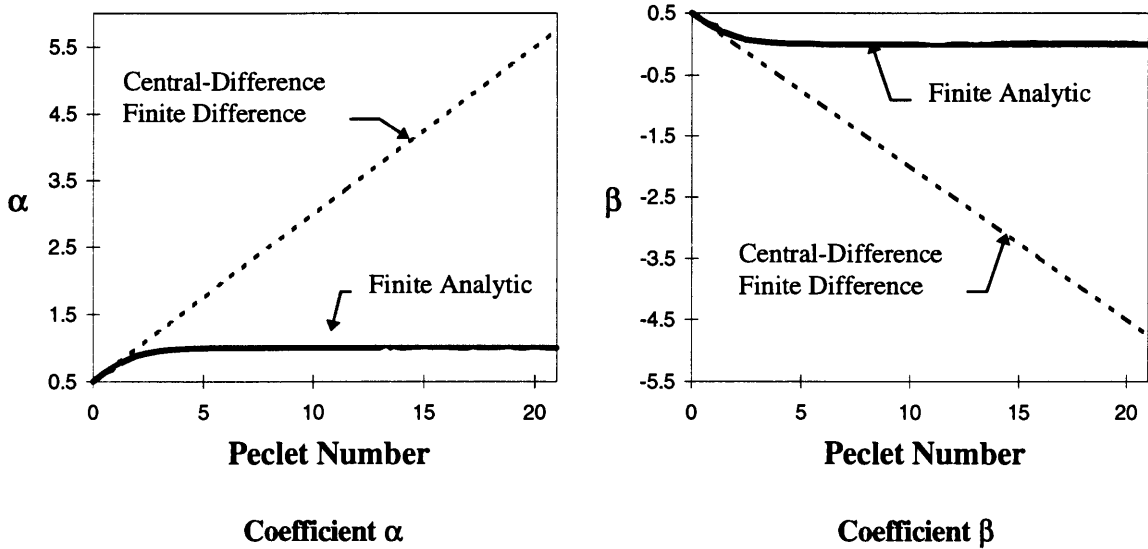
2.2.3. Discussion and Comparison

These analytically derived coefficients in (2.16) are referred to as finite analytic coefficients. Equation (2.5) based on the finite analytic coefficients is called finite analytic method.

Equation (2.5) shows that concentration at $x = x_i$ in a local computational element is a weighted average of concentration at the two neighboring nodes. The coefficients α_i and β_i can also be regarded as weighting factors or influence coefficients that characterize the influence on concentration at mid point ($x = x_i$) from both upstream and downstream neighboring concentrations. Figure 2-2 shows graphically how the coefficients α_i and β_i vary with the grid Peclet number for the finite analytic method as well as the upwind and central difference methods. In all cases, α_i and β_i add up to unity, with α_i always greater or equal to β_i , reflecting the fact that "information" propagates from upstream and concentration at the upstream node at $x = x_{i-1}$ has more influence on C_i than concentration downstream, and the upstream influence increases as Peclet number increases. However, upwind scheme underestimates α_i or the upstream influence and overestimates the downstream influence, as a result, leading to numerical diffusion. Like the finite analytic coefficients, the two weighting factors of upwind scheme are always positive and add up to unity, the resulting solution is always a physically realistic solution. On the other hand, the central difference method grossly overestimates the upstream influence and underestimates the downstream influence. In fact, the downstream coefficient β_i becomes negative when the Peclet number exceeds 2 and approaches minus infinity as the Peclet number approaches infinity. A negative β_i value means that a decrease (or increase) of concentration at $x = x_{i+1}$ in a local element will cause concentration at the mid point to increase (or decrease). Because of this, a central difference scheme may lead to a physically unrealistic solution when Peclet number exceeds two.



(a). Comparison of finite analytic and upwind finite difference methods



(b). Comparison of finite analytic and central-difference finite difference methods

Figure 2-2: Numerical coefficients as functions of pecelet numbers

The finite analytic coefficients in fact reduces to the coefficients derived from finite difference methods when advection is relatively weak. In the case that the grid Peclet number is small, e^{Pe_i} in (2.16) can be expanded as

$$e^{Pe_i} = 1 + Pe_i + O(Pe_i^2) \quad (2.17)$$

Using (2.17) in (2.6), yields

$$\alpha_i = \frac{e^{Pe_i}}{1 + e^{Pe_i}} = \frac{1 + Pe_i + O(Pe_i^2)}{1 + [1 + Pe_i + O(Pe_i^2)]}$$

$$\beta_i = \frac{1}{1 + e^{Pe_i}} = \frac{1}{1 + [1 + Pe_i + O(Pe_i^2)]} \quad (2.18)$$

Retaining only the first order term, (2.16) can be reduced to (2.7) derived using upwind difference method. If one further makes use of the following expansion

$$\frac{1}{1 + Pe_i} = 1 - Pe_i + Pe_i^2 - Pe_i^3 + \dots \quad (2.19)$$

Then the equation (2.18) reduces to the coefficients derived from central difference method as given in (2.6).

The analysis presented above clearly demonstrates the advantage of the finite analytic method and its relationship with the conventional finite difference methods.

2.3. Basic Formulation of Finite Analytic Method for Multi-Dimensional Transport

The usefulness of any newly developed numerical methods for solving groundwater transport problems lies in its extendibility to multi-dimensional problems since real world groundwater transport is inherently multi-dimensional. Chen and Chen [1982] extended the finite analytic method to two dimensional steady state transport and applied to a wide range of fluid flow and heat transfer problems . In this section the basic formulation is briefly reviewed and the problems and limitations are discussed.

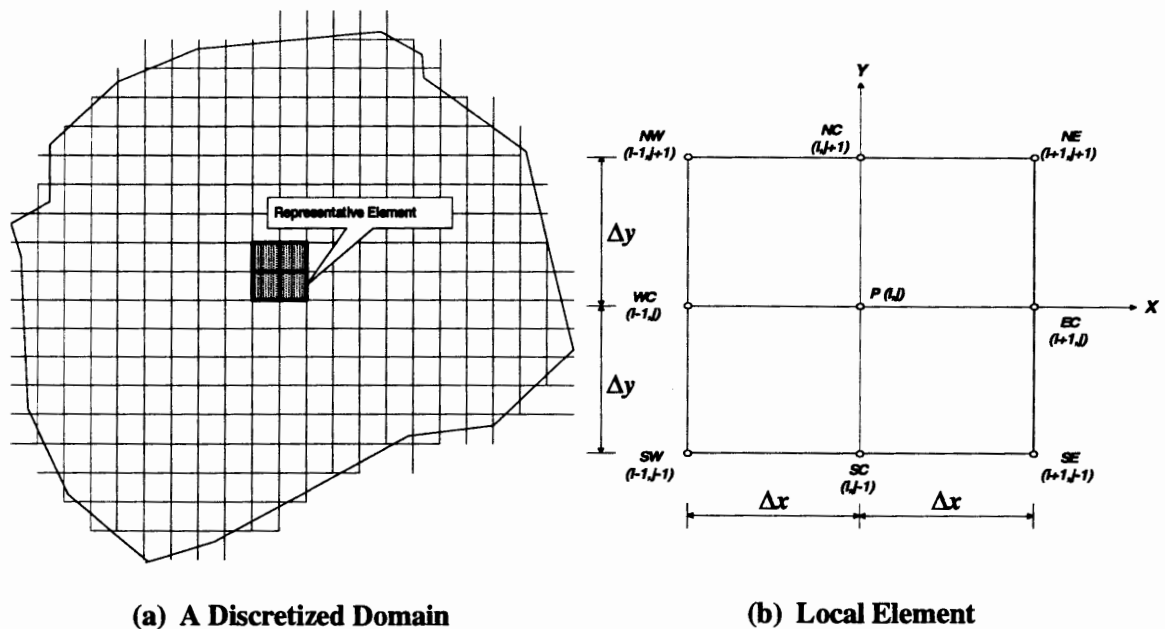


Figure 2-3: A discretized domain and local element of the finite analytic method

For illustration purpose, consider steady transport of a conservative solute in a variable velocity field. The governing equation is

$$u(x, y) \frac{\partial C}{\partial x} + v(x, y) \frac{\partial C}{\partial y} = \frac{\partial}{\partial x} \left[D(x, y) \frac{\partial C}{\partial x} \right] + \frac{\partial}{\partial y} \left[D(x, y) \frac{\partial C}{\partial y} \right] \quad (2.20)$$

where x and y are Cartesian spatial coordinates, $u(x,y)$ and $v(x,y)$ are advective velocities, $D(x,y)$ is diffusion coefficient and is function of x and y , and C is a dependent solute concentration.

Let the boundary conditions be specified so that the problem is well-posed (solution exists, and the solution is unique and stable). The domain is subdivided into small rectangles as shown in Figure 2-2(a). A representative local element (see Figure 2-2(b)) with central node P or (i,j) has neighboring nodes points $SW (i-1,j-1)$, $WC (i-1,j)$, $NW (i-1,j+1)$, $SC (i,j-1)$, $NC (i,j+1)$, $SE (i+1,j-1)$, $EC (i+1,j)$, and $NE (i+1,j+1)$. The grid spacings in both x and y directions are set to be uniform, which are Δx and Δy respectively. An analytic solution can be obtained for the local element as a function of the boundary conditions

$$C(x, y) = f[C_N(x), C_S(x), C_E(y), C_W(y), \Delta x, \Delta y, x, y] \quad (2.21)$$

where $C_N(x)$, $C_S(x)$, $C_E(y)$ and $C_W(y)$ are, respectively, the northern, southern, eastern, and western boundary conditions of the element. Numerically, boundary functions C_N , C_S , C_E and C_W may be approximated in terms of the nodal values along the boundary, for example, $C_N = C_N(C_{NW}, C_{NC}, C_{NE}, x)$.

The natural solution to (2.20) suggests that an exponential and linear function in terms of the three nodal values on each boundary may be employed to obtain the approximated boundary conditions for the local element [see Chen and Chen, 1982 for details]. In the local element as shown in Figure 2-2 (b), the south boundary condition, where y is fixed, can be approximated by

$$C_S(x) = a_s(e^{2Ax-1} - 1) + b_s x + c_s \quad (2.22)$$

where

$$A = \frac{1}{2} \frac{u_{i,j}}{D_{i,j}} \quad (2.23)$$

and

$$a_s = \frac{C_{SE} + C_{SW} - 2C_{SC}}{4 \sinh^2 A \Delta x}$$

$$b_s = \frac{1}{2 \Delta x} [C_{SE} - C_{SW} - (C_{SE} + C_{SW} - 2C_{SC}) \coth(A \Delta x)]$$

$$c_s = C_{SC} \quad (2.25)$$

and u_{ij} , v_{ij} and D_{ij} are local values evaluated at node P .

The boundary conditions for north, east and west sides, i.e., $C_N(x)$, $C_E(y)$, and $C_W(y)$ can be similarly approximated by exponential and linear boundary functions. The linear advective transport equation (2.20) with boundary conditions $C_S(x)$, $C_N(x)$, $C_E(y)$, and $C_W(y)$ is then solved analytically by the method of separation of variables. The local analytic solution, when evaluated at the interior point P of the rectangular local element, gives a finite analytic algebraic equation relating the interior nodal value C_P and its 8 neighboring nodal values as

$$C_P = a_{NE} C_{NE} + a_{NW} C_{NW} + a_{SE} C_{SE} + a_{SW} C_{SW} + a_{EC} C_{EC} + a_{WC} C_{WC} + a_{SC} C_{SC} + a_{NC} C_{NC} \quad (2.26)$$

The finite analytic coefficients are

$$\begin{aligned} a_{NE} &= e^{-A \Delta x - B \Delta y} E, & a_{NW} &= e^{A \Delta x - B \Delta y} E \\ a_{SE} &= e^{-A \Delta x + B \Delta y} E, & a_{SW} &= e^{A \Delta x + B \Delta y} E \\ a_{NC} &= e^{-B \Delta y} (EA), & a_{SC} &= e^{B \Delta y} (EA) \end{aligned}$$

$$a_{EC} = e^{-A\Delta x} (EB) \quad , \quad a_{WC} = e^{A\Delta x} (EB) \quad (2.28)$$

where

$$E = \frac{1}{4 \cosh(A\Delta x) \cosh(B\Delta y)} - A\Delta x \coth(A\Delta x) E_2 - B\Delta y \coth(B\Delta y) E'_2 \quad (2.29)$$

$$EA = 2A\Delta x \cosh(A\Delta x) \coth(A\Delta x) E_2 \quad (2.30)$$

$$EB = 2B\Delta y \cosh(B\Delta y) \coth(B\Delta y) E'_2 \quad (2.31)$$

and

$$E_2 = \sum_{m=1}^{\infty} \frac{-(-1)^m (\lambda_m \Delta x)}{\left[(A\Delta x)^2 + (\lambda_m \Delta x)^2 \right]^2 \cosh\left(\sqrt{A^2 + B^2 + \lambda_m'^2} \Delta x \right)} \quad (2.32)$$

$$E'_2 = \frac{\Delta x^2}{\Delta y^2} E_2 + \frac{A\Delta y \tanh(B\Delta y) - B\Delta x \tanh(A\Delta x)}{4AB\Delta y^2 \cosh(A\Delta x) \cosh(B\Delta y)} \quad (2.33)$$

with

$$B = \frac{1}{2} \frac{v_{i,j}}{D_{i,j}} \quad (2.34)$$

$$\lambda_m \Delta x = \left(m - \frac{1}{2}\right)\pi \quad , \quad \lambda'_m \Delta y = \left(m - \frac{1}{2}\right)\pi \quad (2.35)$$

The existing finite analytic method exhibits a gradual upwind shift, which is considerably better than those given by conventional finite difference and finite element

methods. Its solution, because of the analytic nature of the solution for the well-posed problem, is stable and relatively accurate. However, disadvantages can still be found in the existing finite analytic methods.

2.4. Problems and Limitations of Existing Finite Analytic Methods

2.4.1. Computational Efficiency

The existing finite analytic coefficients in the finite analytic algebraic equation are obtained from the analytic solution. The coefficients include one or more terms of summation series, which are considered to be time-consuming to evaluate. This problem becomes more severe when the flow field is highly variable, since for each node, calculation of the summation series has to be done individually in order to capture the plume for the changing velocities. In general, the summation E_2 may need 10 to 25 terms; but with larger Peclet number, the number of summation series will be higher. Furthermore, the situation will be even worse when the finite analytic solution is extended to dynamic problems. Because at each time step, the computer has to calculate the summation terms node-by-node; if the number of time steps is large, this computing process will become very messy. However, as will be discussed in later chapters, improvements can be made to reduce the complexity of the formulation and the computational expense for both steady and unsteady problems.

The finite analytic method is not popular not only due to the complexity of the formulations, but also because of the difficulties in evaluating the analytic coefficients. The following section explains these difficulties in the existing finite analytic methods.

2.4.2. Difficulties in Evaluating Finite Analytic Coefficients

There are many ways to approximate the boundary conditions in the finite analytic method. However, as mentioned above, the exponential and linear boundary approximation is recommended in the existing finite analytic methods because there is only one summation term in the finite analytic coefficients. The formulation of this method is

still complex due to the effort of solving the advection-diffusion equation analytically for both advection and diffusion terms. The calculation of the finite analytic coefficient also requires a great deal of computational time. Therefore the evaluation is expensive.

While the finite analytic solution is accurate, the computation of finite analytic coefficients demands the accurate summation of a series with alternately positive and negative terms of large exponential values when the Peclet number is large. When the local Peclet numbers are moderate such as $Pe_x=50$, $Pe_y=50$, most computers do not have difficulty in evaluating E_2 (or E'_2) given in equation (2.32) or (2.33). However, when both Pe_x and Pe_y become large, calculation of the summation E_2 (or E'_2) will require to tabulate terms with large exponential value and to sum terms with alternate terms. A serious

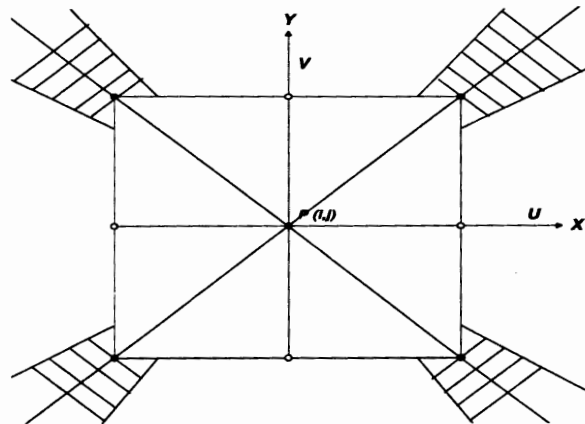


Figure 2-4: Inaccuracy of finite analytic coefficients in cross-hatched region

consequence will lose more and more digit in the summation of E_2 , i.e. subtractive cancellations will occur. Thus Pe_x and Pe_y become greater than 120, the computed results give erroneous values. This kind of error is especially large on the order of 20% for the largest finite analytic coefficient along the lines when $v\Delta x/u\Delta y = \pm 1$ [Zhang and Chen, 1987]. The cross-hatched part in Figure 2-4 shows the region where the existing finite analytic coefficient is not accurate enough. Therefore, when highly variable velocity fields are encountered where there are large local Peclet numbers, the finite analytic solution

loses its accuracy or even has computer floating-point errors. Besides, the finite analytic exponential and linear approximation method can not handle pure advection transport problems because the dispersion coefficient is in the denominator.

2.4.3. Boundary Approximations

Another problem occurs in the existing finite analytic methods is the boundary approximations. In the finite analytic solution, the only source of numerical errors is introduced by boundary approximations. Boundary approximations can be obtained by other approximation functions, besides the exponential and linear boundary approximation function. Some alternative and simpler boundary approximations can be used as boundary conditions. They are, for example, second-order polynomial and piece-wise linear boundary approximations.

All these three existing finite analytic formulations exhibit a gradual upwind shift when advective velocities become large. Both finite analytic formulations based on exponential and linear boundary approximation and piecewise linear boundary approximation give all-positive finite analytic coefficients for the range of advective velocities. But negative analytic coefficients are found in finite analytic formulation based on second-order polynomial boundary approximation when Peclet number becomes large. These negative finite analytic coefficients, although small, are physically unrealistic. The finite analytic solution based on piecewise linear boundary approximation overestimates the diffusion effect at the corner due to the less accurate piecewise linear boundary approximation.

The formulations based on second-order polynomial boundary approximation and piecewise-linear boundary approximations have three summation series terms respectively. Therefore, the finite analytic formulation based on exponential and linear boundary approximation is recommended.

2.4.4. Transient Extensions

Theoretically, the finite analytic exponential and linear solution can provide accurate and stable results. The finite analytic method has been tested to be superior to conventional finite difference and finite element methods [Chen and Chen, 1982]. However, in the development of the formulation for the unsteady problems, the temporal term is handled by using finite difference method [Chen and Chen, 1982]. At each time level, the steady-state finite analytic solution is used to solve the advection-diffusion equation analytically.

Although the finite analytic method is an accurate numerical method, the finite difference method, unfortunately, gives relatively inaccurate results. Experience by Li et al. [1992] shows that a good space approximation needs to be applied with a good temporal approximation in order to obtain satisfactory results. An old saying of “A chain is only as strong as the weakest link” summarizes the use of the hybrid method using the finite analytic method for the steady portion of the partial differential equation and the finite difference method for the temporal portion.

A space-time accurate method will be presented in Chapter 4, where finite analytic/Laplace transform hybrid method is used to obtain stable and accurate results for transient solute transport problems when advection dominates.

Chapter 3

Improved Finite Analytic Methods for Steady Transport

This chapter addresses the issues raised in Chapter 2 and presents the accurate, efficient and robust finite analytic methods for solving the advection-dominated diffusion transport equation.

3.1. Governing Equation

Consider two-dimensional steady-state reactive contaminant transport in heterogeneous porous media. The governing equation is

$$u(x, y) \frac{\partial C}{\partial x} + v(x, y) \frac{\partial C}{\partial y} = \frac{\partial}{\partial x} \left[D_x(x, y) \frac{\partial C}{\partial x} \right] + \frac{\partial}{\partial y} \left[D_y(x, y) \frac{\partial C}{\partial y} \right] - \lambda(x, y)C + S(x, y) \quad (3.1)$$

where u and v are advective velocities in x and y directions respectively, D_x and D_y are the diffusion coefficients, λ is the first-order decay constant, and S is the external source/sink term, C is the solute concentration. For heterogeneous porous media, the coefficient and parameter in (3.1) are generally spatial variable. Also, the flow and transport domain are usually bounded and irregular, thus (3.1) has to be solved numerically.

3.2. Approximation of Local Analytic Solution

3.2.1. Approximation of Diffusion Terms

As in conventional finite difference and existing finite analytic methods, the solution domain is first discretized as shown in Figure 2-3. Figure 3-1 shows a representative computational element centered at node (x_i, y_i) , where a typical interior

point P is surrounded by eight neighboring nodes. For illustration purpose and notational convenience, we assume uniform grid spacings Δx and Δy .

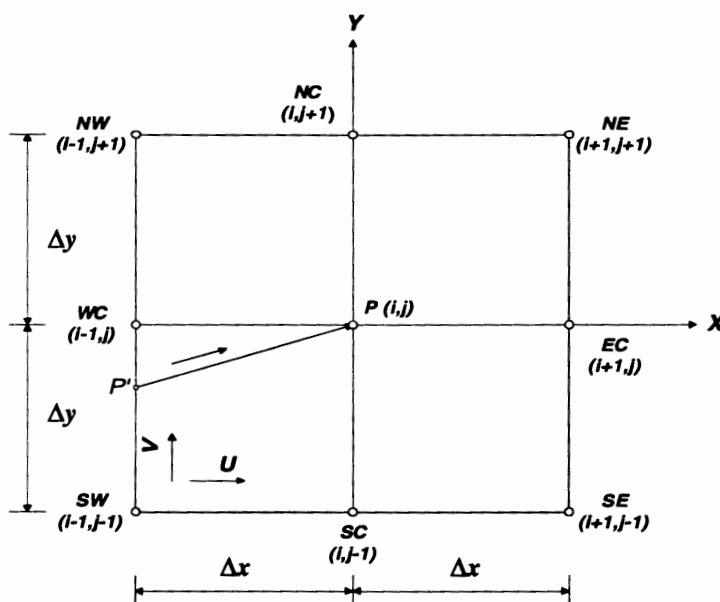


Figure 3-1: A computational element for finite analytic method with linear interpolation

In a local computational element, the coefficients and parameters in the governing equation vary little and can be approximated by locally constant values

$$\begin{aligned}
 u(x, y) &\approx u_{i,j}; & v(x, y) &\approx v_{i,j}; \\
 D_x(x, y) &\approx D_{x_{i,j}}; & D_y(x, y) &\approx D_{y_{i,j}}; \\
 \lambda(x, y) &\approx \lambda_{i,j}; \\
 S(x, y) &\approx S_{i,j}
 \end{aligned}
 \tag{3.2}$$

where $x_{i-1} \leq x \leq x_{i+1}$ and $y_{i-1} \leq y \leq y_{i+1}$. This assumption is also found in conventional numerical methods as well as in existing finite analytic methods. The local governing equation can then be written as

$$u_{i,j} \frac{\partial C}{\partial x} + v_{i,j} \frac{\partial C}{\partial y} = D_{x,i,j} \frac{\partial^2 C}{\partial^2 x} + D_{y,i,j} \frac{\partial^2 C}{\partial^2 y} - \lambda_{i,j} C + S_{i,j} \quad (3.3)$$

Equation (3.3) is a differential equation with constant coefficients defined on a simple rectangular element. The equation can be solved analytically given proper local boundary conditions. The resulting local analytical solution can be used to derive a local algebraic representation of the original differential equation. However, as discussed earlier, the analytically derived algebraic formulation is complex and involves infinite series which is difficult and expensive to evaluate. Careful examination of the solution procedure of (3.3) reveals that the elliptic diffusion terms make the analytical solution complicated. The analytical based numerical approaches were being developed. Because standard numerical methods have difficulty in approximating the hyperbolic advection terms. Standard finite difference or finite element methods can often accurately approximate diffusion type differential operators, or more generally differential operators which involve even order derivatives in the original partial differential equation. To exploit the advantages of the existing finite analytic methods and the standard numerical methods, the diffusion terms in the equation are first approximated locally by standard finite difference, and then the modified equation of (3.3) is solved analytically. Using a central-difference finite difference scheme, we get

$$\frac{\partial^2 C}{\partial x^2} \approx \frac{C_{i+1,j} - 2C_{i,j} + C_{i-1,j}}{\Delta x^2} \quad (3.4)$$

$$\frac{\partial^2 C}{\partial y^2} \approx \frac{C_{i,j+1} - 2C_{i,j} + C_{i,j-1}}{\Delta y^2} \quad (3.5)$$

Inserting (3.4) and (3.5) into (3.3), a modified equation of (3.3) is obtained locally as

$$u_{i,j} \frac{\partial C}{\partial x} + v_{i,j} \frac{\partial C}{\partial y} + \lambda_{i,j} C = (f_{x_{i,j}} + f_{y_{i,j}}) + S_{i,j} \quad (3.6)$$

where

$$f_{x_{i,j}} = D_{x_{i,j}} \frac{C_{i+1,j} - 2C_{i,j} + C_{i-1,j}}{\Delta x^2} \quad (3.7)$$

$$f_{y_{i,j}} = D_{y_{i,j}} \frac{C_{i,j+1} - 2C_{i,j} + C_{i,j-1}}{\Delta y^2} \quad (3.8)$$

Note that the numerically delicate advection and reaction terms in (3.3) are kept intact and retained in their original differential forms. Equation (3.6) is formally a hyperbolic differential equation and has the following analytical solution (see Appendix A for the detailed solution developing process).

$$C(x, y) = e^{\left[\frac{-\lambda_{i,j}}{\sqrt{u_{i,j}^2 + v_{i,j}^2}} \sqrt{(x-x_{p'})^2 + (y-y_{p'})^2} \right]} \left[C(x_{p'}, y_{p'}) - \frac{f_{x_{i,j}} + f_{y_{i,j}} + S_{i,j}}{\lambda_{i,j}} \right] + \frac{f_{x_{i,j}} + f_{y_{i,j}} + S_{i,j}}{\lambda_{i,j}} \quad (3.9)$$

where P' is where flowline (that passes the interior node P) intersects with local element boundaries (see Figure 3-1), $x_{p'}$ and $y_{p'}$ are local coordinates of P' .

Evaluating $C(x, y)$ at interior node P at $x = x_p$ and $y = y_p$, yields

$$C_{i,j} = e^{\frac{\lambda_{i,j} \Delta \eta}{U_{i,j}}} C_{p'} + \frac{f_{x_{i,j}} + f_{y_{i,j}} + S_{i,j}}{\lambda_{i,j}} \left(1 - e^{\frac{-\lambda_{i,j} \Delta \eta}{U_{i,j}}} \right) \quad (3.10)$$

where

$$U_{i,j} = \sqrt{u_{i,j}^2 + v_{i,j}^2} \quad (3.11)$$

$$\Delta\eta = \sqrt{\Delta x^2 + \Delta y^2 r_{i,j}^2} \quad \text{if } r_{i,j} \leq 1 \quad (3.12)$$

$$\Delta\eta = \sqrt{\frac{\Delta x^2}{r_{i,j}^2} + \Delta y^2} \quad \text{if } r_{i,j} > 1 \quad (3.13)$$

with

$$r_{i,j} = \left| \frac{v_{i,j} \Delta x}{u_{i,j} \Delta y} \right| \quad (3.14)$$

Substituting (3.7) and (3.8) into (3.10), and rearranging, the latter becomes

$$C_{i,j} = R_{p'} C_{p'} + R_x (C_{i+1,j} + C_{i-1,j}) + R_y (C_{i,j+1} + C_{i,j-1}) + R_{i,j} \quad (3.15)$$

where

$$R_0 = 1 + \left(\frac{2D_{x i,j}}{\lambda_{i,j} \Delta x^2} + \frac{2D_{y i,j}}{\lambda_{i,j} \Delta y^2} \right) \left(1 - e^{-\frac{\lambda_{i,j} \Delta \eta}{U_{i,j}}} \right) \quad (3.16)$$

$$R_{p'} = e^{-\frac{\lambda_{i,j} \Delta \eta}{U_{i,j}}} \frac{1}{R_0} \quad (3.17)$$

$$R_x = \frac{D_{x i,j}}{\lambda_{i,j} \Delta x^2} \left(1 - e^{-\frac{-\lambda_{i,j} \Delta \eta}{U_{i,j}}} \right) \frac{1}{R_0} \quad (3.18)$$

$$R_y = \frac{D_{y i,j}}{\lambda_{i,j} \Delta y^2} \left(1 - e^{-\frac{-\lambda_{i,j} \Delta \eta}{U_{i,j}}} \right) \frac{1}{R_0} \quad (3.19)$$

$$R_{i,j} = \frac{S_{i,j}}{\lambda_{i,j}} \left(1 - e^{-\frac{-\lambda_{i,j} \Delta \eta}{U_{i,j}}} \right) \frac{1}{R_0} \quad (3.20)$$

In the special case of non-reactive solution transport, $\lambda_{i,j} = 0$, (3.16) through (3.20) are reduced to, respectively

$$R_0 = 1 + \frac{2\Delta\eta}{U_{i,j}} \left(\frac{D_{x i,j}}{\Delta x^2} + \frac{D_{y i,j}}{\Delta y^2} \right) \quad (3.21)$$

$$R_{p'} = \frac{1}{R_0} \quad (3.22)$$

$$R_x = \frac{D_{x i,j} \Delta \eta}{U_{i,j} \Delta x^2} \frac{1}{R_0} \quad (3.23)$$

$$R_y = \frac{D_{y i,j} \Delta \eta}{U_{i,j} \Delta y^2} \frac{1}{R_0} \quad (3.24)$$

$$R_{i,j} = \frac{S_{i,j} \Delta \eta}{U_{i,j}} \frac{1}{R_0} \quad (3.25)$$

Here L'Hospital Rule is applied to evaluate the following limit in the process of deriving the above equations

$$\lim_{\lambda_{i,j} \rightarrow 0} \frac{1 - e^{-\frac{\lambda_{i,j} \Delta \eta}{U_{i,j}}}}{\lambda_{i,j}} = \lim_{\Delta \eta \rightarrow 0} \frac{\left(1 - e^{-\frac{\lambda_{i,j} \Delta \eta}{U_{i,j}}}\right)'}{(\lambda_{i,j})'} = \frac{\Delta \eta}{U_{i,j}} \quad (3.26)$$

Equation (3.15) provides a new analytically derived local algebraic representation of the partial differential equation given in (3.3). The algebraic equation applies for all interior nodal points in the flow domain.

However, that (3.15) involves a non-nodal concentration value $C_{P'}$, which must be approximated in terms of nodal concentrations before the equation can be used as a normal numerical scheme for solving nodal concentrations throughout the discretized domain.

3.2.2. Linear Interpolation Boundary Approximation

The simplest way to approximate the non-nodal concentration at P' is to linearly interpolate $C_{P'}$ in terms of concentrations at the nearest two nodes on the local cell boundaries. If, for example, P' falls between nodes $(i-1, j)$ and $(i-1, j-1)$ as shown in Figure 3-1, $C_{P'}$ can be interpolated as

$$C_{P'} = r_{i,j} C_{i-1, j-1} + (1 - r_{i,j}) C_{i-1, j} \quad (3.27)$$

where $r_{i,j}$ has been defined previously in (3.14).

Using (3.27) in (3.15), the latter becomes

$$C_{i,j} = (R_{P'} r_{i,j})C_{i-1,j-1} + [R_{P'}(1-r_{i,j}) + R_x]C_{i-1,j} + (0)C_{i-1,j+1} + (R_y)C_{i,j-1} + (R_y)C_{i,j+1} + (0)C_{i+1,j-1} + (R_x)C_{i+1,j} + (0)C_{i+1,j+1} + R_{i,j} \quad (3.28)$$

Equation (3.28) applies only when $0 \leq r_{i,j} \leq 1$. Obviously, depending on local flow direction in a cell, P' may fall on different local boundaries, and the concentration $C_{P'}$ should be always interpolated using the nearest two nodal concentrations.

There are a total of eight different local numerical formulations depending on the value and the direction of $r_{i,j}$ in the local domain. The details of development of the numerical formulations are given in Appendix A. The final formulations for all the cases encountered are summarized as follows

Case 1, when $r_{i,j} \leq 1$, $u_{i,j} > 0$, and $v_{i,j} \geq 0$, the formulation is given in equation (3.28).

Case 2, when $r_{i,j} \leq 1$, $u_{i,j} > 0$, and $v_{i,j} < 0$,

$$C_{i,j} = (0)C_{i-1,j-1} + [R_{P'}(1-r_{i,j}) + R_x]C_{i-1,j} + (R_{P'} r_{i,j})C_{i-1,j+1} + (R_y)C_{i,j-1} + (R_y)C_{i,j+1} + (0)C_{i+1,j-1} + (R_x)C_{i+1,j} + (0)C_{i+1,j+1} + R_{i,j} \quad (3.29)$$

Case 3, when $r_{i,j} \leq 1$, $u_{i,j} < 0$, and $v_{i,j} < 0$,

$$C_{i,j} = (0)C_{i-1,j-1} + (R_x)C_{i-1,j} + (0)C_{i-1,j+1} + (R_y)C_{i,j-1} + (R_y)C_{i,j+1} + (0)C_{i+1,j-1} + [R_{P'}(1-r_{i,j}) + R_x]C_{i+1,j} + (R_{P'} r_{i,j})C_{i+1,j+1} + R_{i,j} \quad (3.30)$$

Case 4, when $r_{i,j} \leq 1$, $u_{i,j} < 0$, and $v_{i,j} \geq 0$,

$$\begin{aligned}
C_{i,j} = & (0)C_{i-1,j-1} + (R_x)C_{i-1,j} + (0)C_{i-1,j+1} + (R_y)C_{i,j-1} + \\
& (R_y)C_{i,j+1} + (R_{p'} r_{i,j})C_{i+1,j-1} + [R_{p'}(1-r_{i,j}) + R_x]C_{i+1,j} + (0)C_{i+1,j+1} + R_{i,j}
\end{aligned} \tag{3.31}$$

Note that $\Delta\eta$ is expressed as equation (3.12) for Cases 1 to 4.

Case 5, when $r_{ij} > 1$, $u_{ij} \geq 0$, and $v_{ij} > 0$,

$$r'_{i,j} = \left| \frac{u_{i,j}\Delta y}{v_{i,j}\Delta x} \right| \quad \text{or} \quad r'_{i,j} = \frac{1}{r_{i,j}} \tag{3.32}$$

$$\begin{aligned}
C_{i,j} = & (R_{p'} r'_{i,j})C_{i-1,j-1} + (R_x)C_{i-1,j} + (0)C_{i-1,j+1} + [R_{p'}(1-r'_{i,j}) + R_y]C_{i,j-1} + \\
& (R_y)C_{i,j+1} + (0)C_{i+1,j-1} + (R_x)C_{i+1,j} + (0)C_{i+1,j+1} + R_{i,j}
\end{aligned} \tag{3.33}$$

Case 6, when $r_{ij} > 1$, $u_{ij} < 0$, and $v_{ij} > 0$,

$$\begin{aligned}
C_{i,j} = & (0)C_{i-1,j-1} + (R_x)C_{i-1,j} + (0)C_{i-1,j+1} + [R_{p'}(1-r'_{i,j}) + R_y]C_{i,j-1} + \\
& (R_y)C_{i,j+1} + (R_{p'} r'_{i,j})C_{i+1,j-1} + (R_x)C_{i+1,j} + (0)C_{i+1,j+1} + R_{i,j}
\end{aligned} \tag{3.34}$$

Case 7, when $r_{ij} > 1$, $u_{ij} > 0$, and $v_{ij} < 0$,

$$\begin{aligned}
C_{i,j} = & (0)C_{i-1,j-1} + (R_x)C_{i-1,j} + (R_{p'} r'_{i,j})C_{i-1,j+1} + (R_y)C_{i,j-1} + \\
& [R_{p'}(1-r'_{i,j}) + R_y]C_{i,j+1} + (0)C_{i+1,j-1} + (R_x)C_{i+1,j} + (0)C_{i+1,j+1} + R_{i,j}
\end{aligned} \tag{3.35}$$

Case 8, when $r_{ij} > 1$, $u_{ij} < 0$, and $v_{ij} < 0$,

$$\begin{aligned}
C_{i,j} = & (0)C_{i-1,j-1} + (R_x)C_{i-1,j} + (0)C_{i-1,j+1} + (R_y)C_{i,j-1} + \\
& [R_{p'}(1-r'_{i,j}) + R_y]C_{i,j+1} + (0)C_{i+1,j-1} + (R_x)C_{i+1,j} + (R_{p'} r'_{i,j})C_{i+1,j+1} + R_{i,j}
\end{aligned} \tag{3.36}$$

Note that $\Delta\eta$ for Case 5 to 8 is written as equation (3.13)

Equation (3.28) through (3.36) can be also summarized as the following more compact form

$$C_{i,j} = a_{i-1,j-1}C_{i-1,j-1} + a_{i-1,j}C_{i-1,j} + \cdots + R_{i,j} \quad (3.37)$$

where $a_{i,j}$ is a function of $r_{i,j}$.

Equation (3.37) is of the same form as a standard finite difference scheme, except that the coefficients are derived analytically instead of using truncated Taylor series approximation. This analytically derived finite difference scheme is called a finite analytic scheme, and the coefficients $a_{i,j}$'s are referred to as finite analytic coefficients. Equation (3.37) is also of the same form as the existing finite analytic form developed by Chen and his co-workers [Chen and Chen, 1982; Chen et al., 1981] except that the finite analytic coefficients are considerably simplified. The new finite analytic scheme, despite the additional approximation for the diffusion terms, is as accurate as the existing one, as will be demonstrated in Chapter 5.

We would like to point out that the standard upwind finite difference method, in the case when there is no chemical reaction involved, is the same as the new finite analytic scheme, except that $C_{p'}$ is estimated or "interpolated" differently. For example when $0 < r_{i,j} < 1$, or when the local flow points northwest, the upwind finite difference method always uses the concentration at the west-central $(i-1, j)$ node and south-central node $(i, j-1)$ for estimating $C_{p'}$ or

$$C_{p'} = \frac{r_{i,j}}{1+r_{i,j}}C_{i-1,j} + \frac{1}{1+r_{i,j}}C_{i,j-1} \quad (3.38)$$

The finite analytic method, however, is able to switch between $(i-1, j)$ and $(i-1, j-1)$ when flow is moving more from west ($0 \leq r_{i,j} \leq 1$) to between $(i-1, j-1)$ and $(i, j-1)$ when flow is moving more from south ($r_{i,j} > 1$). Figure 3-2 provides a schematic illustration of the numerical error associated with “upwind” interpolation as well as linear interpolation used the new finite analytic scheme. As expected, interpolation error (error of numerical approximation compared to analytical solution) depends on the flow direction or the value of $r_{i,j}$. finite analytic method has zero interpolation error when the flow is diagonal because of the use of corner node for interpolation, while the upwind finite difference method becomes worst when $r_{i,j} = 1$. The interpolation error is largest for the finite analytic scheme when P' is half way between the two interpolation nodes or $r_{i,j} = \frac{1}{2}$ (for the case of $0 < r_{i,j} < 1$), although the interpolation error is reduced significantly.

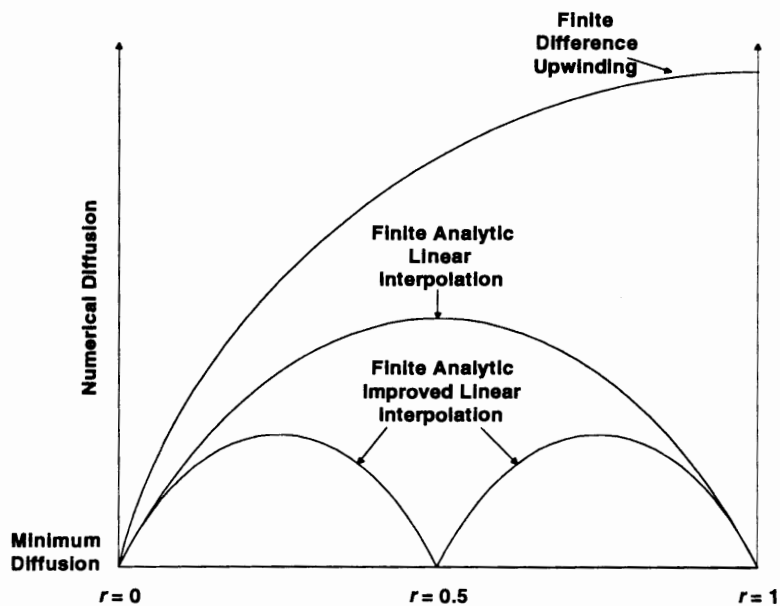


Figure 3-2. Schematic of comparison of numerical diffusion as functions of $r_{i,j}$

One obvious way to improve the boundary interpolation and reduce the associated numerical error is to refine the grid size. However, this often becomes infeasible for real

world problems of realistic size and complexities since grid refinement may increase computational cost considerably. For a three-dimensional problem, the number of computational nodes would increase by a factor of eight when grid size is halved. The computer CPU time for solving a three-dimensional problem increases exponentially with the total number of nodes. Furthermore, the convergence of iterates decreases quickly with the decreasing grid size, especially for a heterogeneous groundwater system.

3.2.3. Improved Linear Interpolation Boundary Approximation

This subsection presents a new interpolation scheme that improves the accuracy of boundary interpolation without refining the grid. For illustrating purpose, only the solution to pure advection transport problem is described.

To motivate the idea, consider first the case that $r_{i,j} = \frac{1}{2}$ or P' falls half way between node $(i-1,j)$ and $(i-1,j-1)$. This corresponds to the case that the error associated with the basic interpolation scheme is greatest since the distance between P' and the two neighbor nodes is maximal. But in a advection-dominated system, the information propagates mostly from upstream; then concentration at non-nodal point P' as shown in Figure 3-3, can be directly related to nodal concentration at node $(i-2,j-1)$ without interpolation.

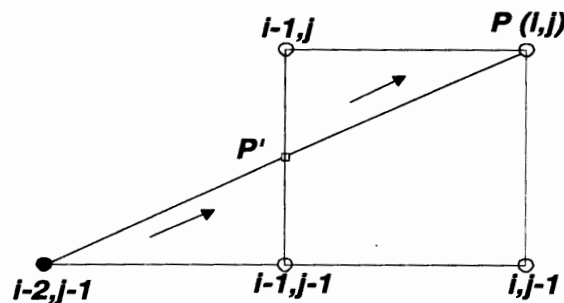


Figure 3-3: Local flowline and P' for $r_{i,j} = \frac{1}{2}$

In the case of pure advection,

$$C_{P'} = C_{i-2,j-1} \quad (3.39)$$

For reaction transport, an equation similar to (3.10) applies between node $(i-2,j-1)$ and P' . This equation is

$$C_{P'} = e^{-\frac{\lambda_{i,j} \Delta \eta}{U_{i,j}}} C_{i-2,j-1} + \frac{S_{i,j}}{\lambda_{i,j}} \left(1 - e^{-\frac{\lambda_{i,j} \Delta \eta}{U_{i,j}}} \right) \quad (3.40)$$

where the velocity is assumed constant locally, so the velocity from node $(i-2,j-1)$ to P' is assumed approximately the same as that from P' to node (i,j) . If equation (3.40), instead of (3.27), is used to estimate the non-nodal concentration $C_{P'}$, the error from interpolation can be entirely eliminated. But, of course, (3.40) applies only for $r_{i,j} = \frac{1}{2}$. In a more general situation P' may not always lie right in the middle of the two interpolating nodes,

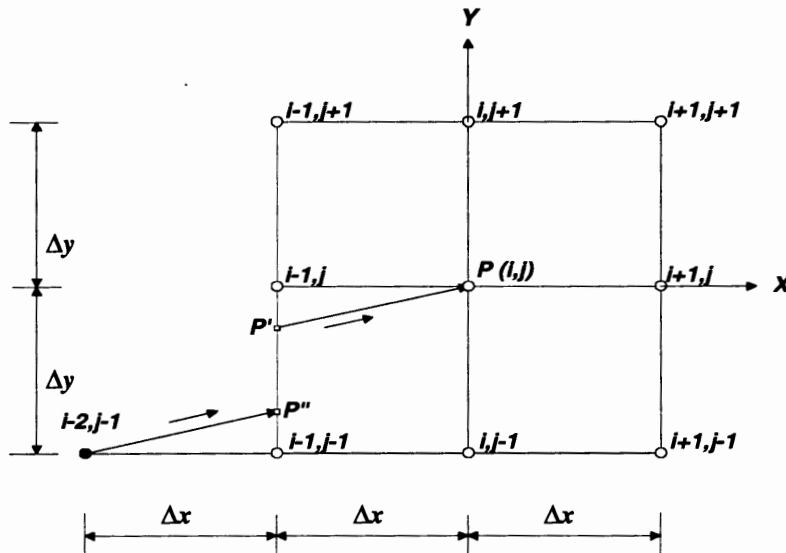


Figure 3-4: A computational local element for finite analytic method with improved linear interpolation

the flowline originating from node $(i-2,j-1)$ may not intersect with local cell boundary exactly at P' but normally at a different point P'' (see Figure 3-4). The concentration at P'' can be analytically related to concentration at the node directly upstream at $(i-2,j-1)$

$$C_{P''} = e^{-\frac{\lambda_{i,j}\Delta\eta}{U_{i,j}}} C_{i-2,j-1} + \frac{S_{i,j}}{\lambda_{i,j}} \left(1 - e^{-\frac{\lambda_{i,j}\Delta\eta}{U_{i,j}}} \right) \quad (3.41)$$

The concentration at P' still needs to be interpolated. However, a much more accurate estimate for $C_{P'}$ can be obtained if interpolation is done between P'' and the node on the local boundary nearest to P' . In the case that P' is closer to node $(i-1,j)$ than to node $(i-1,j-1)$ or $r_{i,j} \leq \frac{1}{2}$,

$$C_{P'} = r_{1i,j} C_{P''} + (1 - r_{1i,j}) C_{i-1,j} \quad (3.42)$$

where $r_{1i,j} = \frac{r_{i,j}}{1 - r_{i,j}}$.

When P' is closer to node $(i-1,j-1)$ than to node $(i-1,j)$ or $0.5 < r_{i,j} \leq 1$, $C_{P'}$ is expressed as:

$$C_{P'} = r'_{1i,j} C_{P''} + (1 - r'_{1i,j}) C_{i-1,j-1} \quad (3.43)$$

where $r'_{1i,j} = \frac{1 - r_{i,j}}{r_{i,j}}$.

The new improved interpolation scheme has the effect of halving the grid size since interpolation error is reduced to zero for $r_{i,j} = \frac{1}{2}$, where the interpolation error of the

basic interpolation is worst. Figure 3-2 also shows schematically the performance of the improved linear interpolation scheme relative to others discussed earlier.

Substituting equation (3.42) into equation (3.15), the following new finite analytic scheme is obtained

For $r_{i,j} \leq 0.5$

$$C_{i,j} = r_{1i,j} R_1 C_{i-2,j-1} + (1 - r_{1i,j}) R_2 C_{i-1,j} + (1 + R_2 r_{1i,j}) R_3 \quad (3.44)$$

For $0.5 < r_{i,j} \leq 1$

$$C_{i,j} = r'_{1i,j} R_1 C_{i-2,j-1} + (1 - r'_{1i,j}) R_2 C_{i-1,j-1} + (1 + R_2 r'_{1i,j}) R_3 \quad (3.45)$$

where

$$R_1 = e^{\frac{-2\lambda_{i,j}\Delta\eta}{U_{i,j}}} \quad (3.46)$$

$$R_2 = e^{\frac{-\lambda_{i,j}\Delta\eta}{U_{i,j}}} \quad (3.47)$$

$$R_3 = \frac{S_{i,j}}{\lambda_{i,j}} \left(1 - e^{\frac{-\lambda_{i,j}\Delta\eta}{U_{i,j}}} \right) \quad (3.48)$$

Note that when P'' falls on the nodal points, the value of that node will be used for $C_{P''}$.

There are totally sixteen different local numerical formulations depending on the direction and value of r in the local domain. Figure 3-5 shows a bigger local element which includes sixteen nodes that would be used in the development of formulations.

The same procedure of development of formulations (3.44) and (3.45) can be followed to derive numerical formulations for other cases. Details of the formulation development can be found in Appendix A. The following formulations are described for all

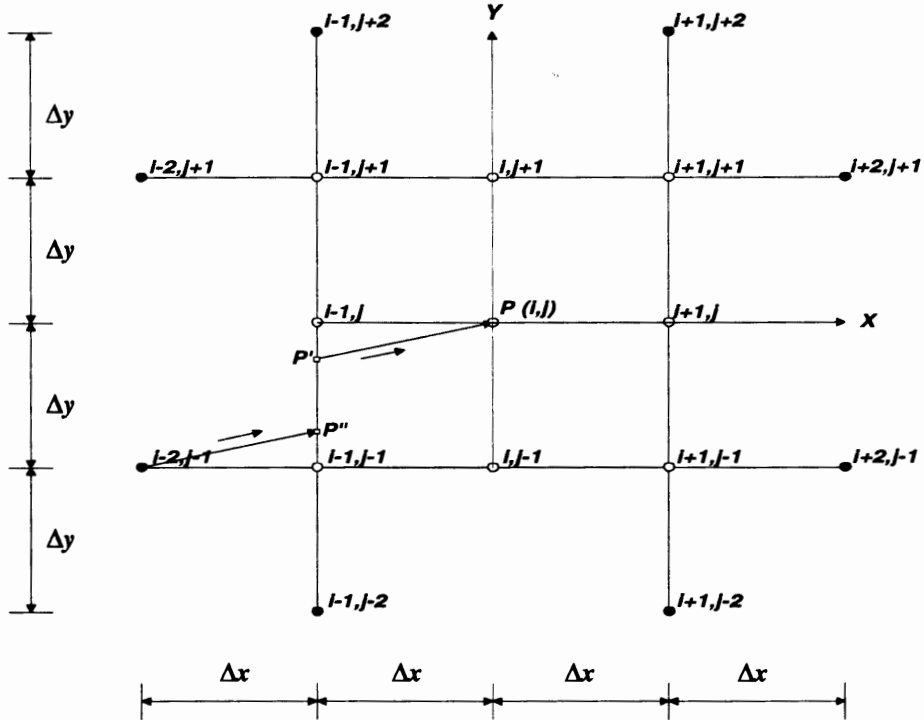


Figure 3-5: A local domain for finite analytic method with improved linear interpolation

the cases that would be encountered in the local element. In each case, there are two subcases. For Cases 1 to 4, subcases are with conditions of (a) $r_{ij} \leq 0.5$ and (b) $0.5 \leq r_{ij} \leq 1$. For Case 5 to 8, subcases are with conditions of (a) $r'_{ij} \leq 0.5$ and $0.5 \leq r'_{ij} \leq 1$. Case 1, when $r_{ij} \leq 1$, $u_{ij} > 0$, and $v_{ij} \geq 0$, for Subcase (a), the formulation is equation (3.43); and for Subcase (b), the formulation is equation (3.45).

Case 2, when $r_{ij} \leq 1$, $u_{ij} > 0$, and $v_{ij} < 0$, for Subcase (a)

$$C_{i,j} = r_{1i,j} R_1 C_{i-2,j+1} + (1 - r_{1i,j}) R_2 C_{i-1,j} + (1 + R_2 r_{1i,j}) R_3 \quad (3.49)$$

and for Subcase (b)

$$C_{i,j} = r'_{1i,j} R_1 C_{i-2,j+1} + (1 - r'_{1i,j}) R_2 C_{i-1,j+1} + (1 + R_2 r'_{1i,j}) R_3 \quad (3.50)$$

Case 3, when $r_{ij} \leq 1$, $u_{ij} < 0$, and $v_{ij} < 0$, for Subcase (a)

$$C_{i,j} = r_{1i,j} R_1 C_{i+2,j+1} + (1 - r_{1i,j}) R_2 C_{i+1,j} + (1 + R_2 r_{1i,j}) R_3 \quad (3.51)$$

and for Subcase (b)

$$C_{i,j} = r'_{1i,j} R_1 C_{i+2,j+1} + (1 - r'_{1i,j}) R_2 C_{i+1,j+1} + (1 + R_2 r'_{1i,j}) R_3 \quad (3.52)$$

Case 4, when $r_{ij} \leq 1$, $u_{ij} < 0$, and $v_{ij} \geq 0$, for Subcase (a)

$$C_{i,j} = r_{1i,j} R_1 C_{i+2,j-1} + (1 - r_{1i,j}) R_2 C_{i+1,j} + (1 + R_2 r_{1i,j}) R_3 \quad (3.53)$$

and for Subcase (b)

$$C_{i,j} = r'_{1i,j} R_1 C_{i+2,j-1} + (1 - r'_{1i,j}) R_2 C_{i+1,j-1} + (1 + R_2 r'_{1i,j}) R_3 \quad (3.54)$$

Note that $\Delta\eta$ is expressed as equation (3.12) for Cases 1 to 4.

Case 5, when $r_{ij} > 1$, $u_{ij} \geq 0$, and $v_{ij} > 0$

$$r_{2i,j} = \frac{r'_{i,j}}{1 - r'_{i,j}} \quad (5.55)$$

$$r'_{2i,j} = \frac{1 - r'_{i,j}}{r'_{i,j}} \quad (3.56)$$

For Subcase (a), the formulation is

$$C_{i,j} = r_{2i,j} R_1 C_{i-1,j-2} + (1 - r_{2i,j}) R_2 C_{i,j-1} + (1 + R_2 r_{2i,j}) R_3 \quad (3.57)$$

and for Subcase (b)

$$C_{i,j} = r'_{2i,j} R_1 C_{i-1,j-2} + (1 - r'_{2i,j}) R_2 C_{i-1,j-1} + (1 + R_2 r'_{2i,j}) R_3 \quad (3.58)$$

Case 6, when $r_{ij} > 1$, $u_{ij} < 0$, and $v_{ij} > 0$, for Subcase (a)

$$C_{i,j} = r_{2i,j} R_1 C_{i+1,j-2} + (1 - r_{2i,j}) R_2 C_{i,j-1} + (1 + R_2 r_{2i,j}) R_3 \quad (3.59)$$

and for Subcase (b)

$$C_{i,j} = r'_{2i,j} R_1 C_{i+1,j-2} + (1 - r'_{2i,j}) R_2 C_{i+1,j-1} + (1 + R_2 r'_{2i,j}) R_3 \quad (3.60)$$

Case 7, when $r_{ij} > 1$, $u_{ij} > 0$, and $v_{ij} < 0$, for Subcase (a)

$$C_{i,j} = r_{2i,j} R_1 C_{i-1,j+2} + (1 - r_{2i,j}) R_2 C_{i,j+1} + (1 + R_2 r_{2i,j}) R_3 \quad (3.61)$$

and for Subcase (b)

$$C_{i,j} = r'_{2i,j} R_1 C_{i-1,j+2} + (1 - r'_{2i,j}) R_2 C_{i-1,j+1} + (1 + R_2 r'_{2i,j}) R_3 \quad (3.62)$$

Case 8, when $r_{ij} > 1$, $u_{ij} < 0$, and $v_{ij} < 0$, for Subcase (a)

$$C_{i,j} = r_{2i,j} R_1 C_{i+1,j+2} + (1 - r_{2i,j}) R_2 C_{i,j+1} + (1 + R_2 r_{2i,j}) R_3 \quad (3.63)$$

and for Subcase (b)

$$C_{i,j} = r'_{2i,j} R_1 C_{i+1,j+2} + (1 - r'_{2i,j}) R_2 C_{i+1,j+1} + (1 + R_2 r'_{2i,j}) R_3 \quad (3.64)$$

where $\Delta\eta$ for Case 5 to 8 is written as equation (3.13)

Note that the new interpolation based finite analytic scheme is derived only for pure advection transport. Extension to include diffusion is straightforward, but the scheme will involve more nodal points. The new finite analytic scheme with refined linear interpolation represents a significant improvement over existing finite analytic method and the new finite analytic method based on basic linear interpolation, as will be demonstrated in Chapter 5.

3.3. Properties of Improved Finite Analytic Methods

A numerical scheme, either finite analytic scheme or finite difference scheme, can be represented in a following general form

$$C_{i,j} = \sum_{\substack{l \neq i \\ m \neq j}} a_{lm} C_{lm} + R_{i,j} \quad (3.65)$$

where a_{lm} dictates the performance of a particular scheme, $R_{i,j}$ often reflects contribution from a solute source/sink.

This subsection discusses the properties of new finite analytic coefficients and compares them with existing finite analytic coefficients and standard finite difference

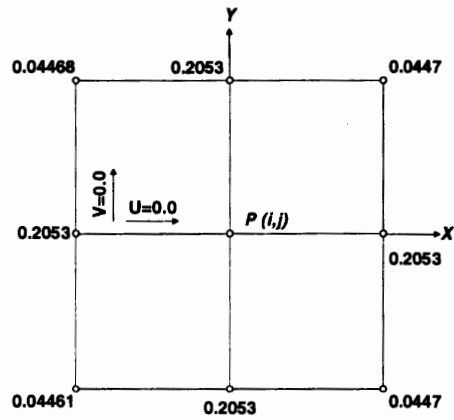
coefficients. In particular, the discussion focuses on how these numerical coefficients vary with changing flow direction and Peclet number that characterizes the relative strength of advection and diffusion.

First, consider solute transport for pure diffusion. Assume that the diffusion coefficients $D_x = D_y = 0.005 \text{ m}^2/\text{day}$. The values of the numerical coefficients obtained from existing finite analytic, upwind finite difference and improved finite analytic linear interpolation methods are shown in Figure 3-6, where the value at the node is the coefficient of the corresponding node. These coefficients are all-positive and sum up to 1 for each method. Because of the approximation of the diffusion by central difference method, the upwind finite difference and the improved finite analytic linear interpolation methods have same non-zero values for numerical coefficients at the four central nodal points but zeros elsewhere. The coefficients of existing finite analytic occur at all nodal points in the local element and are different from the other methods. For pure diffusion condition, results of the existing finite analytic method is more accurate than the improved finite analytic method.

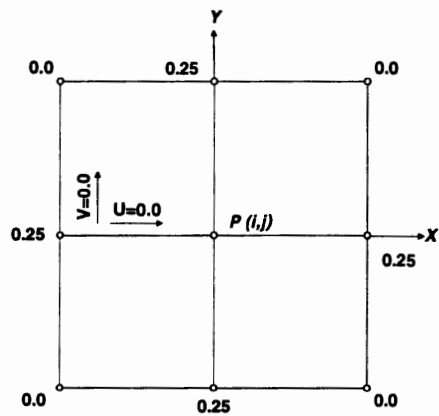
Now consider a small horizontal flow in the above three methods and $Pe_x = 1$. Figure 3-7 illustrates the changes in the coefficients under this flow condition compared to Figure 3-6. Increased values are seen at the west-central node, which means this nodal values have larger influence on the values at interior node P . The coefficients for the upwind finite difference and the improved finite analytic methods are the same at four central nodes, while the existing finite analytic method spreads the coefficient values on each surrounding node.

Figure 3-8 shows another comparison when the horizontal flow becomes stronger, where $Pe_x = 20$. In this case, the advection has large influence on the coefficients, in particular, the values at the west-central node become the major portion of the overall sum of the coefficients.

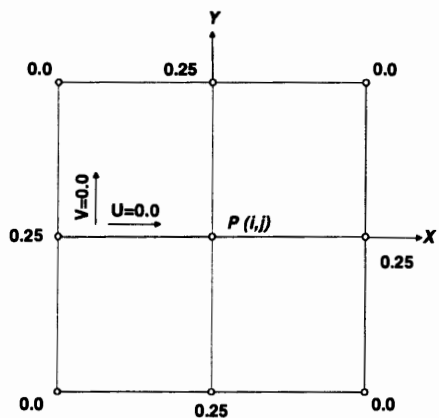
For the pure diffusion case and for the one-dimensional horizontal flow, both the upwind finite difference method and improved finite analytic method have identical coefficients. When the Peclet number becomes large, the coefficients of existing finite



(a). Existing Finite Analytic Method

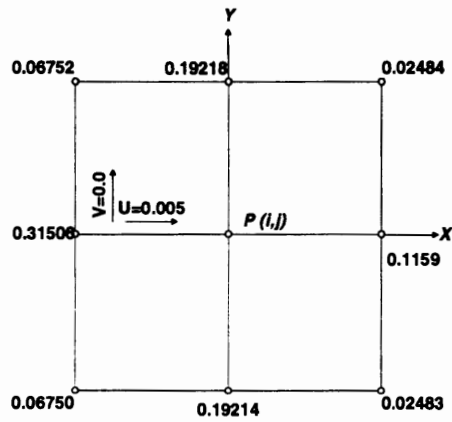


(b). Finite Analytic Linear Interpolation Method

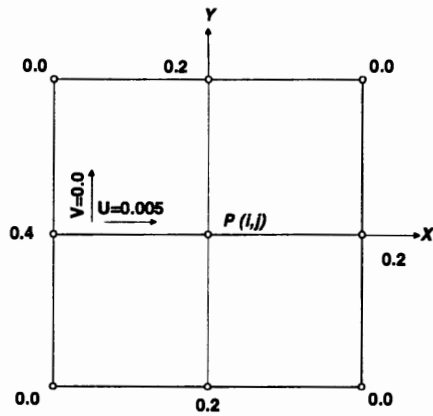


(c). Upwind Finite Difference Method

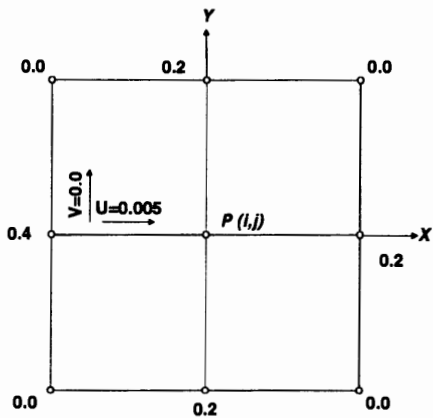
Figure 3-6: Coefficients for pure diffusion problem ($Pe_x = Pe_y = 0$)



(a). Existing Finite Analytic Method

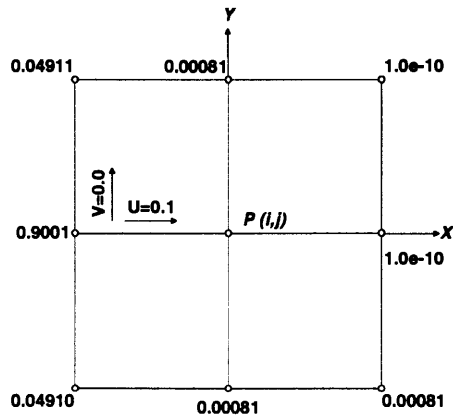


(b). Finite Analytic Linear Interpolation Method

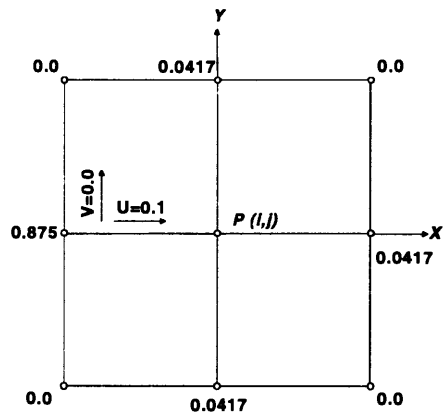


(c). Upwind Finite Difference Method

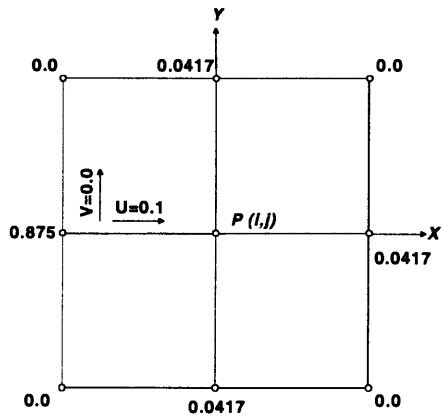
Figure 3-7: Coefficients for transport in horizontal flow ($Pe_x = 1, Pe_y = 0$)



(a). Existing Finite Analytic Method

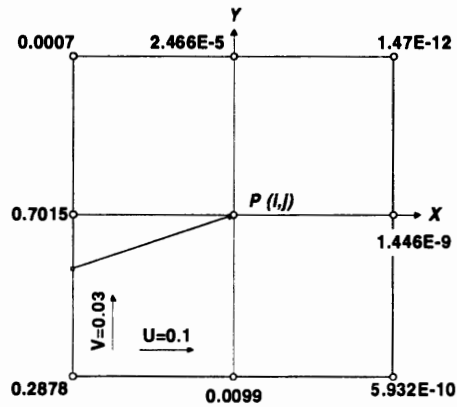


(b). Finite Analytic Linear Interpolation Method

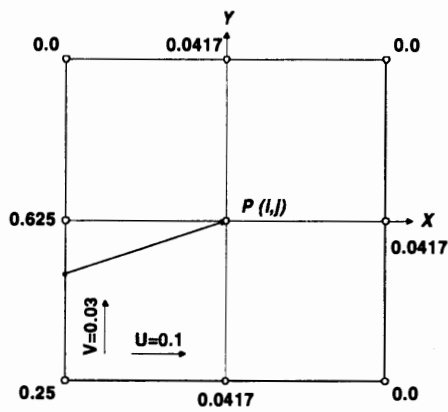


(c). Upwind Finite Difference Method

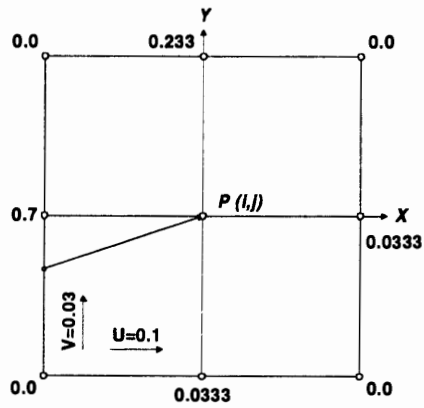
Figure 3-8: Coefficients for transport in horizontal flow ($Pe_x = 20, Pe_y = 0$)



(a). Existing Finite Analytic Method

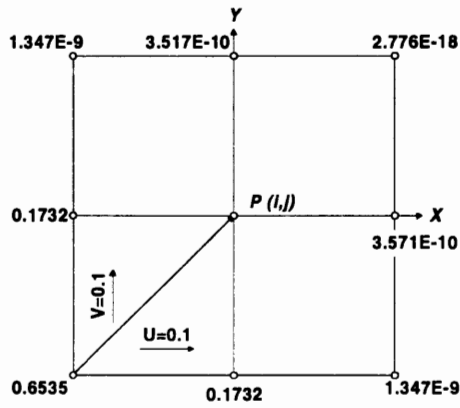


(b). Finite Analytic Linear Interpolation Method

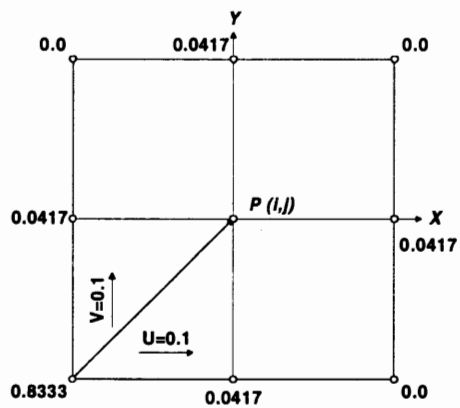


(c). Upwind Finite Difference Method

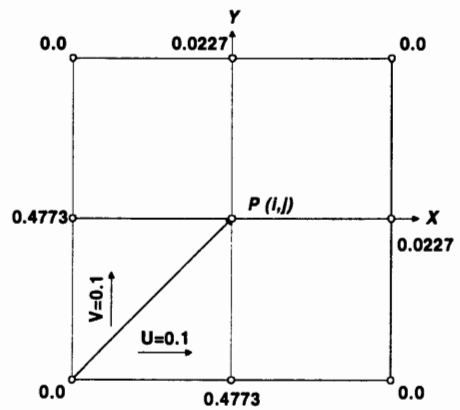
Figure 3-9: Coefficients for 2-D transport ($Pe_x = 20, Pe_y = 6$)



(a). Existing Finite Analytic Method

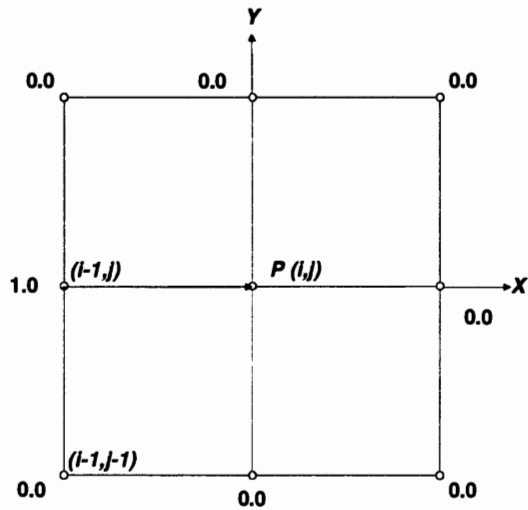


(b). Finite Analytic Linear Interpolation Method

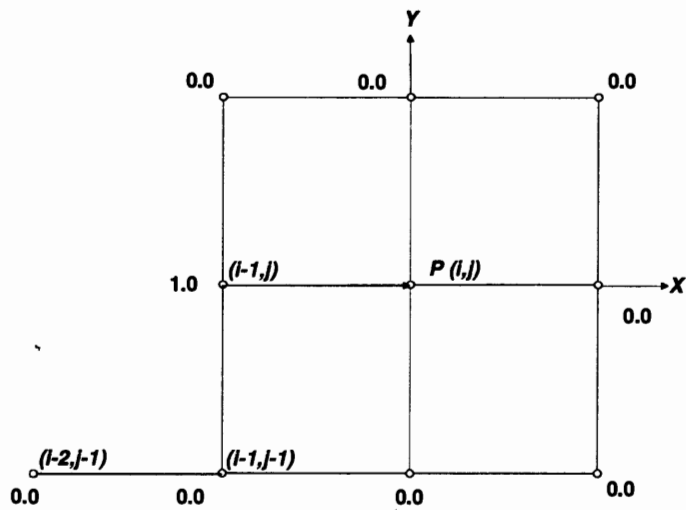


(c). Upwind Finite Difference Method

Figure 3-10: Coefficient for 2-D transport ($Pe_x = 20, Pe_y = 20$)

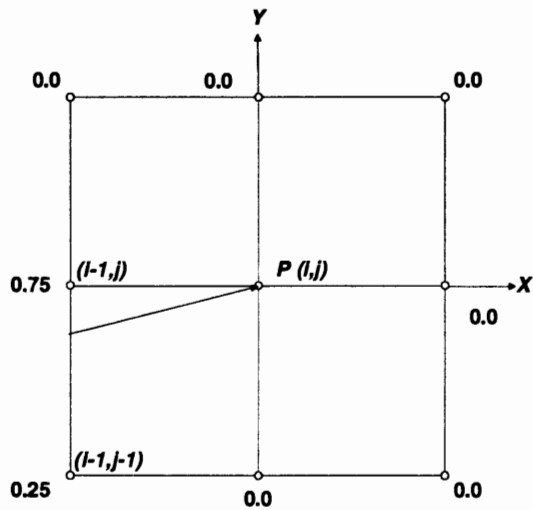


(a). Finite Analytic - Basic Linear Interpolation

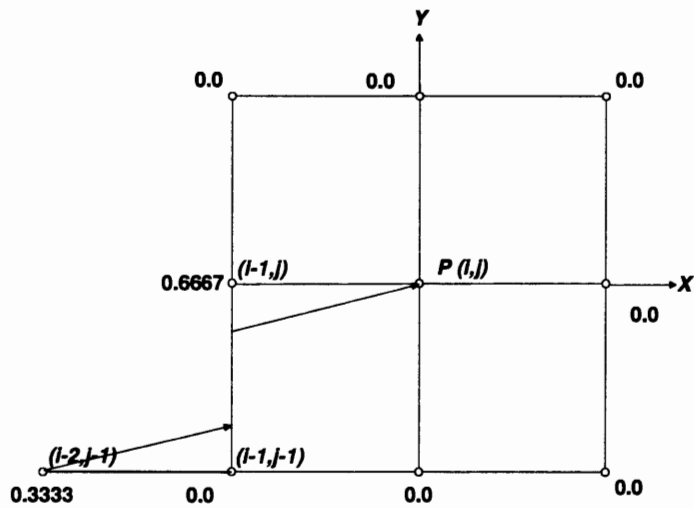


(b). Finite Analytic - Improved Linear Interpolation

Figure 3-11: Coefficients for pure advection problem ($v/u = 0.0$)

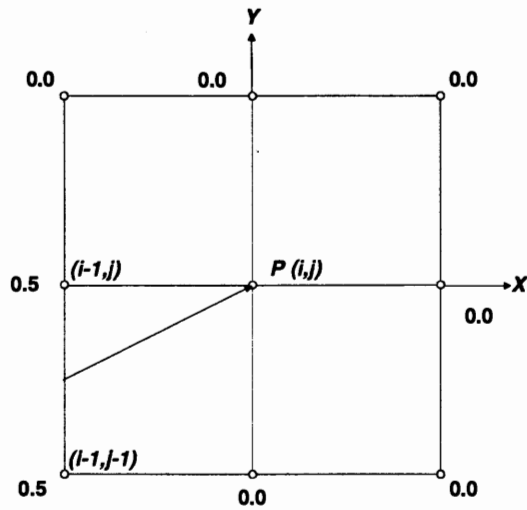


(a) Finite Analytic - Basic Linear Interpolation

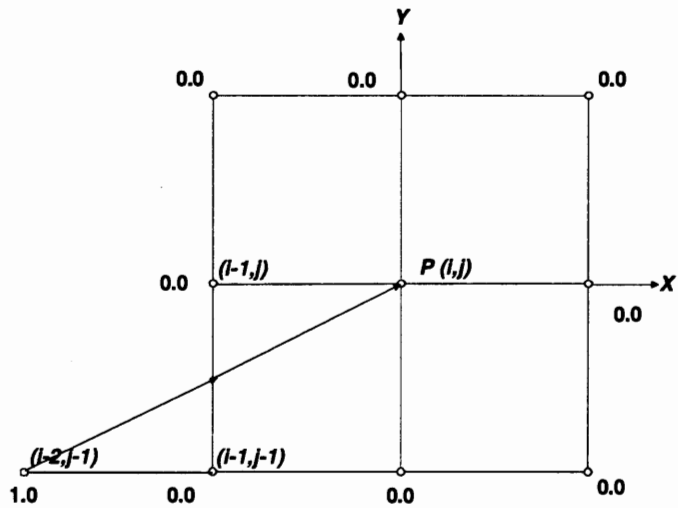


(b). Finite Analytic - Improved Linear Interpolation

Figure 3-12: Coefficients for pure advection problem ($v/u = 0.25$)

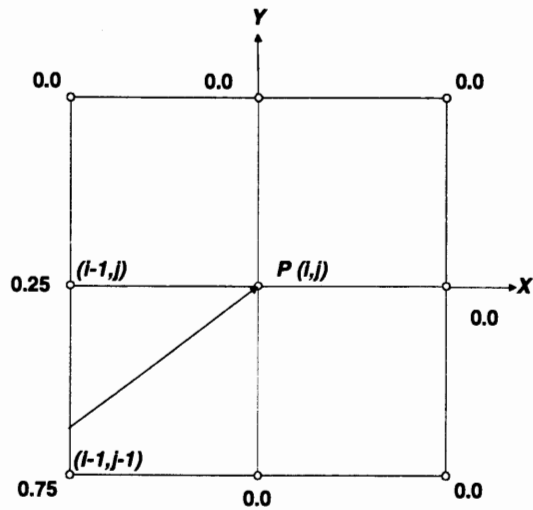


(a) Finite Analytic- Basic Linear Interpolation

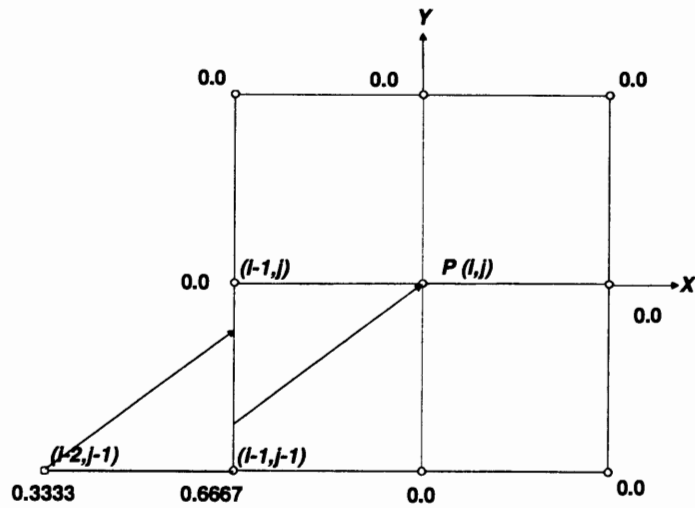


(b). Finite Analytic - Improved Linear Interpolation

Figure 3-13: Coefficients for pure advection problem ($v/u = 0.5$)

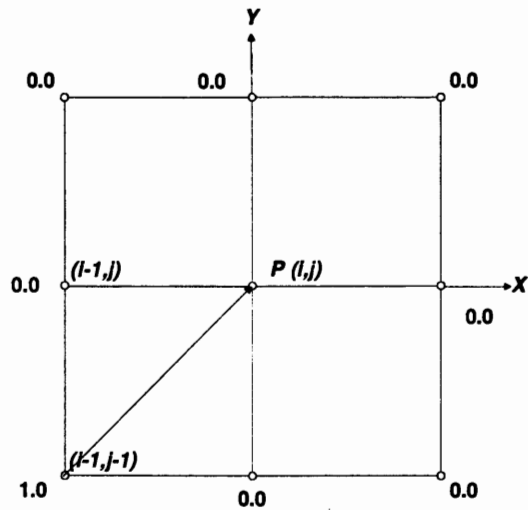


(a) Finite Analytic - Basic Linear Interpolation

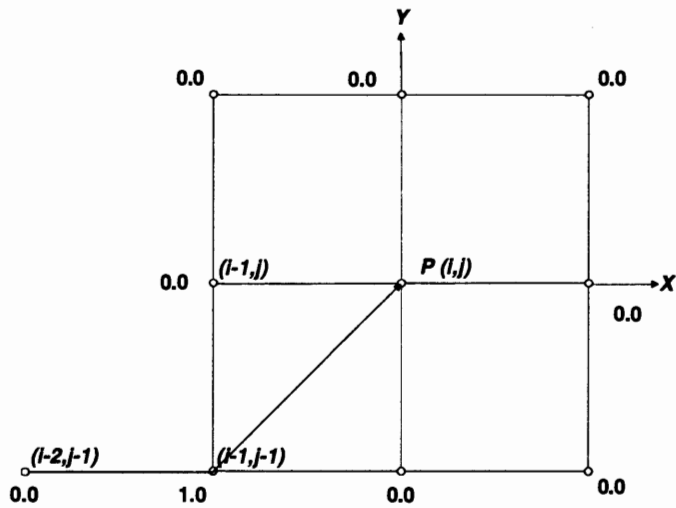


(b). Finite Analytic - Improved Linear Interpolation

Figure 3-14: Coefficients for pure advection problem ($v/u = 0.75$)



(a) Finite Analytic - Basic Linear Interpolation



(b). Finite Analytic - Improved Linear Interpolation

Figure 3-15: Coefficients for pure advection problem ($v/u = 1.0$)

analytic method are close to those of the other two methods. A horizontal plume comparison for these three methods will be presented in Chapter 5, where the resulting plumes are basically identical. All three methods have shown so far all-positive coefficients, and are able to shift the weights of influence on the nodal values according to the magnitude of the horizontal advection or the value of Peclet number. Since the magnitude and the direction of the flow in groundwater varies spatially, the properties of the improved finite analytic method are further analyzed when two-dimensional flow is considered.

Adding a vertical flow to the uniform flow used in Figure 3-8, now $Pe_x = 20$, and $Pe_y = 6$. Similar comparison is shown in Figure 3-9. Notice that coefficients at the south-west corners become a lot larger than the ones shown in Figure 3-8 for both existing and improved finite analytic methods, while the corresponding coefficient of upwind finite difference stays unchanged, which is zero. No influence from the south-west corner by the vertical component of the advection velocity is taken into account when evaluating the value at the interior node for upwind finite difference method. The method loses its proper upwind shift nature when the flow becomes two-dimensional. Both magnitude and direction of the advection have great and natural impact on the weighting factors for the finite analytic methods. Since the horizontal velocity is greater than the vertical one, the coefficients of the west-central nodes have largest values. The existing finite analytic method considers the diffusion effect coming from all local nodes, and needs to spread the weights to each node. Therefore, the coefficients may look different from those given by the improved finite analytic method.

Increasing the vertical component of the advection again to $Pe_x = Pe_y = 20$, the flow is diagonal pointing from the south-west corner to the interior node. The greatest influence is now coming from the south-west corner node. Figure 3-10 illustrates this case. For both finite analytic methods, the coefficient at this node is the greatest. The nature of the upwind shift is shown again for finite analytic methods, but not properly for upwind finite difference method.

The above figures are used to describe the properties of the analytical coefficients of finite analytic linear interpolation method and compare them with the existing finite analytic and upwind finite difference methods. However, the properties of the finite analytic method with improved linear interpolation are also important to know. Figures 3-11 to 3-15 are shown for the pure advection cases, where the magnitude of velocity in y direction is gradually changed and the direction of the flow is changed from horizontal to diagonal. Both improved finite analytic methods are shown in pair for each flow condition. For the improved linear interpolation, the weighting factor of the surrounding nodes is changed according to the magnitude and the direction of the flow, indicating that for different flow condition the influence from the same and/or different nodes is changed. For horizontal and diagonal flows, as shown in Figures 3-11 and 3-15, the two methods have the same coefficients at the corresponding nodes. In Figure 3-12 the highest coefficient value for two methods indicates that influence comes mostly from node $(i-1, j)$. However, the rest of the influence comes from nodes $(i-1, j-1)$ and $(i-2, j-1)$ respectively for linear interpolation and improved linear interpolation. Both nodes are located in upstream directions, but the improved linear interpolation describes the upwind influence more precisely. Similarly, Figure 3-14 can be described. Note that the coefficients in Figure 3-13 are placed at totally different nodes for the two methods. For the improved linear interpolation method and under pure advection condition, the weight is only estimated at the upwind node $(i-2, j-1)$, but at node $(i-1, j-1)$ and node $(i-1, j)$ for linear interpolation method. This figure explains why there is more numerical diffusion occurring in the method of finite analytic linear interpolation in this case of flow condition.

Collectively, for the improved finite analytic methods, for all one-dimensional and two-dimensional cases considered, they provide all-positive coefficients, which are considered physically realistic, since the contribution from diffusion should be positive for all physical problems. With the improved finite analytic methods, one can shift the weights of influence on the determination of nodal values at the interior point P according to the grid size, advective velocity direction and magnitude, and Peclet number.

The finite analytic coefficients of both finite analytic linear interpolation and improved linear interpolation methods add up to 1, that is

$$\sum_{\substack{l \neq i \\ m \neq j}} a_{lm} = 1 \quad (3.66)$$

This property reflects the fact that the concentration at the interior node P is a weighted average of the surrounding nodal values. Equation (3.66) is a necessary condition for mass conservation but not sufficient.

Chapter 4

Improved Finite Analytic Methods for Unsteady Transport

In this chapter, extension of the improved finite analytic methods to unsteady solute transport problem is illustrated. The space-time accurate numerical method for unsteady problem is derived by taking the Laplace transform of the transient equation.

4.1. Basic Idea

It is known that numerical solutions of the transient advection-diffusion equation are complicated by the first-order spatial derivatives describing the advective flux. When advection dominates, advective terms are generally obtained more attention in solving the steady-state advection-diffusion equation. The emphasis on the advective terms when solving transient cases usually leads one to a wrong impression that the temporal term can be handled with simple methods, such as a traditional finite difference methods.

A good space approximation combined with a poor temporal approximation does not give satisfactory results [Li et al., 1992]. Certain choices for the time discretization scheme, such as a fully implicit scheme, or improper selection of a time step size can lead to artificial smearing of oscillations in the solution. This type of unacceptable behavior is particularly problematic when dealing with the advection-diffusion equation describing solute transport in groundwater [Sudicky, 1989]. The unsteady two-dimensional finite analytic formulations [Chen and Chen, 1982] are derived from the hybrid method, which is a combination of the finite analytic method for the steady terms and the finite difference method for the unsteady term in the transient governing equation. This hybrid method may produce unfavorable results in advection-dominated problems, although the finite analytic method itself for the steady-state problem is a good approximation method.

In fact, the time derivative interacts very closely with the spatial terms and it becomes increasingly important and difficult to approximate as the first-order spatial

derivatives become significant. Therefore, the accurate numerical solution of the transient advective transport equation requires that both space and time derivatives should be considered carefully. An inability to properly approximate either of these derivatives can destroy the accuracy of the overall solution [Li et al., 1992].

Laplace transform methods have been used before in numerical algorithms for solving time-dependent partial differential equations. Recently, hybrid methods, for example, Laplace transform/finite element method [Sudicky, 1989] and Laplace transform/finite analytic method [Li et al., 1992], have been applied to solute transport problems. The results of these hybrid methods are accurate and the solutions are robust over a practical range of Peclet numbers.

Therefore, the Laplace transform method is chosen for the temporal approximation in the following sections, when the improved finite analytic methods are extended to transient problems. The basic idea is to use the Laplace transform to convert the transient advection-diffusion equation to a steady state expression which can then be solved with the improved finite analytic methods.

4.2. Formulation

4.2.1. Governing Equation

The general non-conservative contaminant transport problem with sources and sinks is governed by the following partial differential equation

$$\frac{\partial C}{\partial t} + u(x, y) \frac{\partial C}{\partial x} + v(x, y) \frac{\partial C}{\partial y} = \frac{\partial}{\partial x} \left[D_x(x, y) \frac{\partial C}{\partial x} \right] + \frac{\partial}{\partial y} \left[D_y(x, y) \frac{\partial C}{\partial y} \right] - \lambda(x, y)C + S(x, y) \quad (4.1)$$

with initial condition

$$C(x, y, 0) = g(x, y)$$

4.2.2. Laplace Transformation

The Laplace transformation, L , of a function $h(t)$ is defined as (Carslaw and Jaeger, 1959)

$$L[h(t)] = \tilde{h}(p) = \int_0^{\infty} h(t)e^{-pt} dt \quad (4.2)$$

where \tilde{h} is the transform of h and p is the Laplace transform parameter that is in general complex-valued.

The Laplace transformation provides a convenient tool to solve linear time-dependent differential equations. This transformation is especially useful for solving the transient advection-dominated transport equation since it avoids direct approximation of the time derivative. Taking the Laplace transform on both sides of equation (4.1), the transformed governing equation is then obtained

$$u(x, y) \frac{\partial \tilde{C}}{\partial x} + v(x, y) \frac{\partial \tilde{C}}{\partial y} = \frac{\partial}{\partial x} \left[D_x(x, y) \frac{\partial \tilde{C}}{\partial x} \right] + \frac{\partial}{\partial y} \left[D_y(x, y) \frac{\partial \tilde{C}}{\partial y} \right] - [p + \lambda(x, y)] \tilde{C} + \tilde{S}(x, y, p) + g(x, y) \quad (4.3)$$

where the accent indicates the complex-valued Laplace transform. Note that the time derivative has been analytically removed and the transient transport equation becomes a complex-valued “steady-state” advection-diffusion equation, with the initial condition appearing as an inhomogeneous source term.

4.2.3. Finite Analytic Approximation in the Laplace Domain

Equation (4.3) has similar form of equation (3.1). Therefore, improved finite analytic method as developed can be applied to the transformed “steady-state” solute transport equation in a Laplace domain. In the local element as shown in Figure 3-1, the differential equation (4.3) of transformed “steady-state” is written as

$$U_{i,j} \frac{\partial \tilde{C}}{\partial \eta} = D_{x,i,j} \frac{\partial^2 \tilde{C}}{\partial x^2} + D_{y,i,j} \frac{\partial^2 \tilde{C}}{\partial y^2} - (\lambda_{i,j} + p) \tilde{C} + \tilde{S}_{i,j} + g_{i,j} \quad (4.4)$$

where $g_{i,j}$ and $\tilde{S}_{i,j}$ are the local values evaluated at point (i,j) , and other terms are described in Chapter 3. The local numerical solution to equation (4.4) is developed according to the same procedure as used in Chapter 3. For illustrating purpose, only the formulation for this particular case as shown in Figure 3-1 is described. The general solution to equation (4.4) is written as

$$\tilde{C}(\eta) = e^{-\frac{\lambda_{i,j}+p}{U_{i,j}}\eta} \tilde{C}_{P'} + \frac{f'_{x,i,j} + f'_{y,i,j} + (\tilde{S}_{i,j} + g_{i,j})}{\lambda_{i,j} + p} \left(1 - e^{-\frac{\lambda_{i,j}+p}{U_{i,j}}\eta} \right) \quad (4.5)$$

where

$$f'_{x,i,j} = D_{x,i,j} \frac{\tilde{C}_{i+1,j} - 2\tilde{C}_{i,j} + \tilde{C}_{i-1,j}}{\Delta x^2}$$

$$f'_{y,i,j} = D_{y,i,j} \frac{\tilde{C}_{i,j+1} - 2\tilde{C}_{i,j} + \tilde{C}_{i,j-1}}{\Delta y^2}$$

At the interior node P , value of $\tilde{C}_{i,j}$ is then solved

$$\tilde{C}_{i,j} = e^{-\frac{\lambda_{i,j}+p}{U_{i,j}}\Delta\eta} \tilde{C}_{P'} + \frac{f'_{x,i,j} + f'_{y,i,j} + (\tilde{S}_{i,j} + g_{i,j})}{\lambda_{i,j} + p} \left(1 - e^{-\frac{\lambda_{i,j}+p}{U_{i,j}}\Delta\eta} \right) \quad (4.6)$$

Applying linear interpolation for \tilde{C}_p and substituting the finite difference approximation for diffusion terms in equation (4.4), the solution which includes nodal values is derived as

$$\begin{aligned} \tilde{C}_{i,j} = & (R'_{p'} r_{i,j})\tilde{C}_{i-1,j-1} + [R'_{p'}(1-r_{i,j}) + R'_x]\tilde{C}_{i-1,j} + (0)\tilde{C}_{i-1,j+1} + (R'_y)\tilde{C}_{i,j-1} + \\ & (R'_y)\tilde{C}_{i,j+1} + (0)\tilde{C}_{i+1,j-1} + (R'_y)\tilde{C}_{i+1,j} + (0)\tilde{C}_{i+1,j+1} + R'_s \end{aligned} \quad (4.7)$$

where

$$R'_0 = 1 + \left[\frac{2D_{x_{i,j}}}{(\lambda_{i,j} + p)\Delta x^2} + \frac{2D_{y_{i,j}}}{(\lambda_{i,j} + p)\Delta y^2} \right] \left[1 - e^{-\frac{(\lambda_{i,j}+p)\Delta\eta}{U_{i,j}}} \right] \quad (4.8)$$

$$R'_{p'} = e^{-\frac{(\lambda_{i,j}+p)\Delta\eta}{U_{i,j}}} \frac{1}{R'_0} \quad (4.9)$$

$$R'_x = \frac{D_{x_{i,j}}}{(\lambda_{i,j} + p)\Delta x^2} \left[1 - e^{-\frac{(\lambda_{i,j}+p)\Delta\eta}{U_{i,j}}} \right] \frac{1}{R'_0} \quad (4.10)$$

$$R'_y = \frac{D_{y_{i,j}}}{(\lambda_{i,j} + p)\Delta y^2} \left[1 - e^{-\frac{(\lambda_{i,j}+p)\Delta\eta}{U_{i,j}}} \right] \frac{1}{R'_0} \quad (4.11)$$

$$R'_{i,j} = \frac{\tilde{S}_{i,j} + g_{i,j}}{(\lambda_{i,j} + p)} \left[1 - e^{-\frac{(\lambda_{i,j}+p)\Delta\eta}{U_{i,j}}} \right] \frac{1}{R'_0} \quad (4.12)$$

As stated in Chapter 3, steady-state finite analytic solution based on linear interpolation has eight different cases in the local element depending on the value of $r_{i,j}$

and the direction of the flow. The following formulations are for Cases 2 to 8, developed from the local element.

Case 2, when $r_{ij} \leq 1$, $u_{ij} > 0$, and $v_{ij} < 0$,

$$\begin{aligned} \tilde{C}_{i,j} = & (0) \tilde{C}_{i-1,j-1} + [R'_{p'}(1-r_{i,j}) + R'_x] \tilde{C}_{i-1,j} + (R'_{p'} r_{i,j}) \tilde{C}_{i-1,j+1} + (R'_y) \tilde{C}_{i,j-1} + \\ & (R'_y) \tilde{C}_{i,j+1} + (0) \tilde{C}_{i+1,j-1} + (R'_y) \tilde{C}_{i+1,j} + (0) \tilde{C}_{i+1,j+1} + R'_{i,j} \end{aligned} \quad (4.13)$$

Case 3, when $r_{ij} \leq 1$, $u_{ij} < 0$, and $v_{ij} < 0$,

$$\begin{aligned} \tilde{C}_{i,j} = & (0) \tilde{C}_{i-1,j-1} + (R'_x) \tilde{C}_{i-1,j} + (0) \tilde{C}_{i-1,j+1} + (R'_y) \tilde{C}_{i,j-1} + \\ & (R'_y) \tilde{C}_{i,j+1} + (0) \tilde{C}_{i+1,j-1} + [R'_{p'}(1-r_{i,j}) + R'_x] \tilde{C}_{i+1,j} + (R'_{p'} r_{i,j}) \tilde{C}_{i+1,j+1} + R'_{i,j} \end{aligned} \quad (4.14)$$

Case 4, when $r_{ij} \leq 1$, $u_{ij} < 0$, and $v_{ij} \geq 0$,

$$\begin{aligned} \tilde{C}_{i,j} = & (0) \tilde{C}_{i-1,j-1} + (R'_x) \tilde{C}_{i-1,j} + (0) \tilde{C}_{i-1,j+1} + (R'_y) \tilde{C}_{i,j-1} + \\ & (R'_y) \tilde{C}_{i,j+1} + (R'_{p'} r_{i,j}) \tilde{C}_{i+1,j-1} + [R'_{p'}(1-r_{i,j}) + R'_x] \tilde{C}_{i+1,j} + (0) \tilde{C}_{i+1,j+1} + R'_{i,j} \end{aligned} \quad (4.15)$$

Note that $\Delta\eta$ expressed as equation (3.12) for Cases 1 to 4.

Case 5, when $r_{ij} > 1$, $u_{ij} \geq 0$, and $v_{ij} > 0$,

$$\begin{aligned} \tilde{C}_{i,j} = & (R'_{p'} r'_{i,j}) \tilde{C}_{i-1,j-1} + (R'_x) \tilde{C}_{i-1,j} + (0) \tilde{C}_{i-1,j+1} + [R'_{p'}(1-r'_{i,j}) + R'_y] \tilde{C}_{i,j-1} + \\ & (R'_y) \tilde{C}_{i,j+1} + (0) \tilde{C}_{i+1,j-1} + (R'_x) \tilde{C}_{i+1,j} + (0) \tilde{C}_{i+1,j+1} + R'_{i,j} \end{aligned} \quad (4.16)$$

Case 6, when $r_{ij} > 1$, $u_{ij} < 0$, and $v_{ij} > 0$,

$$\begin{aligned} \tilde{C}_{i,j} = & (0)\tilde{C}_{i-1,j-1} + (R'_x)\tilde{C}_{i-1,j} + (0)\tilde{C}_{i-1,j+1} + [R'_{p'}(1-r'_{i,j}) + R'_y]\tilde{C}_{i,j-1} + \\ & (R'_y)\tilde{C}_{i,j+1} + (R'_{p'} r'_{i,j})\tilde{C}_{i+1,j-1} + (R'_x)\tilde{C}_{i+1,j} + (0)\tilde{C}_{i+1,j+1} + R'_{i,j} \end{aligned} \quad (4.17)$$

Case 7, when $r_{ij} > 1$, $u_{ij} > 0$, and $v_{ij} < 0$,

$$\begin{aligned} \tilde{C}_{i,j} = & (0)\tilde{C}_{i-1,j-1} + (R'_x)\tilde{C}_{i-1,j} + (R'_{p'} r'_{i,j})\tilde{C}_{i-1,j+1} + (R'_y)\tilde{C}_{i,j-1} + \\ & [R'_{p'}(1-r'_{i,j}) + R'_y]\tilde{C}_{i,j+1} + (0)\tilde{C}_{i+1,j-1} + (R'_x)\tilde{C}_{i+1,j} + (0)\tilde{C}_{i+1,j+1} + R'_{i,j} \end{aligned} \quad (4.18)$$

Case 8, when $r_{ij} > 1$, $u_{ij} < 0$, and $v_{ij} < 0$,

$$\begin{aligned} \tilde{C}_{i,j} = & (0)\tilde{C}_{i-1,j-1} + (R'_x)\tilde{C}_{i-1,j} + (0)\tilde{C}_{i-1,j+1} + (R'_y)\tilde{C}_{i,j-1} + \\ & [R'_{p'}(1-r'_{i,j}) + R'_y]\tilde{C}_{i,j+1} + (0)\tilde{C}_{i+1,j-1} + (R'_x)\tilde{C}_{i+1,j} + (R'_{p'} r'_{i,j})\tilde{C}_{i+1,j+1} + R'_{i,j} \end{aligned} \quad (4.19)$$

Note that $\Delta\eta$ for Case 5 to 8 can be expressed as equation (3.13)

The overall numerical solution may be summarized as

$$\tilde{C}_{i,j} = \sum_{\substack{l \neq i \\ m \neq j}} a_{lm} \tilde{C}_{lm} + R'_{i,j} \quad (4.20)$$

where a_{lm} is analytical coefficient, and $R'_{i,j}$ is the influence from source/sink.

The formulations of finite analytic solution using linear interpolation boundary approximation are derived for the transformed “steady-state” advection-diffusion equation. The transformed concentration \tilde{C}_{ij} in the Laplace domain must be converted back to the concentration C_{ij} at the same time level, so that the time-dependent variable $C(i,j,t)$ at node (i,j) is available for any further analysis for physical problems.

4.2.4. Numerical Laplace Inversion

In order to obtain the concentration as a function of location and time, the solution (4.7) needs to be inverted. The inverse Laplace transform $C(x, y, t)$ is given by the following well-known inversion formula

$$C(x, y, t) = \frac{1}{2\pi} \int_{-j\infty}^{+j\infty} e^{pt} \tilde{C}(x, y, p) dp \quad (4.21)$$

or, alternatively

$$C(x, y, t) = \frac{e^{vt}}{\pi} \int_0^{\infty} \left\{ \operatorname{Re} [\tilde{C}(x, y, p)] \cos \omega t - \operatorname{Im} [\tilde{C}(x, y, p)] \sin \omega t \right\} d\omega \quad (4.22)$$

where Re and Im denote respectively the real and imaginary parts of their arguments and j is the pure imaginary number: $j = (-1)^{1/2}$. Using a trapezoidal rule with a step size of π/T , the following approximation is obtained

$$C(x, y, t) \approx \frac{e^{vt}}{T} \left\{ \begin{aligned} & -\frac{1}{2} \operatorname{Re} [\tilde{C}(x, y, p)] + \sum_{m=0}^{N_p} \operatorname{Re} \left[\tilde{C} \left(x, v + i \frac{m\pi}{T} \right) \right] \cos \frac{m\pi}{T} t \\ & - \sum_{m=0}^N \operatorname{Im} \left[\tilde{C} \left(x, v + i \frac{m\pi}{T} \right) \right] \sin \frac{m\pi}{T} t \end{aligned} \right\} \quad (4.23)$$

Here, T is the maximum simulation time.

Experience by Sudhicky [1989] in using the inversion formula (4.23) for a wide range of input transport parameters, different boundary condition types and different modes of mass release suggests the following expression of v is adequate for general purposes

$$v = -\ln \left(\frac{1}{1.6t_{\max}} \right) \quad (4.24)$$

where $E = 10^{-6}$ and t_{max} is the maximum simulation time.

Equation (4.23) is the basis of many existing Laplace transform inversion algorithms [Li et al., 1992]. Note that the infinite series have been truncated to N_p terms. The summation kernels in these truncated series may be highly oscillatory. A disadvantage with evaluation of (4.23) is the extremely slow convergence of the series expression, with adverse implications for both accuracy and computation time. Generally, the value of N_p for a typical problem is of the order of 10^3 .

However, numerous algorithms have been developed in an effort to accelerate the convergence of equation (4.23) [Crump, 1976; De Hoog et al., 1982]. Crump [1976] has shown that the truncation error in equation (4.23) can be significantly reduced, and convergence therefore accelerated, in the finite series approximation by means of the epsilon algorithm. Experience by Li et al. [1992] and by Sudicky [1989] using the Crump algorithm to perform the Laplace transform inversion shows that the value of N_p needed for adequate accuracy is dramatically reduced to approximately 7 to 40. An alternative and more robust technique, quotient difference algorithm [De Hoog et al., 1982], was demonstrated to be greatly superior to the epsilon scheme for reducing oscillations of the inverse in the neighborhood of a discontinuity (i.e., sharp front) and is in general more efficient because a smaller N_p is required to achieve a level of accuracy similar to that obtained with the epsilon method.

The Laplace transform can also be applied with the finite analytic improved linear interpolation approximation method to solve the transient advection-dominated solute transport problems. Details of the formulation development are not described in this work.

4.3. Discussion

The Laplace transform, when applied to the unsteady partial differential equation, takes away the temporal term analytically, and leaves the remaining equation in a “steady-state” form. This transformed “steady-state” equation can then be solved by finite analytic

methods. Taking Laplace transform for the temporal part of the transient equation differs from using other approximation methods, because there is no accumulated numerical diffusion on the temporal term at every time step.

The improved finite analytic/Laplace transform method will have significant improvement compared with the finite analytic/finite difference hybrid method [Chen and Chen, 1982], when solving advection-dominated cases. Although some good algorithms are used for the numerical inversion, the computer CPU time necessary to evaluate the inverse transform is still a concern or problem.

Chapter 5

Examples, Results and Discussion

This chapter demonstrates the performance of the new finite analytic methods by applying them for predicting solute transport in homogeneous as well as heterogeneous porous media. The results are systematically compared with those obtained with both the existing finite analytic method and the conventional upwind finite difference method.

5.1. Problem Definition

Consider solute transport at a synthetic hazardous waste site shown in Figure 5-1. The domain is $100\text{ m} \times 100\text{ m}$ in size. The waste source is a $8\text{ m} \times 8\text{ m}$ rectangular area represented as a continuous aerial source. Solute source concentration is assumed steady

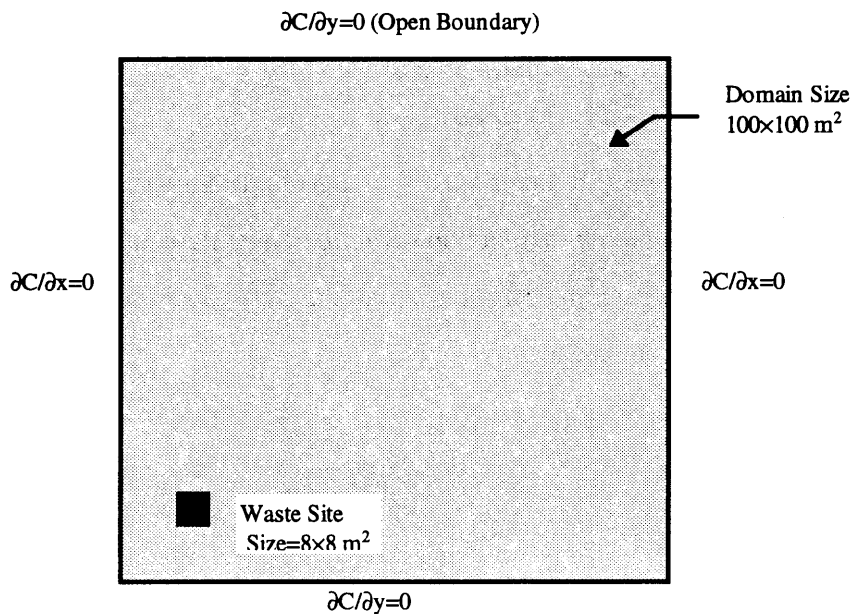


Figure 5-1: Domain of interest and boundary conditions

and constant at the solubility level of 1 ppm and, in the domain of interest, the corresponding solute concentration plume has reached a steady state. The boundaries of simulation are assumed sufficiently far away from the source that concentration gradient can be assumed small and thus a no dispersive solute flux boundary condition can be approximately used at all four boundaries. This type of boundary condition is often called "open" boundary condition since solute plume can still migrate across the site boundaries.

Recognizing that subsurface environment at real field sites are characteristically heterogeneous, the real test for the improved finite-analytic methods lies in their ability and robustness in predicting solute transport in nonuniform, especially, strongly nonuniform, velocity fields. To mimic the extremely variable nature of subsurface environment, log transmissivity is represented as spatially correlated random field characterized by its mean $\ln K$, variance $\sigma_{\ln K}$ and correlation scales λ_x and λ_y . A spatially correlated random field can be roughly visualized as a periodic field with an random amplitude and a random period. The correlation scale corresponds to the mean period and standard deviation (square root of the variance) corresponds to mean amplitude of fluctuation. Transport in a random field provides a stringent test of the new method. Most numerical methods fails when used for predicting solute transport realizations of a random field, especially when log transmissivity variance is high and when correlation scales are small.

Some model parameters like total grid points and site parameters for the nonuniform field are tabulated in Table 5-1.

As discussed in chapter 1, variability in transmissivity translates into variability in groundwater velocity, which in turns causes solute plume irregularity. This work focuses on transport predictions and no attempt is made to predict groundwater flow in heterogeneous media. Given statistics of log transmissivity, the corresponding velocity field is here generated using an existing cross-correlated random field generator developed by Ruan [Ruan, 1994].

The new finite analytic method, along with existing finite analytic method and the conventional upwind method, is used to predict leachate plume migration at the site. The results are summarized in Figure 5-2 through 5-18.

Table 5-1: Total Grid Points and Site Parameters for Nonuniform Fields.

Parameter	Value
Domain length (x direction)	100 (m)
Domain width (y direction)	100 (m)
Number of grids in x direction (for methods comparison)	100
Number of grids in y direction (for methods comparison)	100
Porosity	0.3
Geometric mean transmissivity conductivity	7.4 (m ² /day)
Correlation scales ($\lambda_x=\lambda_y$)	8.0 (m)
Regional mean hydraulic gradient	0.002

5.2. Numerical Results

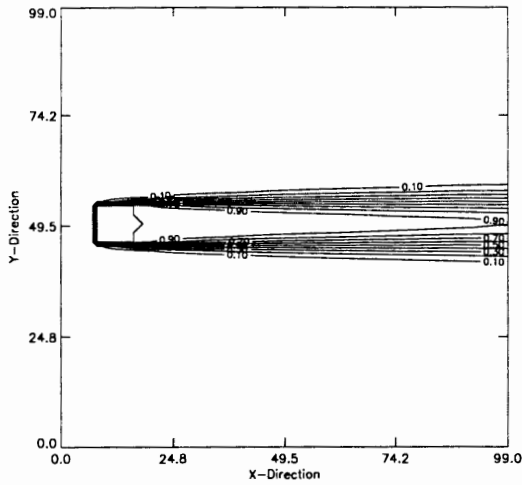
Figures 5-2 and 5-3 shows the predicted plume when mean flow is aligned with x -axis at the site using, respectively, the improved finite analytic method (with linear interpolation), the existing finite analytic method and the upwind method. Figure 5-4 shows the plots of the log mean hydraulic conductivity and highly variable velocity fields that are used in Figure 5-3. Note that the log mean hydraulic conductivity fields plotted here and latter are shown qualitatively. Value r represents the mean flow direction. The mean flow Peclet numbers, which are the products of the mean flow velocity and the dispersion coefficient, are 20 for the uniform flow and 16.7 for the nonuniform flow, and the variance of log transmissvity is 1.5. All three methods tested in this case performs well especially in the case of uniform flow. In fact, as has been shown in Chapter 3, for conservative solute transport in a uniform flow aligned with x coordinate axis, the upwind

method is identical to the improved finite analytic method with the simple linear boundary interpolation. In Figure 5-3, solution from upwind finite difference method in the case of nonuniform flow shows more numerical dispersion than those obtained from the finite analytic methods. This is because flow in this case does not always go along the axis and upwind solution degrades significantly when flow direction is not aligned with the coordinate axis as will be discussed in the next paragraph. The two finite analytic methods perform well here and the improved finite analytic method is as accurate as the existing finite analytic.

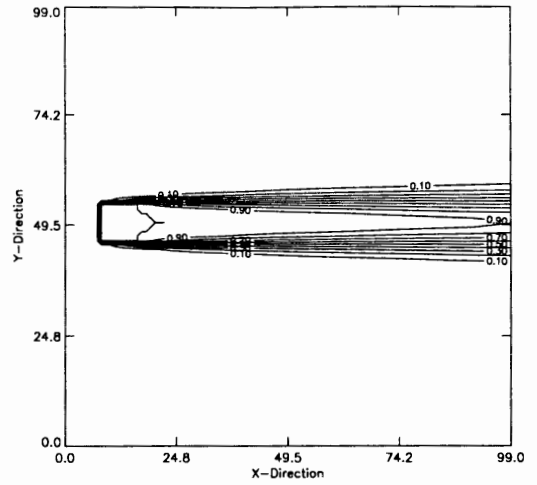
Figure 5-5 through Figure 5-7 show plume predictions obtained from the same three methods when mean flow direction is at an angle with x direction and with $r = 0.5$. Figure 5-8 is the random flow field realization corresponding to the nonuniform field used in Figures 5-6 and 5-7. The mean flow Peclet number in x and y direction are 20 and 10 for uniform flow, and 16.7 and 8.5 for nonuniform flow, respectively. The "exact" plume in Figure 5-5 is also presented for comparison (note results from a fine resolution simulation by the improved finite analytic methods are used as "exact" solution for comparison). In these cases, the performance of upwind method degrades, while both the improved and existing finite analytic methods remain reasonably accurate. Although for some cases, the existing finite analytic performs slightly better, because for $r = 0.5$, the improved finite analytic methods with linear interpolation has the worst case scenario. However, the finite analytic methods may be considered of the same accuracy especially under nonuniform flow. The upwind solution shown in Figure 5-5 is more dispersive than the exact solution. This is caused by the fact that upwind method does not make use of the corner nodes in the computational element when information propagates from upstream.

In Figure 5-7 mean Peclet numbers were raised up to 83.4 and 41.7 respectively in the x and y directions. Note that the plume by the existing finite analytic method is not shown because the output result does not exist due to over-flow point computer error.

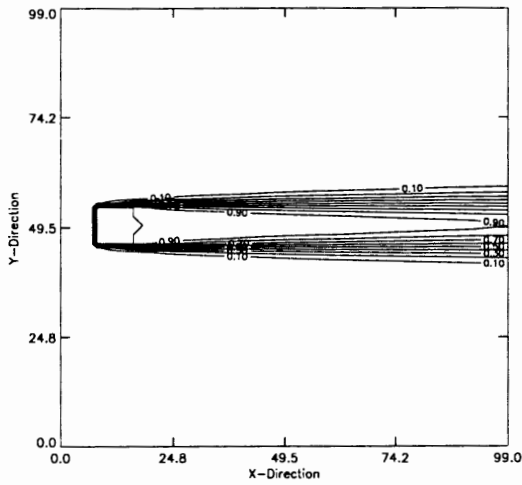
In order to test the highest range of Peclet values the existing finite analytic exponential and linear approximation method can handle, and to find out and compare



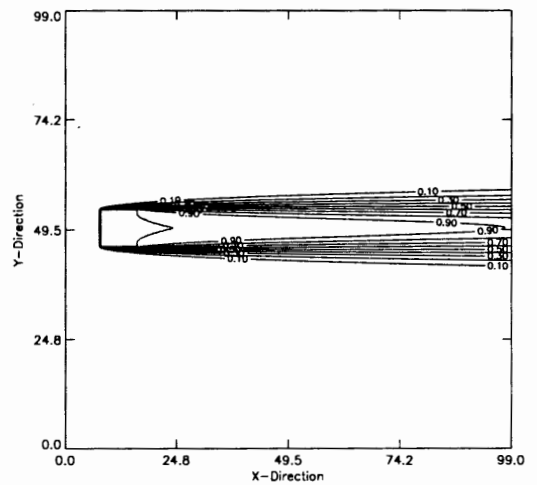
a. Upwind Finite Difference Method



b. Existing Finite Analytic Method

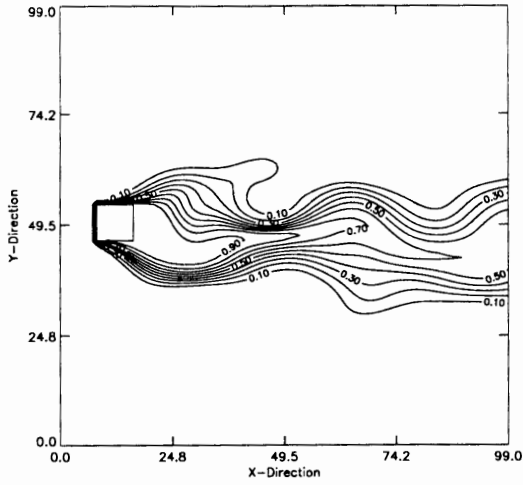


c. Finite Analytic Method with Basic Linear Interpolation

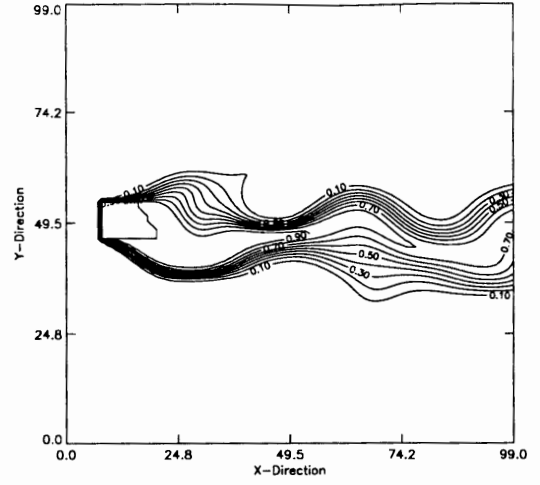


d. "Exact" Solution (Total Number of Grid Points = 500 x 500)

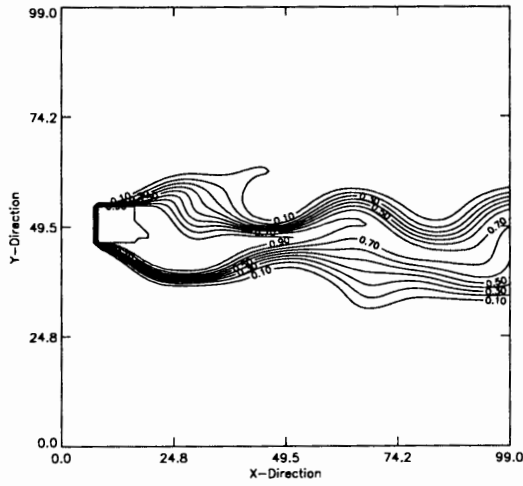
Figure 5-2: Solute transport in homogeneous porous media for $r = 0$ (Peclet number: $Pe_x = 20$)



a. Upwind Finite Difference Method

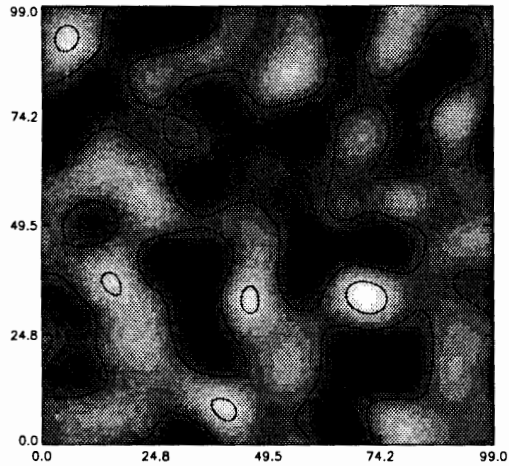


b. Existing Finite Analytic Method



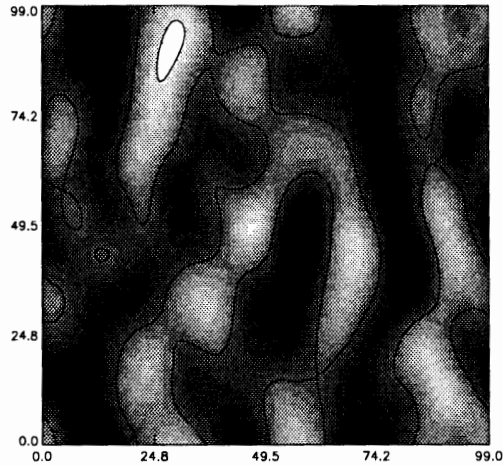
c. Finite Analytic Method with Basic Linear Interpolation

**Figure 5-3: Solute transport in heterogeneous porous media for $r = 0$
($\sigma_{LK}^2 = 1.0$; mean Peclet numbers: $Pe_x = 16.7$, $Pe_y = 0.0$)**



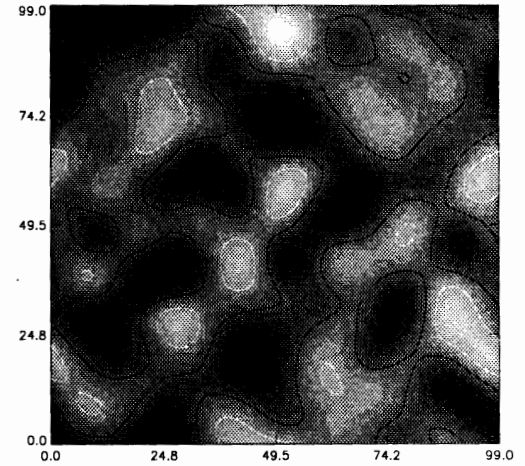
a. LnK

Value Range (Black - White): (-3.0, 2.5)



b. Velocity u

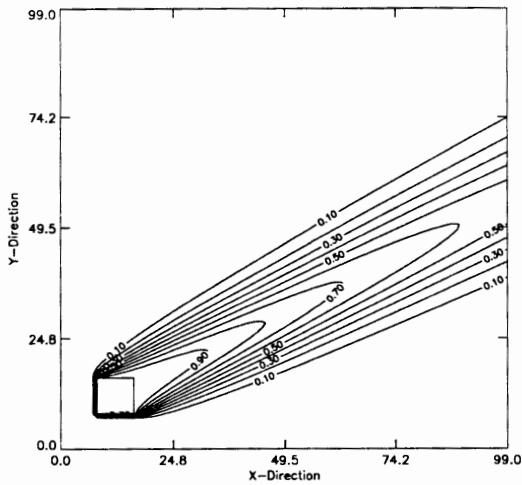
Value Range (Black - White): (-0.03, 0.12)



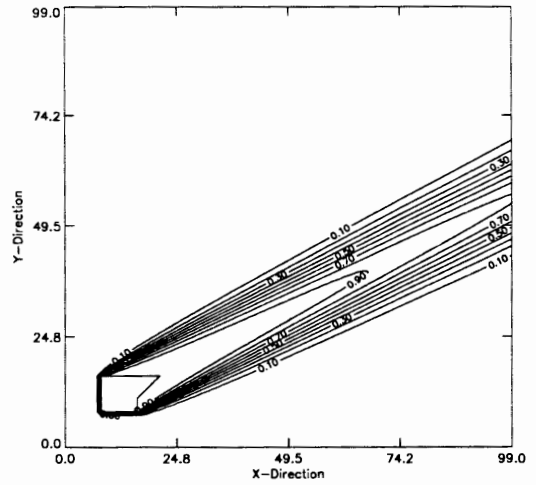
c. Velocity v

Value Range (Black - White): (-0.03, 0.05)

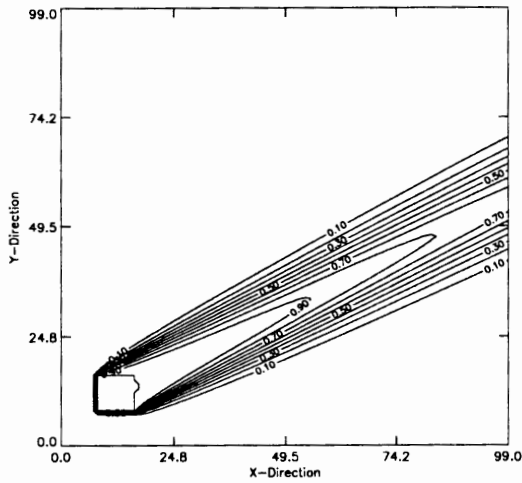
Figure 5-4: Highly variable velocity flow field realization
 ($\lambda_x = \lambda_y = 8.0$ m; $\sigma^2_{Lnk} = 1.5$; mean flow velocities: $u_0 = 0.0417$ m/day, $v_0 = 0.0$ m/day)



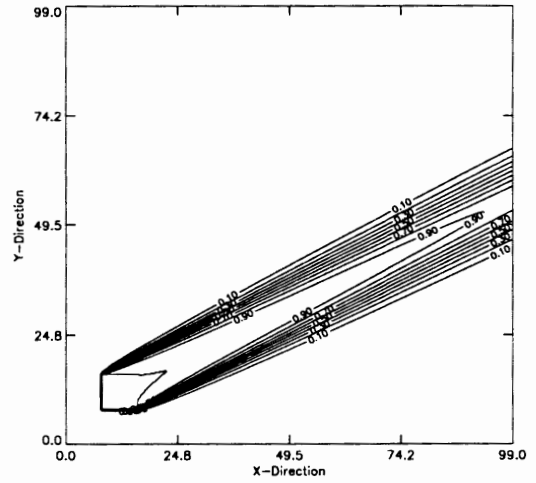
a. Upwind Finite Difference Method



b. Existing Finite Analytic Method

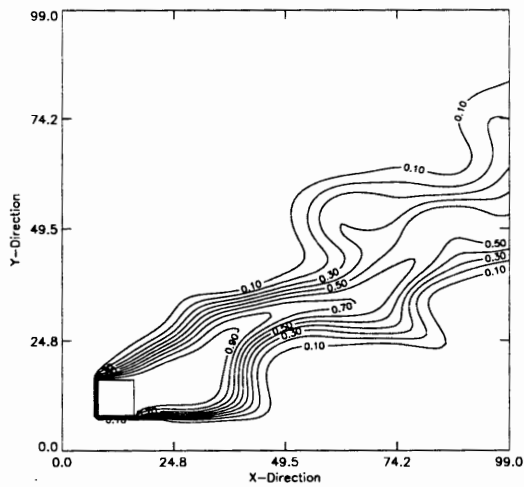


c. Finite Analytic Method with Linear Interpolation

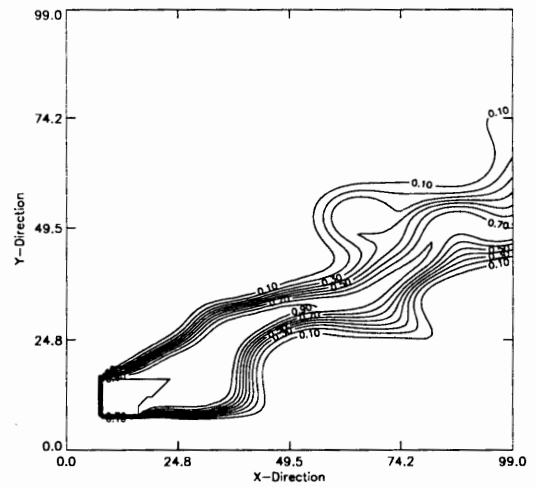


d. "Exact" Solution (Total Number of Grid Points = 500 x 500)

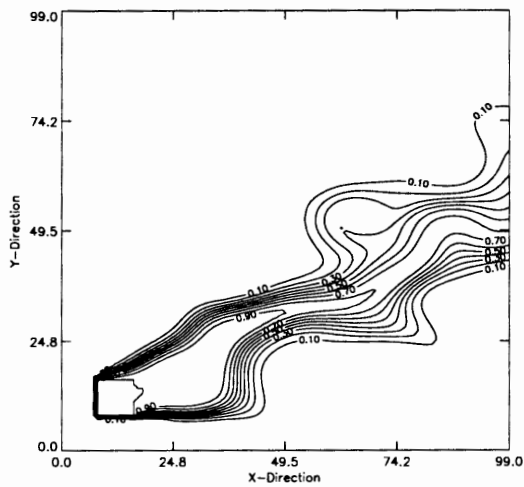
Figure 5-5: Solute transport in heterogeneous porous media for $r = 0.5$ (Peclet numbers: $Pe_x = 20$, $Pe_y = 10$)



a. Upwind Finite Difference Method

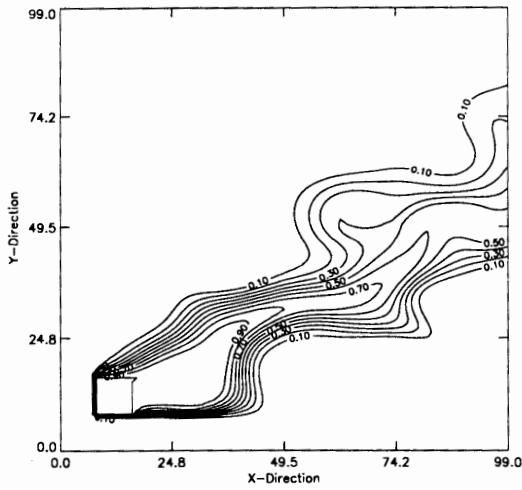


b. Existing Finite Analytic Method

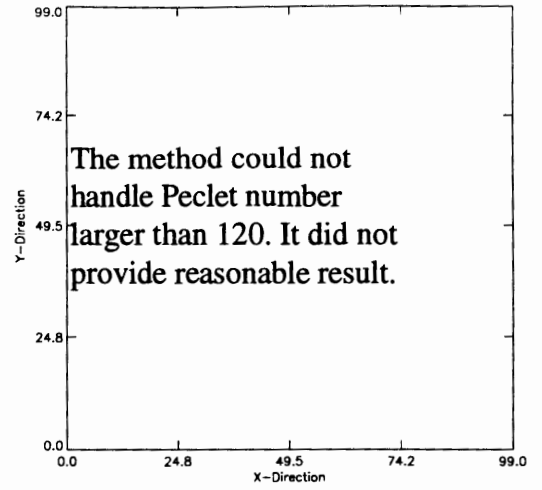


c. Finite Analytic Method with Basic Linear Interpolation

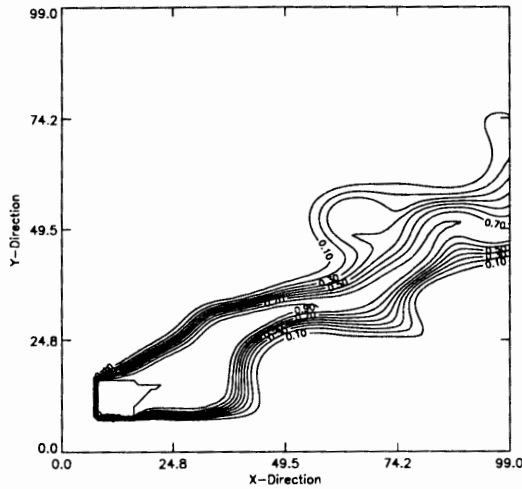
**Figure 5-6: Solute transport in heterogeneous porous media for $r = 0.5$
 $(\sigma_{LK}^2 = 1.5; \text{mean Peclet numbers: } Pe_x = 16.7, Pe_y = 8.34)$**



a. Upwind Finite Difference Method

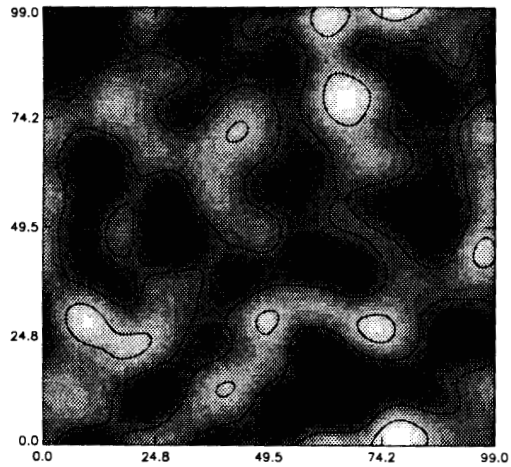


b. Existing Finite Analytic Method



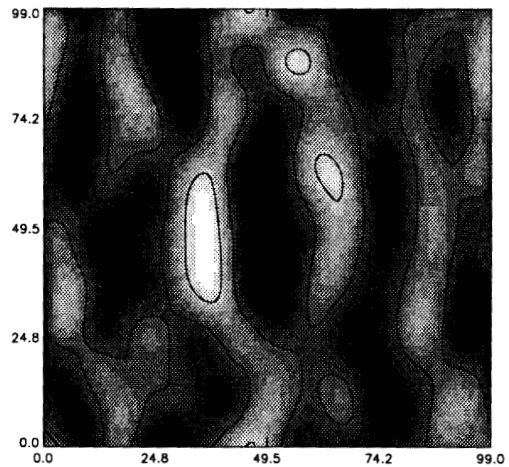
c. Finite Analytic Method with Basic Linear Interpolation

Figure 5-7: Solution transport in heterogeneous porous media for $r = 0.5$ ($\sigma_{LnK}^2 = 1.5$; mean Peclet numbers: $Pe_x = 83.4$, $Pe_y = 41.7$)



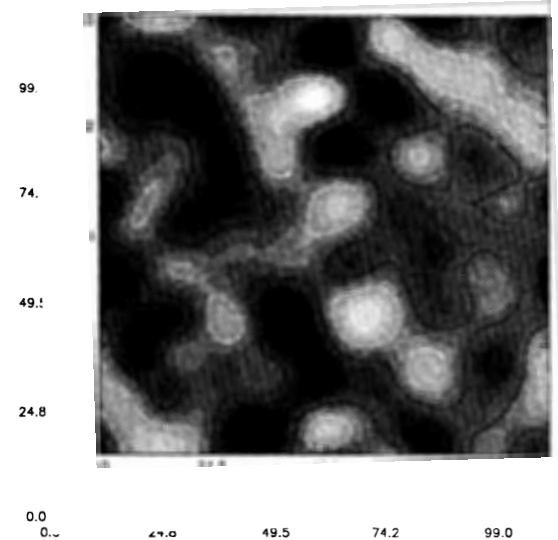
a. LnK

Value Range (Black -White): (-3.0, 3.0)



b. Velocity u

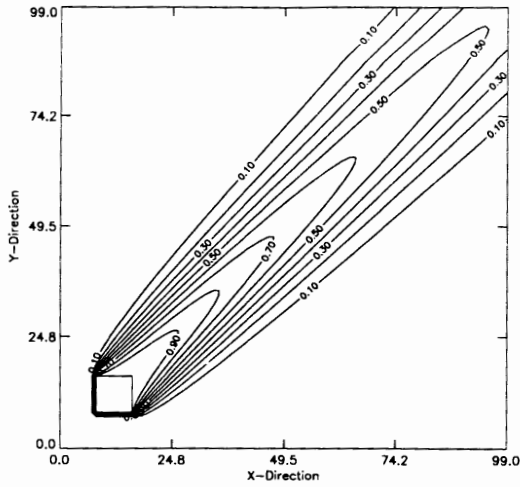
Value Range (Black -White): (-0.05, 0.12)



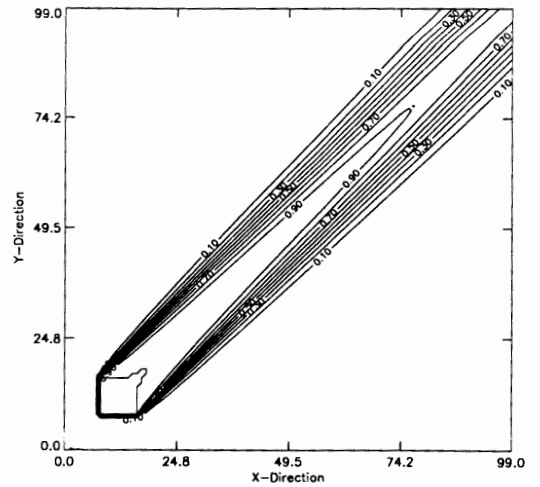
c. Velocity v

Value Range (Black -White): (-0.04, 0.08)

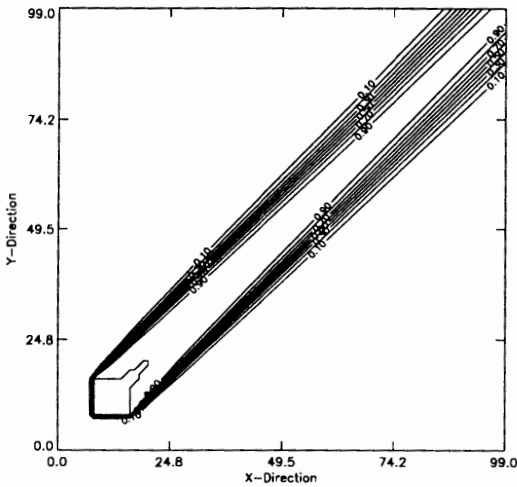
Figure 5-8: Highly variable velocity flow field realization
 ($\lambda_x = \lambda_y = 8.0$ m; $\sigma^2_{LnK} = 1.5$; mean flow velocities: $u_0 = 0.0417$ m/day, $v_0 = 0.0208$ m/day)



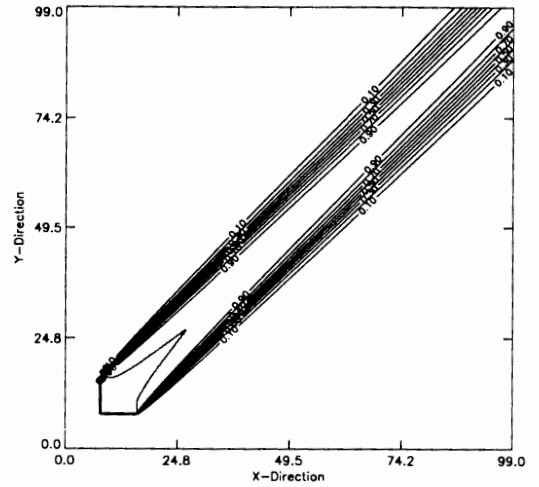
a. Upwind Finite Difference Method



c. Existing Finite Analytic Method

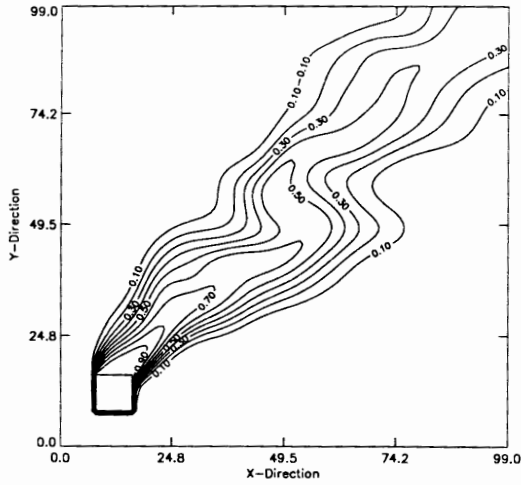


c. Finite Analytic Method with Basic Linear Interpolation

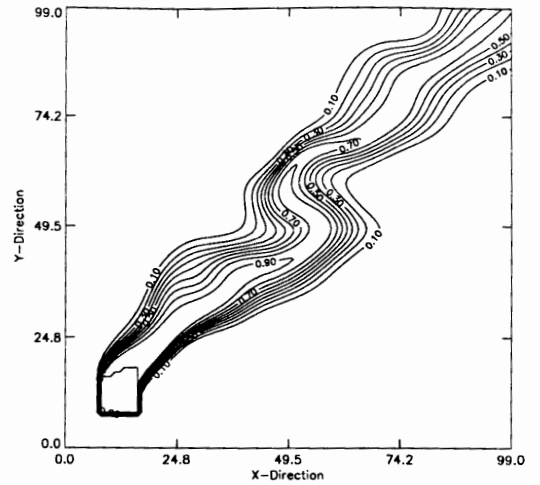


d. "Exact" Solution (Total Number of Grid Points = 500 x 500)

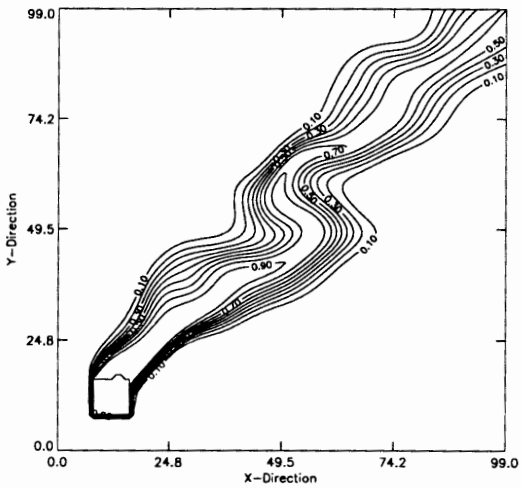
Figure 5-9: Solute transport in homogeneous porous media for $r = 1.0$ (Peclet numbers: $Pe_x = 20$, $Pe_y = 20$)



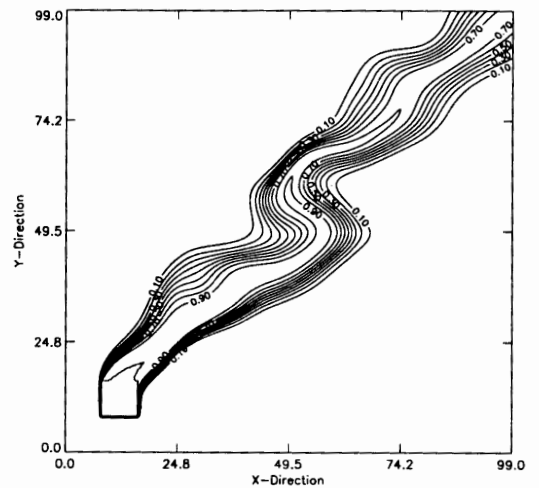
a. Upwind Finite Difference Method



b. Existing Finite Analytic Method

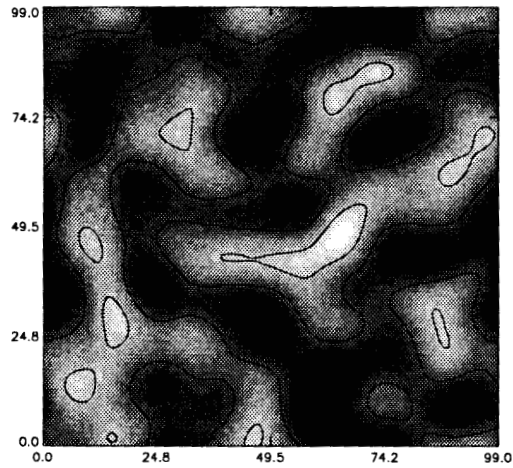


c. Finite Analytic Method with Basic Linear Interpolation



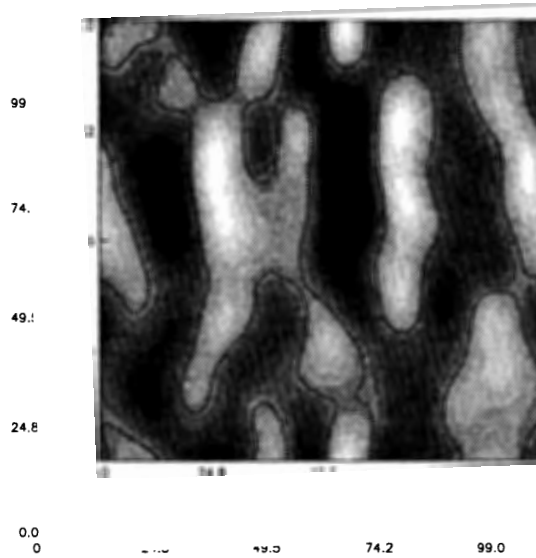
d. "Exact" Solution (Total Number of Grid Points = 400 x 400)

**Figure 5-10: Solution transport in heterogeneous porous media for $r = 1.0$
 $(\sigma_{L\&K}^2 = 1.5; \text{mean Peclet numbers: } Pe_x = 16.7, Pe_y = 16.7)$**



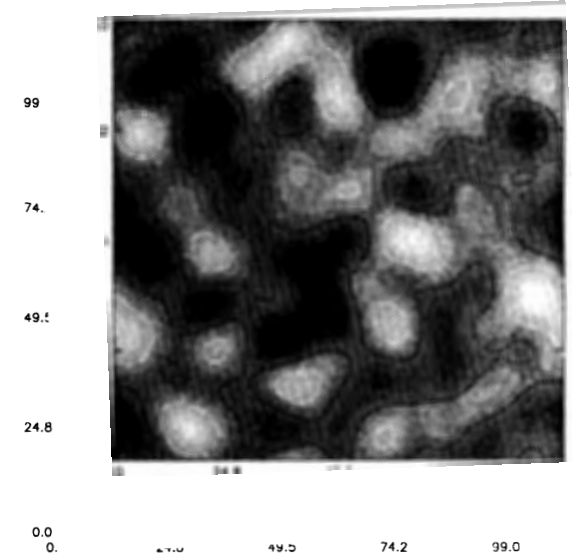
a. LnK

Value Range (Black -White): (-3.0, 3.0)



b. Velocity u

Value Range (Black -White): (-0.08, 0.12)



c. Velocity v

Value Range (Black -White): (-0.02, 0.1)

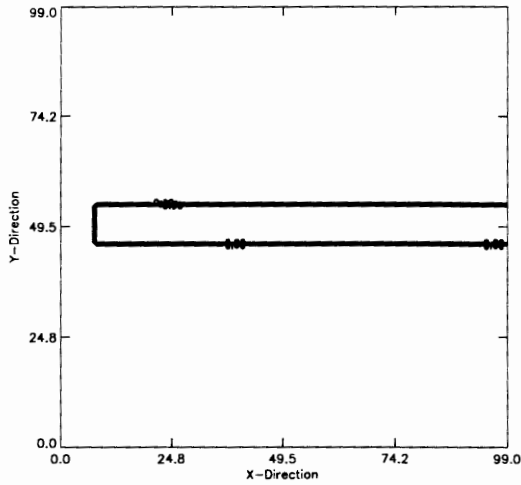
Figure 5-11: Highly variable velocity flow field realization
 ($\lambda_x = \lambda_y = 8.0$ m; $\sigma^2_{Lnk} = 1.5$; mean flow velocities: $u_0 = 0.0417$ m/day, $v_0 = 0.0417$ m/day)

that with the finite analytic linear interpolation method, both methods are applied to uniform velocity fields. The existing finite analytic method can only handle Peclet numbers up to 120 as mentioned in Chapter 2, while the improved finite analytic method can solve the problems with Peclet numbers greater than 1,000. When both Pe_x and Pe_y are greater than 120, any further summation of E_2 as written in equation (2.32) can not be obtained with enough accuracy because the computer used in double precision can provide an accuracy of 14 digits. Large round off error is found in calculating the series solution when Peclet number is large. In the extreme case the series may give such an erroneous value as to cause instability in the computation [Zhang and Chen, 1987]. The finite analytic linear interpolation method does not have this kind of problem because of the simplified boundary approximation and formulations.

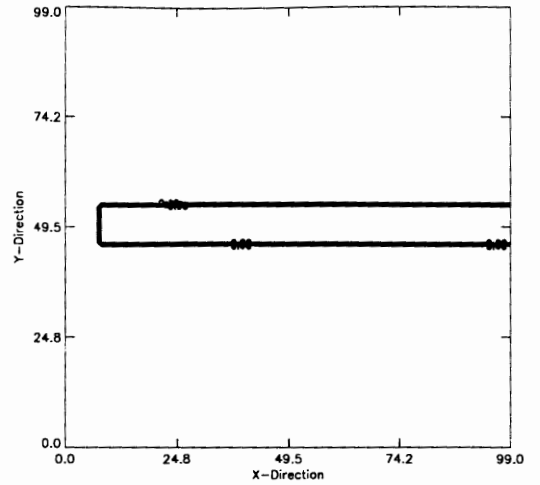
Therefore, when finite analytic exponential and linear boundary method is applied to highly variable velocity fields without causing run-time floating point errors, one has to make sure that the Peclet numbers in the entire domain will not exceed 120. Furthermore, the method is not applicable to pure advection cases due to the diffusion coefficient in the denominator in the equations (2.24) and (2.34) for coefficient A and B .

Figures 5-9 and 5-10 show the comparisons of finite analytic and upwind solutions when plume orientation is diagonal. In these flow conditions, upwind solution involves maximum numerical dispersion. Numerical dispersion becomes more and more significant further downstream away from the source. Note that the improved finite analytic solution is more accurate than the existing finite analytic method when compared to the “exact” solution, even when the diffusion portion of the transport equation is treated with standard finite difference.

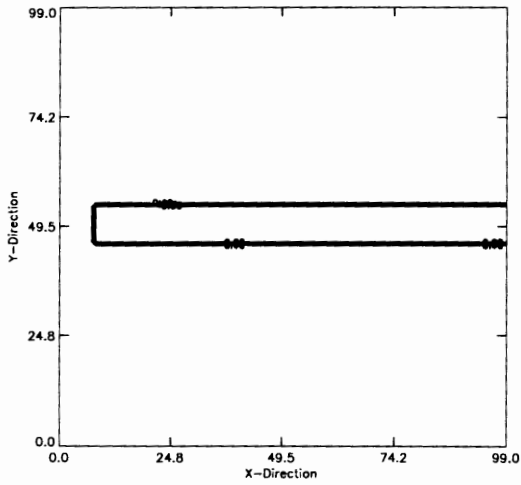
The above comparisons are done by comparing improved finite analytic (with basic linear interpolation) with upwind finite difference and existing finite analytic method. It is concluded that the new finite analytic method is as accurate as the existing one except for $r = 0.5$. Under the some circumstances, it actually performs even better than the existing



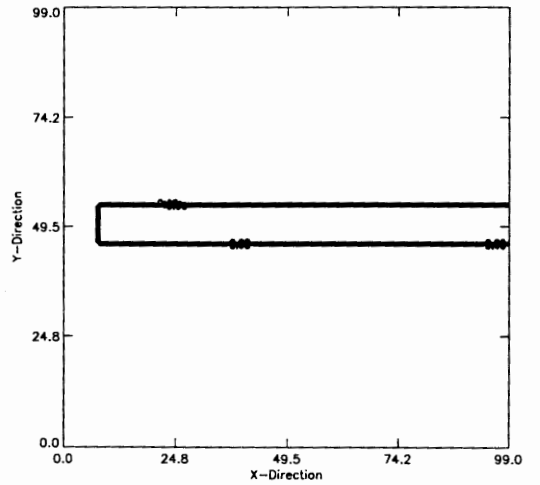
a. Upwind Finite Difference Method



b. Finite Analytic Method with Basic Linear Interpolation

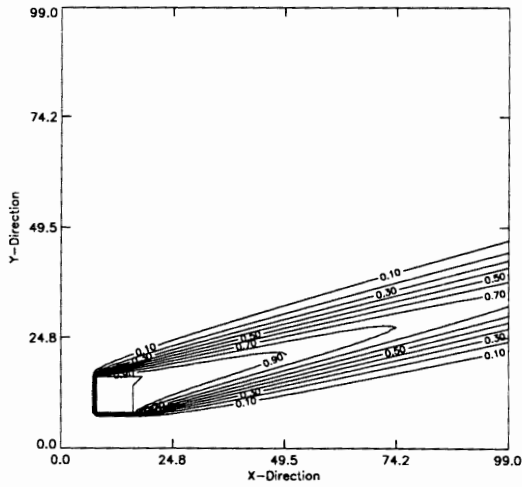


c. Finite Analytic Method with Improved Linear Interpolation

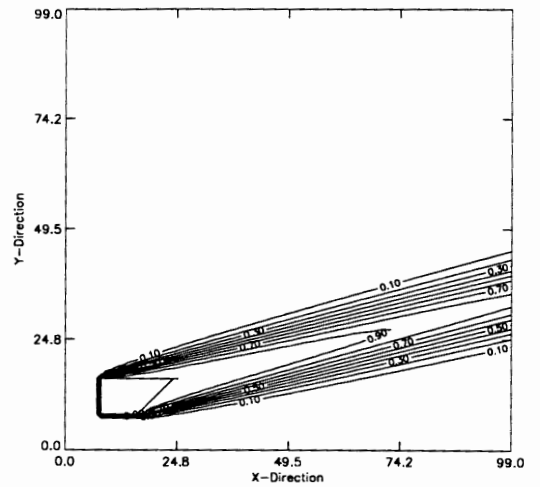


d. Exact Solution

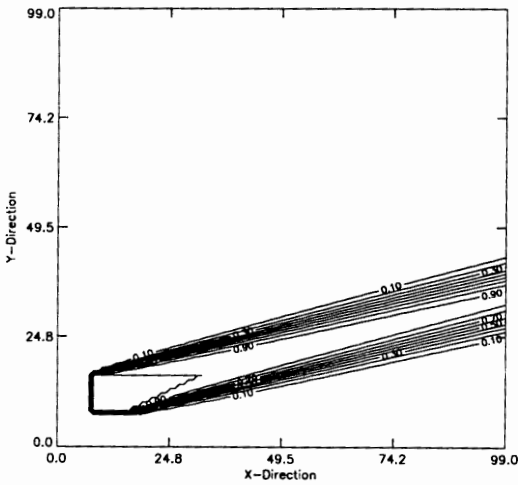
Figure 5-12: Solute transport in homogeneous porous media for $r = 0.0$ and $Pe \rightarrow \infty$



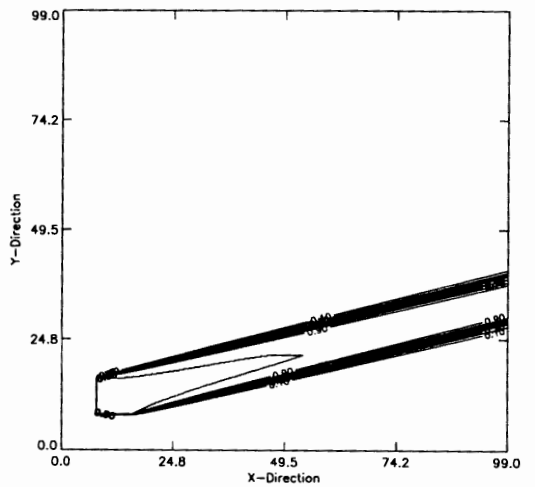
a. Upwind Finite Difference Method



b. Finite Analytic Method with Basic Linear Interpolation

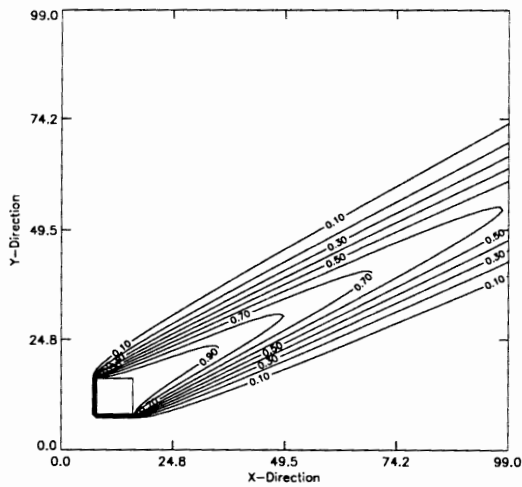


c. Finite Analytic Method with Improved Linear Interpolation

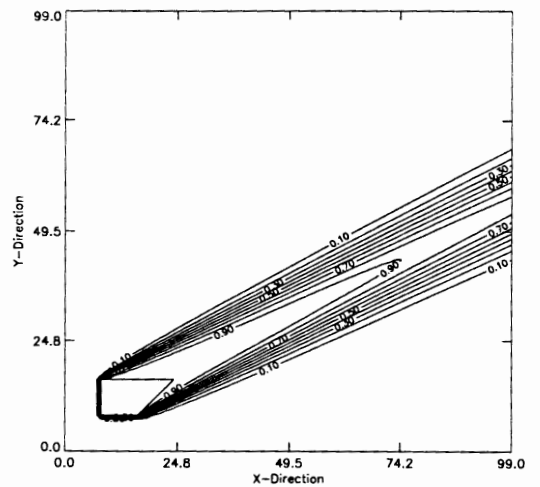


**d. "Exact" Solution
(Total Grid Points = 500 x 500)**

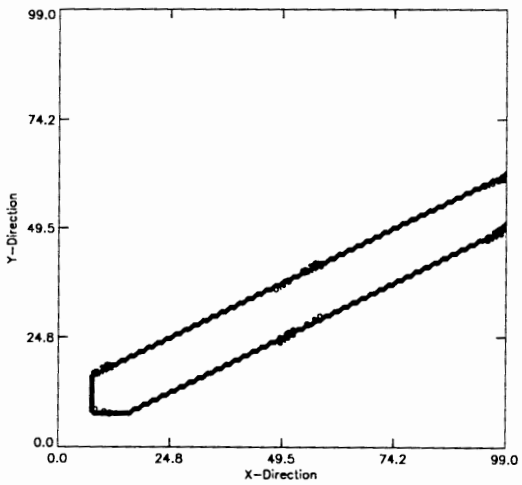
**Figure 5-13: Solute transport in homogeneous porous media
for $r = 0.25$ and $Pe \rightarrow \infty$**



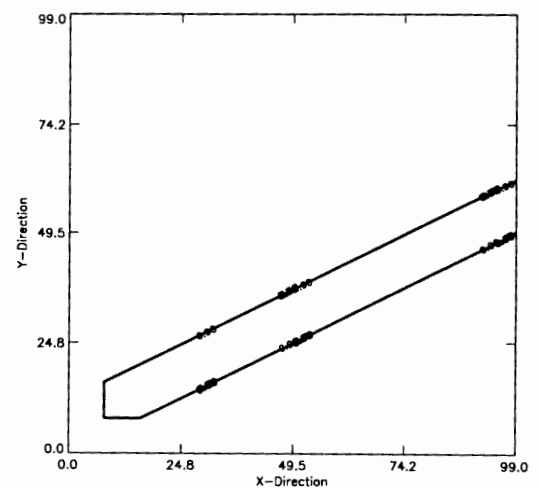
a. Upwind Finite Difference Method



b. Finite Analytic Method with Basic Linear Interpolation

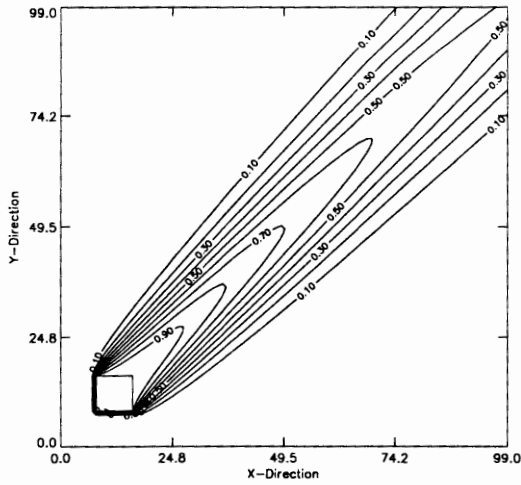


c. Finite Analytic Method with Improved Linear Interpolation

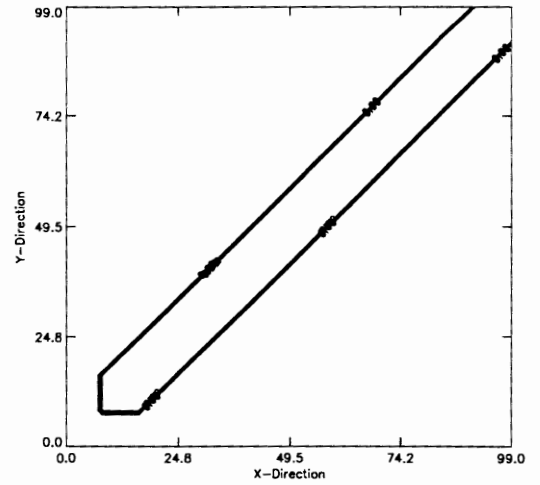


d. Exact Solution

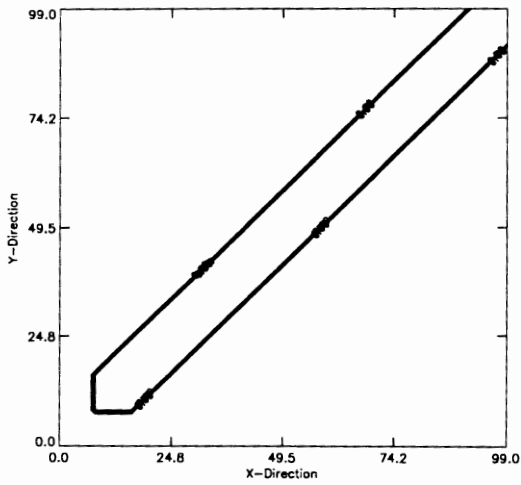
Figure 5-14: Solute transport in homogeneous porous media for $r = 0.5$ and $Pe \rightarrow \infty$



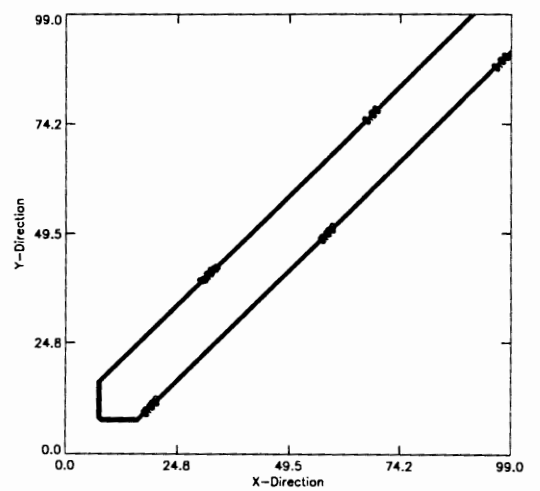
a. Upwind Finite Difference Method



b. Finite Analytic Method with Basic Linear Interpolation

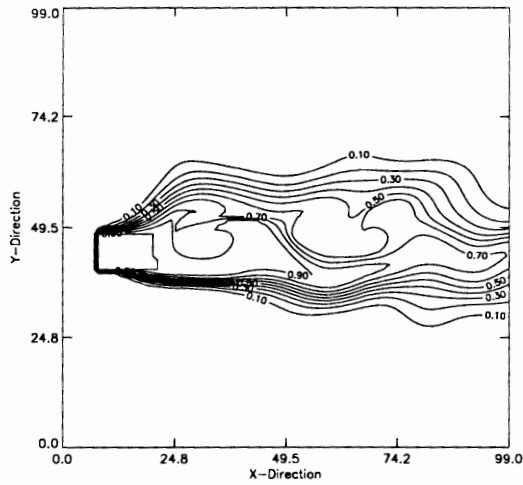


c. Finite Analytic Method with Improved Linear Interpolation

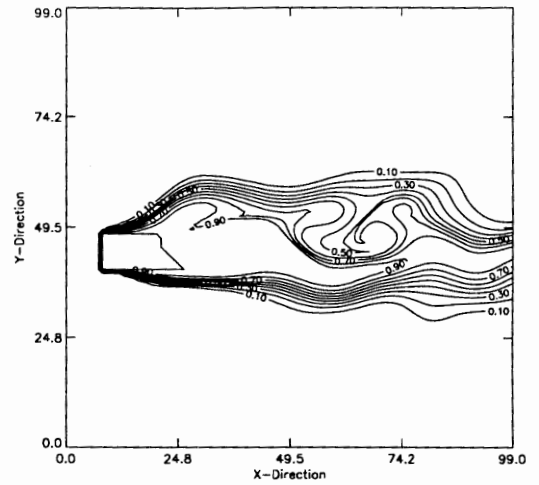


d. Exact Solution

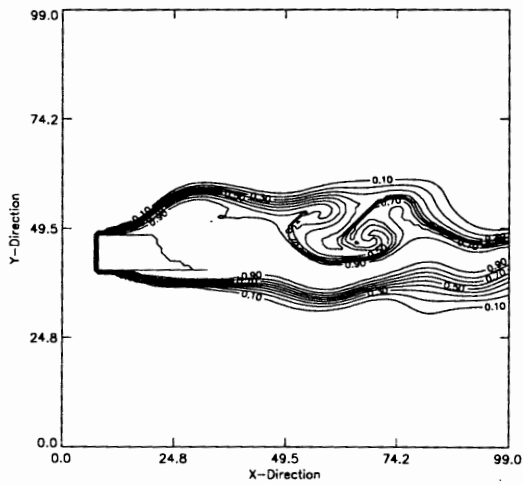
Figure 5-15: Solute transport in homogeneous porous media for $r = 1.0$ and $Pe \rightarrow \infty$



a. Upwind Finite Difference Method

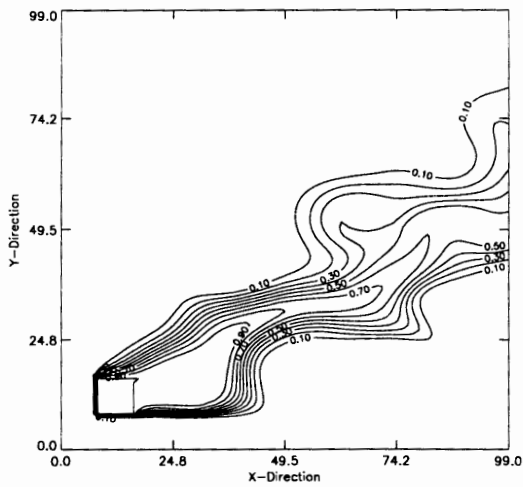


b. Finite Analytic Method with Basic Linear Interpolation

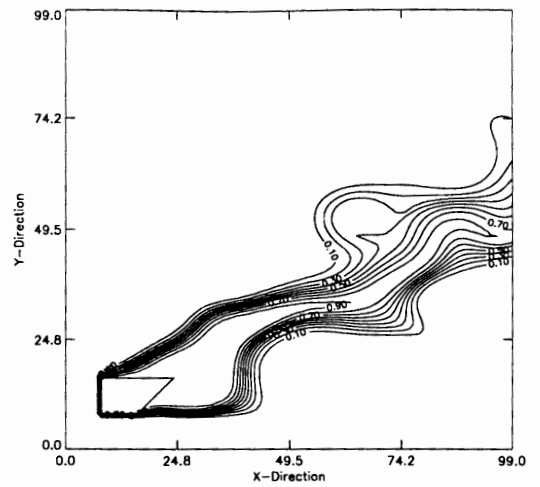


c. Finite Analytic Method with Improved Linear Interpolation

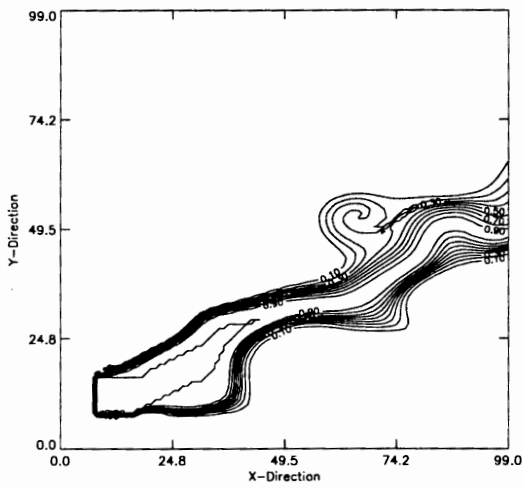
**Figure 5-16: Solute transport in heterogeneous porous media for $r = 0.0$
 $(\sigma_{LnK}^2 = 1.5; \text{mean flow velocity: } u_0 = 0.0417 \text{ m/day})$**



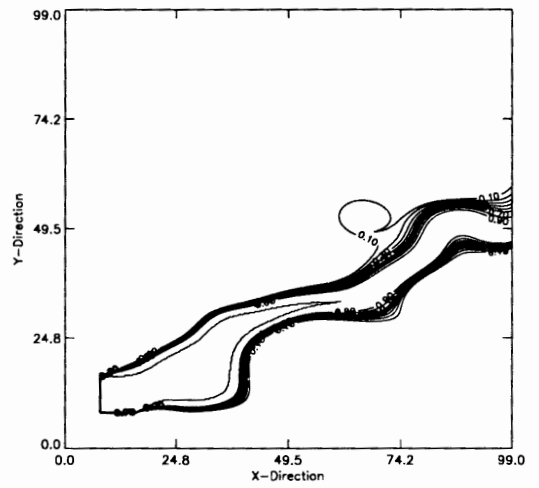
a. Upwind Finite Difference Method



b. Finite Analytic Method with Basic Linear Interpolation

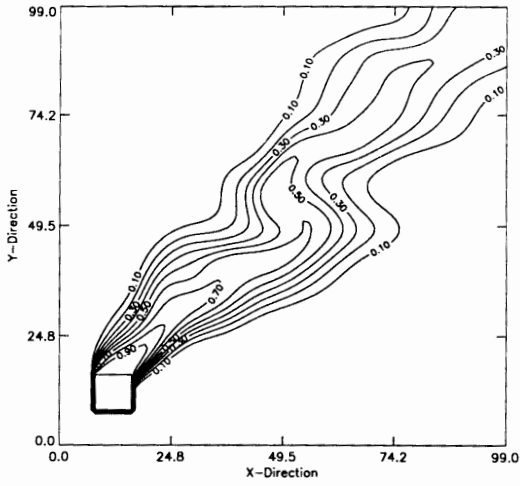


c. Finite Analytic Method with Improved Linear Interpolation

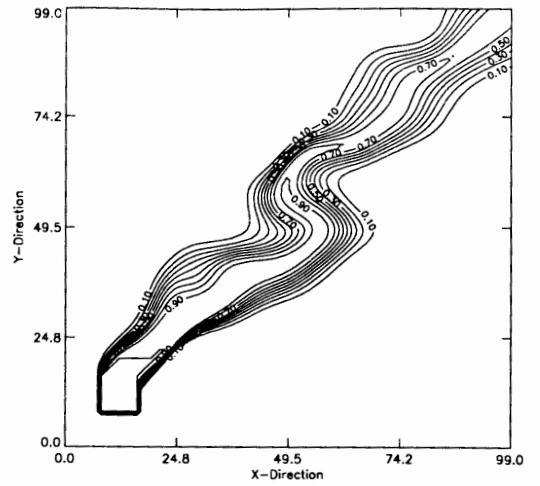


d. "Exact" Solution (Total Number of Grid Points = 400 x 400)

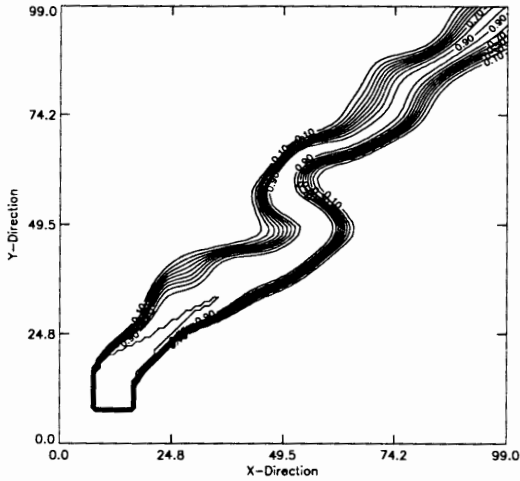
**Figure 5-17: Solution transport in heterogeneous porous media for $r = 0.5$
 ($\sigma_{LK}^2=1.5$; mean flow velocities: $u_0=0.0417$ m/day, $v_0=0.0208$ m/day)**



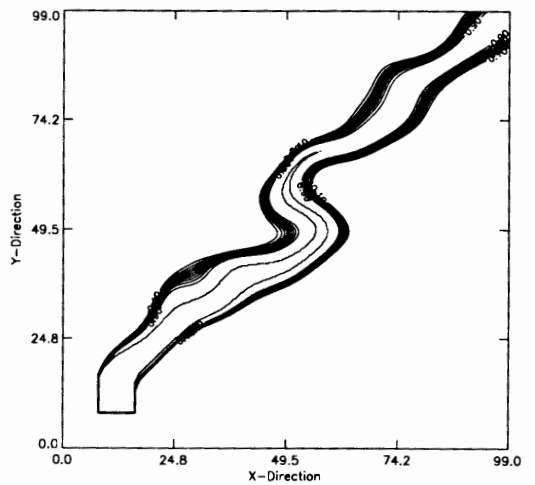
a. Upwind Finite Difference Method



b. Finite Analytic Method with Basic Linear Interpolation



c. Finite Analytic Method with Improved Linear Interpolation



d. "Exact" Solution (Total Number of Grid Points = 400 x 400)

**Figure 5-18: Solution transport in heterogeneous porous media for $r = 1.0$
 $(\sigma^2_{Lk}=1.5; \text{mean flow velocities: } u_o=0.0417 \text{ m/day, } v_o=0.0417 \text{ m/day})$**

finite analytic method. These comparisons are also made when Peclet numbers are small or moderate. However, in the real world, groundwater flow field is generally highly variable as well as advection-dominated. Consider an extreme case which advection is highly dominated and Peclet number approaches infinity. In this case, only the new finite analytic methods along with the upwind finite difference method will be shown and discussed in the comparisons. Here the existing finite analytic method is no longer valid. It has been shown that, for most of the problems considered, finite analytic method with basic linear interpolation has at least the same accuracy as the existing one, even when Peclet number is small and moderate.

Figures 5-12 through 5-18 show predicted plumes using various numerical methods tested when advection dominates and Peclet number approaches infinity. Comparisons under uniform flows are shown in Figures 5-12 to 5-15. When mean flow is aligned with the axis, predicted plumes using all different methods tested look good. In fact, the solutions are all exact in the case that flow is uniform. However, when the flow is at an angle with the axis. The performance of different methods becomes dramatically different. Upwind solution degrades with increasing angles between flow and coordinate axis, with numerical dispersion being at maximum when the mean flow is diagonal. The new finite-analytic method with linear interpolation is most accurate when the mean flow is horizontal as well as diagonal, and it leads to exact solution in the case of uniform flow. But the method still produces varying degree of numerical dispersion with the maximum occurring $r = 0.5$ or when mean flow direction is half way between horizontal and diagonal. The finite analytic method with improved linear interpolation performs best for all the cases considered. The solution is consistently more accurate, and the solution is exact when flow is horizontal, diagonal or half way in between. The small oscillatory effect in Figure 5-14 (c) is not caused by numerical error but roundoff error. If we can keep more decimal point in the computation, the effect will be vanished. Figures 5-16 through 5-18 are shown for nonuniform flows with three different mean flow directions, respectively, $r = 0$, $r = 0.5$ and $r = 1$. Plumes by upwind method is more dispersed than those of the finite analytic methods. The finite analytic method with basic

linear interpolation performs well but with some degree of dispersion. The finite analytic method with improved linear interpolation is always the best. Plumes by this method showed less numerical diffusion, and are more close to the “exact” solution than the other two methods.

Chapter 6

Conclusions

6.1. Summary of Original Contributions

The accurate and robust finite analytic solutions based on linear interpolations for boundary approximations are derived for two-dimensional steady-state advection-dominated solute transport problems. They are the finite analytic solution based on classic linear interpolation boundary approximation and the finite analytic solution based on improved linear interpolation boundary approximation. The new finite analytic methods are developed to exploit the advantages of the existing finite analytic and traditional finite difference approaches. They differ from the existing finite analytic method, when advection dominates, instead of solving the entire governing equation including diffusion terms analytically, the new methods approximate the diffusion by finite difference and then solve the modified governing equation analytically. The new finite analytic methods differ from the existing one also because they are applying simple linear interpolation for boundary approximation. These finite analytic methods reduce the complexity of the existing finite analytic formulations and enhance the efficiency of the coefficient calculations. When advection dominates, the finite analytic linear interpolation approximation solution is tested to be of the same accuracy as the recommended existing finite analytic method [Chen and Chen, 1982]. The solution of finite analytic improved linear interpolation approximation has higher accuracy than the solution of finite analytic linear interpolation approximation, when applying to two-dimensional steady-state problems.

The finite analytic methods based on linear interpolations provide all-positive coefficients. The methods are also able to shift the weight of influence from upstream, according to flow direction and Peclet number. These new finite analytic methods are mass-conservative, if chemical reaction is not involved.

The improved finite analytic methods have been applied to various highly variable velocity fields where the advection is dominated. These methods have significant improvement with handling large Peclet numbers (i.e., $Pe > 1000$), while the existing finite analytic methods suffer large round off error when Peclet number is greater than 120 due to the inability of the computer to provide an accurate summation of a series with alternately positive and negative terms of large exponential value. Moreover, the new finite analytic methods can handle pure advection or when Peclet number approaches infinity.

The existing finite analytic methods also have “weak” areas in the local domain, when $v\Delta x/u\Delta y$ or r is close to 1. Within these area, if Peclet number is large, the finite analytic solution loses its accuracy not due to the theory used but due to the inability of computer in providing accurate summation of the analytic series. The finite analytic linear interpolation approximation method avoids the weakness with using linear interpolation as boundary approximation, and provides the best result around those areas. However, the finite analytic linear interpolation approximation method has its own weak areas. When $v\Delta x/u\Delta y$ or r is close to 0.5, the method results in relatively large numerical diffusion.

The finite analytic method based on improved linear interpolation approximation, which includes more neighboring nodes, avoids both “weak” areas that occur in the existing finite analytic methods and finite analytic method based on simple linear interpolation approximation. The finite analytic improved linear interpolation approximation method is superior to the finite analytic linear interpolation approximation method, and naturally, better than the existing finite analytic methods.

However, the finite analytic improved linear interpolation approximation formulation includes more neighboring nodal points, assumption of using constant local parameters over the element may not be valid, if the local element of grid size is not small enough.

Finally, the Laplace transform method is applied to the transient equation when extending the improved finite analytic methods to transient problems. The analytically transformed expression behaves like a steady state advection-diffusion equation with a

first-order decay term. This expression can be solved with the improved finite analytic methods and time dependence recovered with an efficient inverse Laplace transform algorithm. The Laplace transform/finite analytic method is an accurate approach in space and time for transient problems, but the computer CPU time will be a concern.

6.2. Recommendations for Future Work

The finite analytic improved linear interpolation approximation method is currently derived for pure advection solute transport problem, and can be extended to involve diffusion. Approximation of the diffusion terms may also use the simple finite difference techniques. The formulation of finite analytic based on improved linear interpolation boundary approximation includes more neighboring nodal points, and local parameters are assumed to be constant and have corresponding values at the interior nodal point. This assumption may not be applicable, if the grid size is not small enough.

The finite analytic/Laplace transform solution based on linear interpolation boundary approximation is derived. Future research should focus on further testing the new method for transient solute transport and extending the method to transport in transient velocity fields in three-space dimensions.

Appendix

The Improved Finite Analytic Method with Linear Interpolation for Steady Transport

In this appendix, the finite analytic solution for steady-state two-dimensional advection-diffusion transport equation is derived. To develop the solution of this improved finite analytic method, we first use central-difference finite difference method to approximate the diffusion term, and then solve the modified governing equation by finite analytic method. The boundary approximation used here for the finite analytic solution is the classic linear interpolation.

Consider a steady two-dimensional advection-diffusion transport equation including decay and source/sink terms

$$u(x,y)\frac{\partial C}{\partial x} + v(x,y)\frac{\partial C}{\partial y} = \frac{\partial}{\partial x}\left[D_x(x,y)\frac{\partial C}{\partial x}\right] + \frac{\partial}{\partial y}\left[D_y(x,y)\frac{\partial C}{\partial y}\right] - \lambda(x,y)C + S(x,y) \quad (\text{A.1})$$

where C represents concentration of contaminated plume in groundwater. The velocities u and v , diffusion coefficients D_x and D_y in x and y directions, decay rate λ and source/sink term S and are functions of coordinates x and y . C is solute concentration. In general, an analytic solution of equation (A.1) is not available due to variable parameters, the finite analytic numerical methods are used to obtain the local analytic solution in a local element as shown in Figure A-1.

In order to solve the advective transport equation (A.1) analytically in the local element, the idea of solving analytical solution of one-dimensional advection-diffusion equation is used. When the local element is small enough, one may assume that velocities,

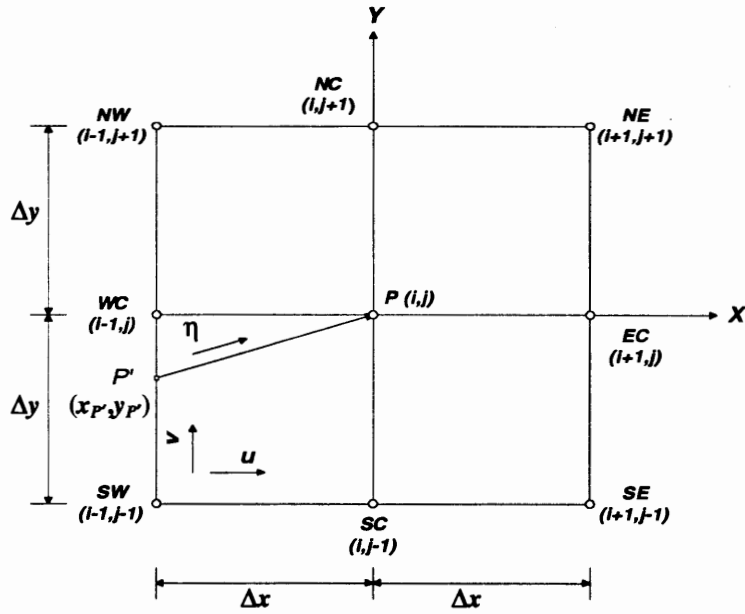


Figure A-1: A local element for improved finite analytic method with linear interpolation boundary approximation

diffusion coefficients, decay rate and source/sink term are constant in the local element and use corresponding values at the interior point P or (i,j) , we get

$$\begin{aligned}
 u(x,y) &\approx u_{i,j}; & v(x,y) &\approx v_{i,j}; \\
 D_x(x,y) &\approx D_{x_{i,j}}; & D_y(x,y) &\approx D_{y_{i,j}}; \\
 \lambda(x,y) &\approx \lambda_{i,j}; \\
 S(x,y) &\approx S_{i,j}
 \end{aligned}
 \tag{A.2}$$

where $x_{i-1} \leq x \leq x_{i+1}$ and $y_{i-1} \leq y \leq y_{i+1}$.

Using $U_{i,j}$ as a combined velocity of $u_{i,j}$ and $v_{i,j}$, equation (A.1) becomes a one-dimensional equation in the local element.

$$U_{i,j} \frac{\partial C}{\partial \eta} = D_{x_{i,j}} \frac{\partial^2 C}{\partial x^2} + D_{y_{i,j}} \frac{\partial^2 C}{\partial y^2} - \lambda_{i,j} C + S_{i,j}
 \tag{A.3}$$

where

$$U_{i,j} = \sqrt{u_{i,j}^2 + v_{i,j}^2} \quad (\text{A.4})$$

and, η is a temporal coordinate with a direction of the combined velocity along the trajectory flow line. The trajectory flow line starts at an arbitrary point P' or $(x_{P'}, y_{P'})$, which is most likely a non-nodal points.

In this work, advection-dominated problem is the major consideration for the development of the numerical solution to equation (A.1). The effect of the diffusion on the solute transport is small compared to the advection. Therefore, central-difference finite difference method is used to approximate the diffusion terms:

$$\frac{\partial^2 C}{\partial x^2} = \frac{C_{i+1,j} - 2C_{i,j} + C_{i-1,j}}{\Delta x^2} \quad (\text{A.5})$$

$$\frac{\partial^2 C}{\partial y^2} = \frac{C_{i,j+1} - 2C_{i,j} + C_{i,j-1}}{\Delta y^2} \quad (\text{A.6})$$

Assuming that the deviation of diffusion between point P' and interior node P is negligible, the equation (A.3) in the local element is further simplified as

$$U_{i,j} \frac{\partial C}{\partial \eta} + \lambda_{i,j} C = f_{x_{i,j}} + f_{y_{i,j}} + S_{i,j} \quad (\text{A.7})$$

where

$$f_{x_{i,j}} = D_{x_{i,j}} \frac{C_{i+1,j} - 2C_{i,j} + C_{i-1,j}}{\Delta x^2} \quad (\text{A.8})$$

$$f_{y_{i,j}} = D_{y_{i,j}} \frac{C_{i,j+1} - 2C_{i,j} + C_{i,j-1}}{\Delta y^2} \quad (\text{A.9})$$

The equation (A.7) can be solved analytically in the local element, and the general solution for C at any point along the flowline is written as

$$C(\eta) = f(C_{P'}, U_{i,j}, \eta, f_{x_{i,j}}, f_{y_{i,j}}, \lambda_{i,j}, S_{i,j}) \quad (\text{A.10})$$

which can be expressed explicitly as follow

$$C(\eta) = e^{\left[\frac{-\lambda_{i,j}\eta}{U_{i,j}}\right]} \left[C_{P'} - \frac{f_{x_{i,j}} + f_{y_{i,j}} + S_{i,j}}{\lambda_{i,j}} \right] + \frac{f_{x_{i,j}} + f_{y_{i,j}} + S_{i,j}}{\lambda_{i,j}} \quad (\text{A.11})$$

where

$$C_{P'} = C(x_{P'}, y_{P'}) \quad (\text{A.12})$$

$$\eta = \sqrt{(x - x_{P'})^2 + (y - y_{P'})^2} \quad (\text{A.13})$$

and, η can be any point in the local element and on element boundaries.

Evaluating $C(\eta)$ at the interior node $P (i,j)$, the solution becomes

$$C_{i,j} = e^{\frac{\lambda_{i,j}\Delta\eta}{U_{i,j}}} C_{P'} + \frac{f_{x_{i,j}} + f_{y_{i,j}} + S_{i,j}}{\lambda_{i,j}} \left(1 - e^{\frac{-\lambda_{i,j}\Delta\eta}{U_{i,j}}} \right) \quad (\text{A.14})$$

where, $\Delta\eta$ is the distance between node P and non-nodal point P' .

The locally analytical solution includes values of a non-nodal point P' and four boundary nodal points which directly connect the interior node P . The numerical solution is described as follow:

$$C_{i,j} = R_{P'} C_{P'} + R_x (C_{i+1,j} + C_{i-1,j}) + R_y (C_{i,j+1} + C_{i,j-1}) + R_{i,j} \quad (\text{A.15})$$

where

$$R_0 = 1 + \left(\frac{2D_{x_{i,j}}}{\lambda_{i,j} \Delta x^2} + \frac{2D_{y_{i,j}}}{\lambda_{i,j} \Delta y^2} \right) \left(1 - e^{\frac{-\lambda_{i,j} \Delta \eta}{U_{i,j}}} \right) \quad (\text{A.16})$$

$$R_{P'} = e^{\frac{-\lambda_{i,j} \Delta \eta}{U_{i,j}}} \frac{1}{R_0} \quad (\text{A.17})$$

$$R_x = \frac{D_{x_{i,j}}}{\lambda_{i,j} \Delta x^2} \left(1 - e^{\frac{-\lambda_{i,j} \Delta \eta}{U_{i,j}}} \right) \frac{1}{R_0} \quad (\text{A.18})$$

$$R_y = \frac{D_{y_{i,j}}}{\lambda_{i,j} \Delta y^2} \left(1 - e^{\frac{-\lambda_{i,j} \Delta \eta}{U_{i,j}}} \right) \frac{1}{R_0} \quad (\text{A.19})$$

$$R_{i,j} = \frac{S_{i,j}}{\lambda_{i,j}} \left(1 - e^{\frac{-\lambda_{i,j} \Delta \eta}{U_{i,j}}} \right) \frac{1}{R_0} \quad (\text{A.20})$$

and $\Delta \eta$, for the case as shown in Figure A-1, is written

$$\Delta\eta = \sqrt{\Delta x^2 + \Delta y^2} r_{i,j}^2 \quad (\text{A.21})$$

where

$$r_{i,j} = \left| \frac{v_{i,j} \Delta x}{u_{i,j} \Delta y} \right| \quad (\text{A.22})$$

Since decay rate λ is in a denominator in equations (A.16), (A.18), (A.19) and (A.20), when λ approaches 0, computational error of division by zero will be encountered.

Noticing that $1/\lambda_{i,j}$ is always accompanied by $\left(1 - e^{-\frac{\lambda_{i,j} \Delta\eta}{U_\eta}}\right)$, to avoid computer run-time

error, the L'Hospital Rule is applied. When $\lambda_{i,j}$ approaches 0, and $\left(1 - e^{-\frac{\lambda_{i,j} \Delta\eta}{U_\eta}}\right)$ also

approaches 0; derivatives of $\lambda_{i,j}$ and $\left(1 - e^{-\frac{\lambda_{i,j} \Delta\eta}{U_\eta}}\right)$ exist and $\left(1 - e^{-\frac{\lambda_{i,j} \Delta\eta}{U_\eta}}\right) \neq 0$; and value

of $\lambda_{i,j}$ over $\left(1 - e^{-\frac{\lambda_{i,j} \Delta\eta}{U_\eta}}\right)$ exists. These conditions are satisfied the L'Hospital Rule. Then

$$\lim_{\eta \rightarrow 0} \frac{1 - e^{-\frac{\lambda_{i,j} \Delta\eta}{U_\eta}}}{\lambda_{i,j}} = \lim_{\eta \rightarrow 0} \frac{\left(1 - e^{-\frac{\lambda_{i,j} \Delta\eta}{U_\eta}}\right)'}{(\lambda_{i,j})'} = \frac{\Delta\eta}{U_\eta} \quad (\text{A.23})$$

Therefore, when λ approaches 0, coefficients in equations (A.16) to (A.20) are rewritten as follows

$$R_0 = 1 + \frac{2\Delta\eta}{U_{i,j}} \left(\frac{D_{x_{i,j}}}{\Delta x^2} + \frac{D_{y_{i,j}}}{\Delta y^2} \right) \quad (\text{A.24})$$

$$R_{p'} = \frac{1}{R_0} \quad (\text{A.25})$$

$$R_x = \frac{D_{x_{i,j}} \Delta\eta}{U_{i,j} \Delta x^2} \frac{1}{R_0} \quad (\text{A.26})$$

$$R_y = \frac{D_{y_{i,j}} \Delta\eta}{U_{i,j} \Delta y^2} \frac{1}{R_0} \quad (\text{A.27})$$

$$R_{i,j} = \frac{S_{i,j} \Delta\eta}{U_{i,j}} \frac{1}{R_0} \quad (\text{A.28})$$

To evaluate $C_{i,j}$, we need to estimate non-nodal value $C_{p'}$, which can be expressed by nodal values. A lot of ways can be used to evaluate $C_{p'}$. In this appendix, the $C_{p'}$ value is approximated using linear interpolation between the values of the two closest nodes along the boundary. In the case (called Case 1) as shown in Figure A-1, the $C_{p'}$ is interpolated as

$$C_{p'} = r_{i,j} C_{i-1,j-1} + (1 - r_{i,j}) C_{i-1,j} \quad (\text{A.29})$$

Thus, we obtained the local finite analytic algebraic equation associating the interior nodal value C_p with its neighboring nodal values

$$C_{i,j} = (R_{p'} r_{i,j})C_{i-1,j-1} + [R_{p'}(1-r_{i,j}) + R_x]C_{i-1,j} + (0)C_{i-1,j+1} + (R_y)C_{i,j-1} + (R_y)C_{i,j+1} + (0)C_{i+1,j-1} + (R_x)C_{i+1,j} + (0)C_{i+1,j+1} + R_{i,j} \quad (\text{A.30})$$

Note that coefficients for nodes $(i-1,j+1)$, $(i+1,j-1)$ and $(i+1,j+1)$ are zeros.

Depending on the direction of the trajectory line (as shown in Figure A-2) and the value of $r_{i,j}$, there are eight cases that may be encountered in the development of the overall solution. In each case, value $C_{p'}$ may have different expressions because of the interpolation between different nodes. Other finite analytic numerical formulations can be described as follows

Case 2: $r_{i,j} \leq 1$, $u_{i,j} > 0$, and $v_{i,j} < 0$

The value of $C_{p'}$ is interpolated using $C_{i-1,j+1}$ and $C_{i-1,j}$

$$C_{p'} = r_{i,j}C_{i-1,j+1} + (1-r_{i,j})C_{i-1,j} \quad (\text{A.30})$$

$$C_{i,j} = (0)C_{i-1,j-1} + [R_{p'}(1-r_{i,j}) + R_x]C_{i-1,j} + (R_{p'} r_{i,j})C_{i-1,j+1} + (R_y)C_{i,j-1} + (R_y)C_{i,j+1} + (0)C_{i+1,j-1} + (R_x)C_{i+1,j} + (0)C_{i+1,j+1} + R_{i,j} \quad (\text{A.31})$$

Case 3: $r_{i,j} \leq 1$, $u_{i,j} < 0$, and $v_{i,j} < 0$

The value of $C_{p'}$ is interpolated using $C_{i+1,j+1}$ and $C_{i+1,j}$

$$C_{p'} = r_{i,j}C_{i+1,j+1} + (1-r_{i,j})C_{i+1,j} \quad (\text{A.32})$$

$$C_{i,j} = (0)C_{i-1,j-1} + (R_x)C_{i-1,j} + (0)C_{i-1,j+1} + (R_y)C_{i,j-1} + (R_y)C_{i,j+1} + (0)C_{i+1,j-1} + [R_{p'}(1-r_{i,j}) + R_x]C_{i+1,j} + (R_{p'} r_{i,j})C_{i+1,j+1} + R_{i,j} \quad (\text{A.33})$$

Case 4: $r_{ij} \leq 1$, $u_{i,j} < 0$, and $v_{i,j} \geq 0$

The value of $C_{p'}$ is interpolated using $C_{i+1,j-1}$ and $C_{i+1,j}$

$$C_{p'} = r_{i,j} C_{i+1,j-1} + (1 - r_{i,j}) C_{i+1,j} \quad (\text{A.34})$$

$$C_{i,j} = (0)C_{i-1,j-1} + (R_x)C_{i-1,j} + (0)C_{i-1,j+1} + (R_y)C_{i,j-1} + \\ (R_y)C_{i,j+1} + (R_{p'} r_{i,j})C_{i+1,j-1} + [R_{p'}(1 - r_{i,j}) + R_x]C_{i+1,j} + (0)C_{i+1,j+1} + R_{i,j} \quad (\text{A.35})$$

where $\Delta\eta$ is expressed as equation (A.21) for Cases 1 to 4.

Case 5: $r_{ij} \geq 1$, $u_{i,j} \geq 0$, and $v_{i,j} > 0$

$$r'_{i,j} = \left| \frac{u_{i,j} \Delta y}{v_{i,j} \Delta x} \right| \quad \text{or} \quad r'_{i,j} = \frac{1}{r_{i,j}} \quad (\text{A.36})$$

The value of $C_{p'}$ is interpolated using $C_{i-1,j-1}$ and $C_{i-1,j}$

$$C_{p'} = r'_{i,j} C_{i-1,j-1} + (1 - r'_{i,j}) C_{i-1,j} \quad (\text{A.37})$$

$$C_{i,j} = (R_{p'} r'_{i,j})C_{i-1,j-1} + (R_x)C_{i-1,j} + (0)C_{i-1,j+1} + [R_{p'}(1 - r'_{i,j}) + R_y]C_{i,j-1} + \\ (R_y)C_{i,j+1} + (0)C_{i+1,j-1} + (R_x)C_{i+1,j} + (0)C_{i+1,j+1} + R_{i,j} \quad (\text{A.38})$$

Case 6: $r_{ij} \geq 1$, $u_{i,j} < 0$, and $v_{i,j} > 0$

The value of $C_{p'}$ is interpolated using $C_{i+1,j-1}$ and $C_{i,j-1}$

$$C_{p'} = r'_{i,j} C_{i+1,j-1} + (1 - r'_{i,j}) C_{i,j-1} \quad (\text{A.39})$$

$$C_{i,j} = (0)C_{i-1,j-1} + (R_x)C_{i-1,j} + (0)C_{i-1,j+1} + [R_{p'}(1-r'_{i,j}) + R_y]C_{i,j-1} + (R_y)C_{i,j+1} + (R_{p'}r'_{i,j})C_{i+1,j-1} + (R_x)C_{i+1,j} + (0)C_{i+1,j+1} + R_{i,j} \quad (\text{A.40})$$

Case 7: $r_{i,j} \geq 1$, $u_{i,j} > 0$, and $v_{i,j} < 0$

The value of $C_{p'}$ is interpolated using $C_{i+1,j-1}$ and $C_{i,j-1}$

$$C_{p'} = r'_{i,j}C_{i-1,j+1} + (1-r'_{i,j})C_{i,j+1} \quad (\text{A.41})$$

$$C_{i,j} = (0)C_{i-1,j-1} + (R_x)C_{i-1,j} + (R_{p'}r'_{i,j})C_{i-1,j+1} + (R_y)C_{i,j-1} + [R_{p'}(1-r'_{i,j}) + R_y]C_{i,j+1} + (0)C_{i+1,j-1} + (R_x)C_{i+1,j} + (0)C_{i+1,j+1} + R_{i,j} \quad (\text{A.42})$$

Case 8: $r_{i,j} \geq 1$, $u_{i,j} < 0$, and $v_{i,j} < 0$

The value of $C_{p'}$ is interpolated using $C_{i+1,j+1}$ and $C_{i,j+1}$

$$C_{p'} = r'_{i,j}C_{i+1,j+1} + (1-r'_{i,j})C_{i,j+1} \quad (\text{A.43})$$

$$C_{i,j} = (0)C_{i-1,j-1} + (R_x)C_{i-1,j} + (0)C_{i-1,j+1} + (R_y)C_{i,j-1} + [R_{p'}(1-r'_{i,j}) + R_y]C_{i,j+1} + (0)C_{i+1,j-1} + (R_x)C_{i+1,j} + (R_{p'}r'_{i,j})C_{i+1,j+1} + R_{i,j} \quad (\text{A.44})$$

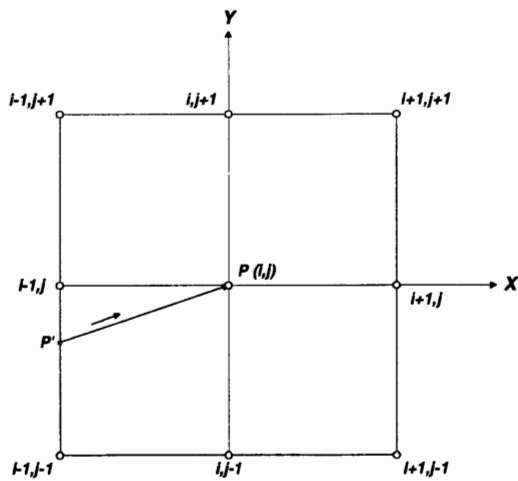
The $\Delta\eta$ for Cases 5 to 8 is written as

$$\Delta\eta = \sqrt{\Delta y^2 + \Delta x^2 r'_{i,j}{}^2} \quad (\text{A.45})$$

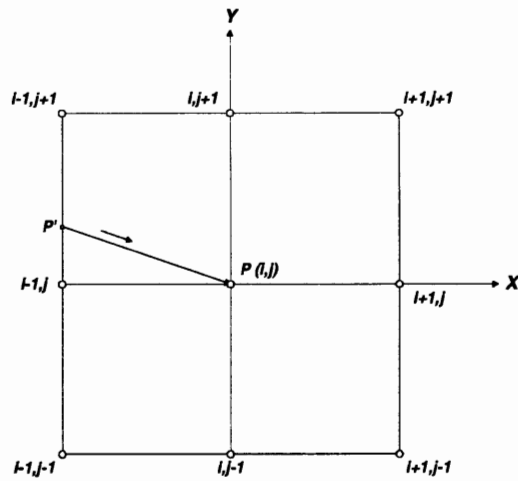
The overall numerical solution may be summarized as

$$C_{i,j} = \sum_n^8 a_n C_n + R_{i,j} \quad (\text{A.32})$$

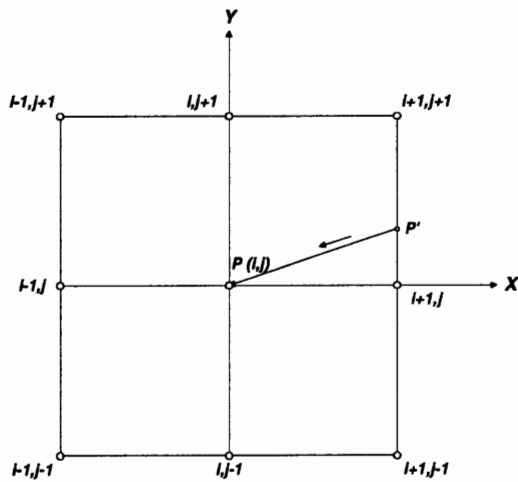
Here, n denoted the eight neighboring boundary nodes in the local element of interior nodal point P ; a_n denotes the finite analytic coefficients associated with the n th node; and $R_{i,j}$ is the effect of source/sink.



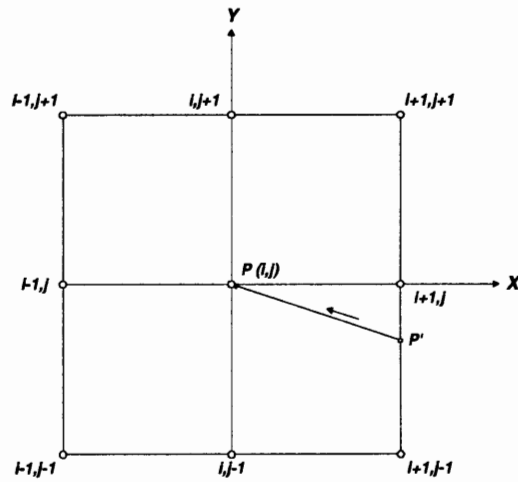
(1). Case 1



(2). Case 2

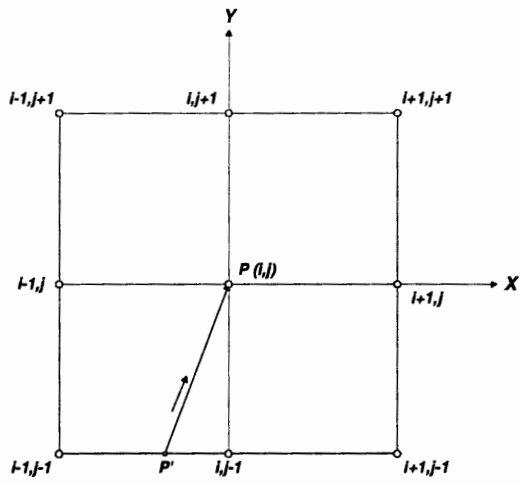


(3). Case 3

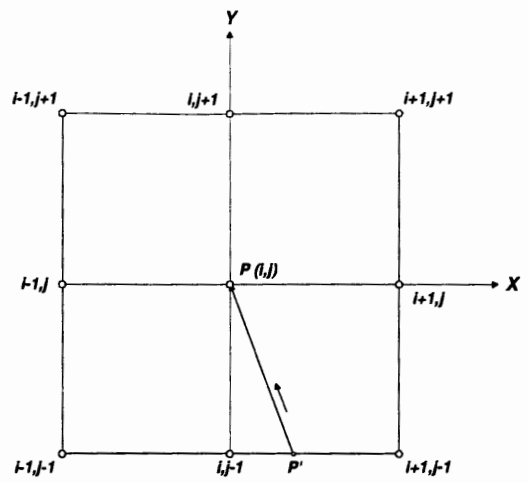


(4). Case 4

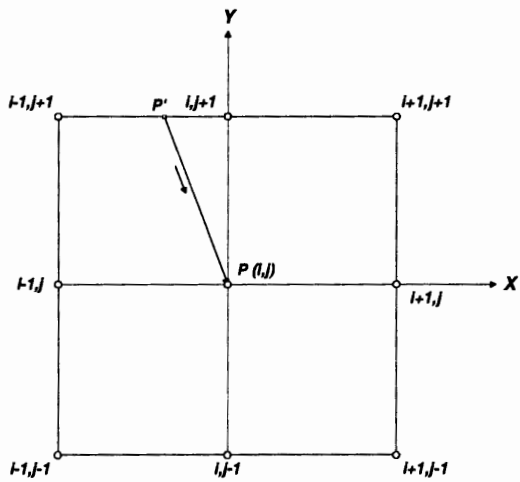
Figure A-2: Local elements for formulation development of finite analytic method based on linear interpolation boundary approximation



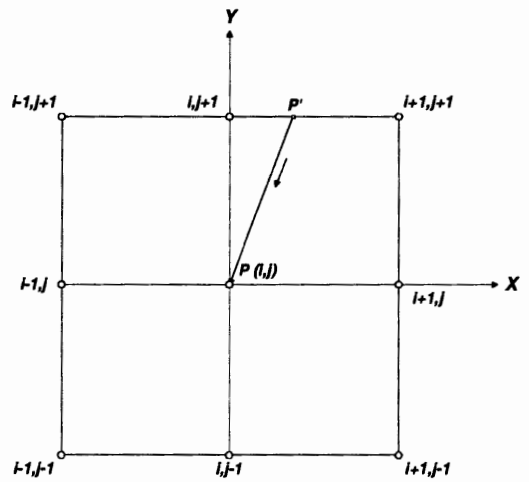
(5). Case 5



(6). Case 6



(7). Case 7



(8). Case 8

Figure A-2: Local elements for formulation development of finite analytic method based on linear interpolation boundary approximation

REFERENCES

1. "Contaminant Transport in Groundwater", edited by Kobus, H. E. and Kinzelbach, W., A.A.Balkema Publishers, 1989.
2. "Cunge, J. A., Holly, F. M. and Verwey, A., "Practical Aspects of Computational River Hydraulics", Pitman Publishing Limited, 1980.
3. "Mathematical Modeling for Flow and Transport Through Porous Media", edited by Dagan, G., Hornung, U. and Knabner, P., Kluwer Academic Publishers, 1991.
4. Anderson, D. A., Tannehill, H. C. and Pletcher, R. H., "Computational Fluid Mechanics and Heat Transfer", Hemisphere Publishing Corporation, McGraw-Hill Book Company, 1984.
5. Anderson, M. P. and Woessner, W. W., "Applied Groundwater Modeling: Simulation of Flow and Advection Transport", Academic Press, Inc., 1992.
6. Baker, A. J., "Finite Element Computational Fluid Mechanics", Hemisphere Publishing Corporation, McGraw-Hill Book Company, 1983.
7. Bear, J. and Verruijt, A., "Modeling Groundwater Flow and Pollution", D. Reidel Publishing Company, 1987.
8. Bear, J. and Verruijt, A., "Modeling Groundwater Flow and Pollution: with Computer Programs for Sample Cases", D. Reidel Publishing Company, 1987.
9. Belytschko, T., "Major Advances in Finite Element Model Technology", Computer Utilization in Structural Engineering, Publication by ASCE, New York, NY, USA, May 1989, pp 11-20.
10. Brannan, J. R. and Haselow, J. S., "Compound Random Field Models of Multiple Scale Hydraulic Conductivity", Water Resources Research, vol. 29, No. 2, Feb. 1993, pp 365-372.
11. Burnett, R. D. and Frind, E. O., "Simulation of Contaminant Transport in Three Dimensions, 1, The Alternating Direction Galerkin Technique", Water Resour. Res., 23, 683-694, 1987.

12. Burnett, R. D. and Frind, E. O., "Simulation of Contaminant Transport in Three Dimensions, 2. Dimensionality Effects", *Water Resources Research*, vol. 23, No. 4, Apr. 1987, pp 695-705.
13. Chen, C. J. and Chen, H. C., "Finite Analytic Numerical Method for Unsteady Two-Dimensional Navier-Stokes Equations", Energy Division and Iowa Institute of Hydraulic Research, University of Iowa, Iowa City, Iowa, Dec. 1982.
14. Chen, C. J. and Li, P., "Finite Differential Method in Heat Conduction-Application of Analytic Solution Technique", ASME Paper 79-WA/HT-50, December 2-7, 1979. ASME Winter Annual Meeting, New York, N.Y., 1979.
15. Chen, C. J. and Wung, T. S., "Finite Analytic Solution of Convection Heat Transfer for Tube Arrays in Crossflow: Part II--Heat Transfer Analysis", *Journal of Heat Transfer*, Transactions ASME, vol. 111, No. 3, Aug 1989, pp 641-648.
16. Chen, C. J., "Finite Analytic Method", in *Handbook of Numerical Heat Transfer*, edited by Minkowycz W. J., Sparrow, E. M., Schneider, G. E., and Pletcher, R. H., John Wiley and Son Inc., 1988.
17. Chen, H. C. and Chen, C. J., "The Finite Analytic Method (IV): Development of Finite Analytic Method for Unsteady Three-Dimensional Navier-Stokes Equations", Doctoral Dissertation, the University of Iowa, Iowa City, Iowa, Aug. 1982.
18. Chen, Y. and Falconer, R. A., "Advection-Diffusion Modelling Using the Modified QUICK Scheme", *International Journal for Numerical Methods in Fluids*, vol. 15, 1992, pp 1171-1196.
19. Chiang, C. Y., Wheeler, M. F., and Bedient, P. B., "A Modified Method of Characteristics technique and mixed finite-element method for simulation of groundwater solute transport", *Water Resource Research*, Vol. 25, No. 7, 1989, pp 1541-1549.
20. Choi, S. K. and Chen, C. J., "Finite Analytic Numerical Solution of Turbulent Flow Past Axisymmetric Bodies By Zone Modeling Approach", ASME, Fluids Engineering Division, FED vol. 66, Publication by ASME, New York, NY, USA, 1985, pp 23-32.
21. Clough, R. W., "Original Formulation of the Finite Element Method", *Computer Utilization in Structural Engineering*, Publication by ASCE, New York, NY, USA, May 1989, pp 1-10.
22. Crump, K. S., "Numerical Inversion of Laplace Transforms Using a Fourier Series Approximation", *Journal of the Association for Computing Machinery*, vol. 23, No. 1, Jan. 1976, pp 89-96.

23. Davies, B. and Martin, B., "Numerical Inversion of the Laplace Transform: a Survey and Comparison of Methods", *Journal of Computational Physics*, vol. 33, 1979, pp 1-32.
24. De Hoog, F. R., J. H. Knight, and A. N. Stokes, "An improved method for numerical inversion of Laplace transforms", *SIAM J. Sci. Stat. Comput.*, vol. 3, No. 3, 1982, pp 357-366.
25. Desai, C. S., "Elementary Finite Element Method", Prentice-Hall, Inc., 1979.
26. Dillon, P. L., "An Analytical Model of Contaminant Transport From Diffuse Sources in Saturated Porous Media", *Water Resources Research*, vol. 25, No. 6, Jun, 1989, pp 1208-1218.
27. Douglas, J., and Russell, T. F., "Numerical Methods for Convection-Dominated Diffusion Problems Based on Combining the Method of Characteristics with Finite Element or Finite Difference Procedure", *SIAM J. Numerical Analysis*, 19, 1982, pp 1-67.
28. Dubner, H. and Abate, J., "Numerical Inversion of Laplace Transforms by Relating Them to the Finite Fourier Cosine Transform", *Journal of the Association for Computing Machinery*, vol. 15, No. 1, Jan. 1968, pp 115-123.
29. El-Kadi, A. I., "Applying the USGS Mass-Transport Model (MOC) to Remedial Actions By Recovery Wells", *Ground Water*, Vol. 26, No. 3, 1988, pp 281-288.
30. Falconer, R. A. and Liu, S., "Modeling Solute Transport Using QUICK Scheme", *Journal of Environmental Engineering*, vol. 114, No. 1, Feb. 1988, pp3-20.
31. Freeze, R. A. and Witherspoon, P. A., "Theoretical Analysis of Region Groundwater Flow, 1. Analytical and Numerical Solutions to the Mathematical Model", *Water Resour. Res.*, Vol. 2, 1966, pp 641-656.
32. Garder, A. O., Peaceman, Jr., D. W. and Pozzi, Jr., A. L., "Numerical Calculation of Multidimensional Miscible Displacement by the Method of Characteristics", *Soc. Pet. Eng. J.* Vol. 6, No. 2, 1964, pp 260-272.
33. Gray, W. G. and Pinder, G. F., "An Analysis of the Numerical Solution of the Transport Equation", *Water Resources Research*, vol. 12, No. 3, Jun. 1976, pp 547-555.
34. Hamilton, D. A., Wiggert, D. C. and Wright, S. J., "Field Comparison of Three Mass Transport Models", *Journal of Hydraulic Engineering*, vol. 111, No. 1, Jan. 1985, pp 1-11.

35. Honig, G. and Hirdes, U., "A Method for the Numerical Inversion of Laplace Transforms", *Journal of Computational and Applied Mathematics*, vol. 10, 1984, pp 113-132.
36. Huyakorn, P. S., Jones, B. G. and Anderson, P. F., "Finite Element Algorithms for Simulating Three-Dimensional Groundwater Flow and Solute Transport in Multi-layered Systems", *Water Resour. Res.*, 22, 361-374, 1986.
37. Hwang, J. C., Chen, C. J., Sheikoslami, M. and Panigrahi, B. K., "Finite-Analytic Numerical Solution for Two Dimensional Groundwater Solute Transport", *Water Resour. Res.*, Vol. 21, No. 9, 1985, pp 1354-1360.
38. Javandel, I., Doughty, C. and Tsang, C. F., "Groundwater Transport: Handbook of Mathematical Models", American Geophysical Union, 1984.
39. Jonathan I., "Groundwater Modeling by the Finite Element Method", American Geophysical, 1989.
40. Kar, A., Chan, C. L. and Mazumber, J., "Comparative Studies on Nonlinear Hyperbolic and Parabolic Heat Conduction for Various Boundary Conditions: Analytic and Numerical Solutions" *Journal of Heat Transfer, Transactions ASME*, vol. 114, No. 1, Feb 1992, pp 14-20.
41. Kazda, I., "Finite Element Techniques in Groundwater Flow Studies With Application in Hydraulic and Geotechnical Engineering", Elsevier, 1990.
42. Kinzelbach W., "The Random Walk Method in Pollutant Transport Simulation", in *Groundwater Flow and Quality Modeling*, D. Reidel Publishing Company, 1988, pp 227-245.
43. Lawson, D. W., "Improvements in the Finite Difference Solution of Two-Dimensional Dispersion Problems", *Water Resources Research*, vol. 7, No. 3, Jun. 1971, pp 721-725.
44. Leendertse, J.J., "A Water-Quality Simulation Model for Well-Mixed Estuaries and Coastal Seas", Vol. I, Principles of Computation, Rand Corporation Memorandum, RM-6230-RC, Feb., 1970.
45. Leon, L. and Pinder, G. F., "Numerical Solution of Partial Differential Equations in Science and Engineering", John Wiley & Sons, 1988.
46. Leonard, B. P. and Noye, B. J., "Second and Third Order Two Level Implicit FDM's for Unsteady One-Dimensional Convection-Diffusion", *Computational Techniques and Applications*, CTAC-89, Hemisphere, New York, 1990, pp 311-317.

47. Li, S. G. and L. Venkataraman, "Discussion on Time Interpolation for the Solution of the Dispersion Equation by J. C. Yang and E. L. Hsu", *J. of Hydraul. Res.*, Vol. 29, No. 4, 568-571, 1991.
48. Li, S. G., Ruan, F. and Mclaughlin, D., "A Space-Time Accurate Method for Solving Solute Transport Problems", *Water Resources Research*, Vol. 28, No. 9, Sep. 1992, pp 2297-2306.
49. Luhar, A. K. and Britter, R. E., "A Random Walk Model for Dispersion in Inhomogeneous Turbulence in a Convective Boundary Layer", *Atmospheric Environment*, Vol. 23, No. 9, 1989, pp 1911-1924.
50. Luhar, A. K. and Britter, R. E., "Random-Walk Modeling of Buoyant-Plume Dispersion in the Convective Boundary Layer", *Atmospheric Environment*, Vol. 26A, No. 7, 1992, pp 1283-1298.
51. Lynn, W. G., "Stochastic Subsurface Hydrology", Prentice Hall, 1993.
52. Matsoukis, P. C., "Tidal Model Using Method of Characteristics", *Journal of Waterway, Port, Coastal and Ocean Engineering*, vol. 118, No. 3, May-Jun. 1992, pp 233-248.
53. McLaughlin, D., Reid, L. B., Li, S. G., and Hyman, J., "A Stochastic Method for Characterizing Ground-Water Contamination", *Ground Water*, Vol. 31, No. 2, Mar.-Apr. 1993, pp 237-249.
54. Narasimhan, T. N. and Witherspoon, P. A., "An Integrated Finite Difference Method for Analyzing Fluid Flow in Porous Media", *Water Resour. Res.*, 12, 57-64, 1976.
55. Neuman, S. P. and Witherspoon, P. A., "Finite-Element Method of Analyzing Steady Seepage with a Free Surface", *Water Resour. Res.*, Vol. 6, No. 3, 1970, pp 889-897.
56. Neuman, S. P., "An Eulerian-Lagrangian Numerical Scheme for the Dispersion-Convection Equation Using Conjugate Space-Time Grids", *Journal of Computational Physics*, 41, 1981, pp 270-294.
57. Neuman, S. P., "Saturated-Unsaturated Seepage By Finite Elements", *Proceedings ASME*, Vol. 99, No. HY12, 1973, pp 2233-2250.
58. Neuman, S. P., and Sorek, S., "Eulerian-Lagrangian Methods for Advection-Dispersion", in *Finite Elements in Water Resources*, Vol. 4, Edited by Holz, K. P., et al., Springer-Verlag, New York, 1982, pp 14.41-14.68.

59. Panday, S., Huyakorn, P. S., Terrien, R. and Nichols, R. L., "Improved Three-Dimensional Finite-Element Techniques for Field Simulation of Variably Saturated Flow and Transport", *Journal of Contaminant Hydrology*, vol. 12, No. 1-2, Feb. 1993, pp 3-33.
60. Pepper, D. W. and Baker, A. J., "Finite Difference Versus Finite Element", in *Handbook of Numerical Heat Transfer*, Edited by Minkowycz W. J., Sparrow, E. M., Schneider, G. E., and Pletcher, R. H., John Wiley and Son Inc., 1988.
61. Pinder, G. F. and Cooper, Jr. H. H., "A Numerical Technique for Calculating the Transient Position of the Saltwater Front", *Water Resour. Res.*, 6, 875-882, 1970.
62. Pinder, G. F. and Frind, E. O., "Application of the Galerkins Procedure to Aquifer Analysis", *Water Resour. Res.*, Vol. 8, No. 1, 1972, pp108-120.
63. Raithby, G. D., "A Critical Evaluation of Upstream Differencing Applied to Problems Involving Fluid Flow", "Computer Methods in Applied Mechanics and Engineering, Vol., 9, 1976, pp75-103.
64. Raithby, G. D., "Skew Upstream Differencing Schemes for Problems Involving Fluid Flow", *Computer Methods in Applied Mechanics and Engineering*, Vol. 9, 1976, pp 153-164.
65. Roache, P. J., "Computational Fluid Mechanics", Hermosa Publishers, 1972.
66. Robin, M. J. L., Gutjahr, A. L., Sudicky, E. A. and Wilson, J. L., "Cross-Correlated Random Field Generation With the Direct Fourier Transform Method", *Water Resources Research*, vol. 29, No. 7, Jul. 1993, pp 2385-2397.
67. Ruan, F., "An Efficient Multivariate Multidimensional Random Field Generator Using the Fast Fourier Transform", SM Thesis, Department of Civil and Environmental Engineering, MIT, May, 1994.
68. Segol, G. and Pinder, G. F., "Transient Simulation of Saltwater Intrusion in Southeastern Florida", *Water Resour. Res.*, 12, 62-70, 1976.
69. Shay, W. A., "Development of a Second Order Approximation for the Navier-Stokes Equations", *Computers and Fluids*, Vol. 9, 1981, pp 279-298.
70. Sibetheros, I. A., Holley, E. R. and Branski, J. M., "Spline Interpolations for Water Hammer Analysis", *Journal of Hydraulic Engineering*, vol. 117, No. 10, Oct. 1991, pp 1332-1369.

71. Smith, S. S., Allen, M. B., Puckett, J. and Edgar, T., "The Finite Layer Method for Groundwater Flow Models", *Water Resources Research*, vol. 28, No. 6, Jun. 1992, pp 1715-1722.
72. Stone, H. L. and Brain, P. T. L., "Numerical Solution of Convective Transport Problems", *AICHE J*, Vol. 9, 1963, pp 681-688.
73. Sudicky, E. A., "The Laplace Transform Galerkin Technique: A Time-Continuous Finite Element Theory and Application to Mass Transport in Groundwater", *Water Resources Research*, vol. 25, No. 8, Aug. 1989, pp 1833-1846.
74. Sudicky, E. A., 1990, "The Laplace Transform Galerkin Technique for Efficient Time-Continuous Solution of Solute Transport in Double-Porosity Media", Elsevier Science Publishers B.V., Amsterdam.
75. Sun, Y. and Militzer, J., "The Piecewise Parabolic Finite Analytic Method, Part 2: Application", *Applied Mathematical Modelling*, vol. 17, No. 3, Mar. 1993, pp 125-132.
76. Taigbenu, A. and Liggett, J. A., "An Integral Solution for the Diffusion-Advection Equation", *Water Resour. Res.*, 22, 1237-1246, 1986.
77. Tang, Y. and Aral, M. A., "Contaminant Transport in Layered Porous Media, 1. General Solution", *Water Resources Research*, vol. 28, No. 5, May 1992, pp 1389-1397.
78. Tompson, A. F. B. and Gelhar, L. W., "Numerical Simulation of Solute Transport in Three-Dimensional, Randomly Heterogeneous Porous Media", *Water Resources Research*, vol. 26, No. 10, Oct. 1990, pp 2541-2562.
79. Tsai, W. F., Chen, C. J. and Tien, H. C., "Finite Analytic Numerical Solutions for Unsaturated Flow with Irregular Boundaries", *Journal of Hydraulic Engineering*, Vol. 119, No. 11, Nov. 1993, pp 1274-1298.
80. Uffink, G. J. M., "Modeling of Solute Transport With the Random Walk Method", in *Groundwater Flow and Quality Modeling*, D. Reidel Publishing Company, 1988, pp 247-265.
81. Uffink, G. J. M., 1985, "A Random Walk Method for the Simulation of Macrodispersion in a Stratified Aquifer", in: "Relation of Groundwater Quantity and Quality", IAHS-Publication Nr. 146, pp 103-114.
82. Walton, W. C., "Groundwater Modeling Utilities", Lewis Publishing, Inc., 1992.

83. Wang, C., Sun, N. Z., and Yeh, W. W. G., "An Upstream Weight Multiple Cell Balance Finite-Element Method for Solving Three-Dimensional Convection-Dispersion Equations", *Water Resour. Res.*, 22, 1575-1589.
84. Wheeler, M. F., and Dawson, C. N., "An Operator-Splitting Method for Advection-Diffusion-Reaction Problems", in *MAFELAP Proceedings*, Vol. VI, Edited by Whiteman, J. A., Academic, San Diego, California, 1988, pp 463-482.
85. Wilson, E., "Numerical Methods for Solution of Finite Element Systems", *Computer Utilization in Structural Engineering*, Publication by ASCE, New York, NY, USA, May 1989, pp 21-30.
86. Wung, T. S. and Chen, C. J., "Finite Analytic Solution of Convection Heat Transfer for Tube Arrays in Crossflow: Part I--Flow Field Analysis", *Journal of Heat Transfer, Transactions ASME*. vol. 111, No. 3, Aug 1989, pp633-640.
87. Zheng, C., "Extension of the Method of Characteristics for Simulation of Solution Transport in Three Dimensions", *Ground Water*, Vol. 31, No. 3, May-June 1993, pp 456 -465.